Summary of workshop 2:
QCD analysis of nucleon structure

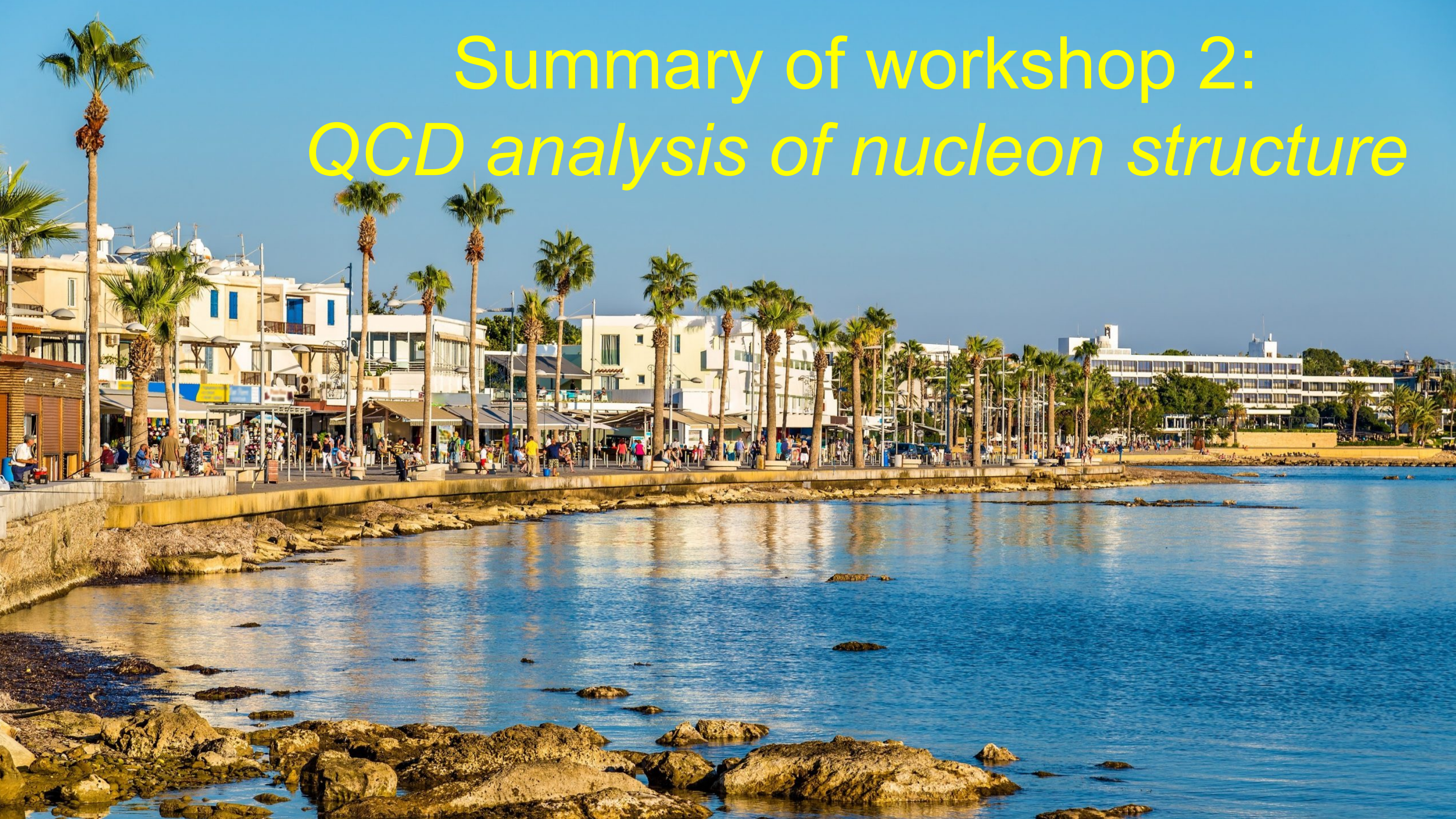

Topics here (and in EIC era!)

Moos
Schlegel
Gamberg
Zurita
Borsa
Magni
Bertone
Braun
Bhattacharya
Pedron
Tomalak
Hobart

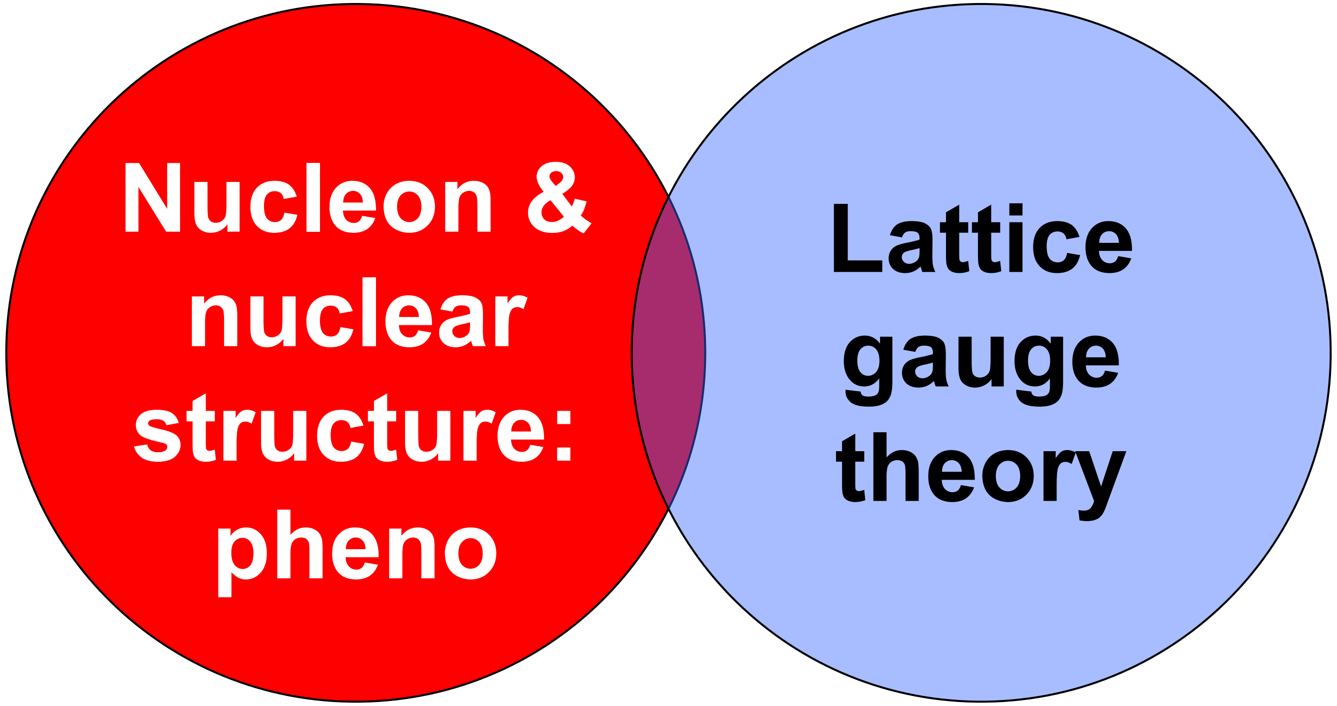

Bacchio
Koutsou
Pefkou
Zhang
Mukherjee
Constantinou
Pittler
Li

Topics here (and in EIC era!)

Moos
Schlegel
Gamberg
Zurita
Borsa
Magni
Bertone
Braun
Bhattacharya
Pedron
Tomalak
Hobart

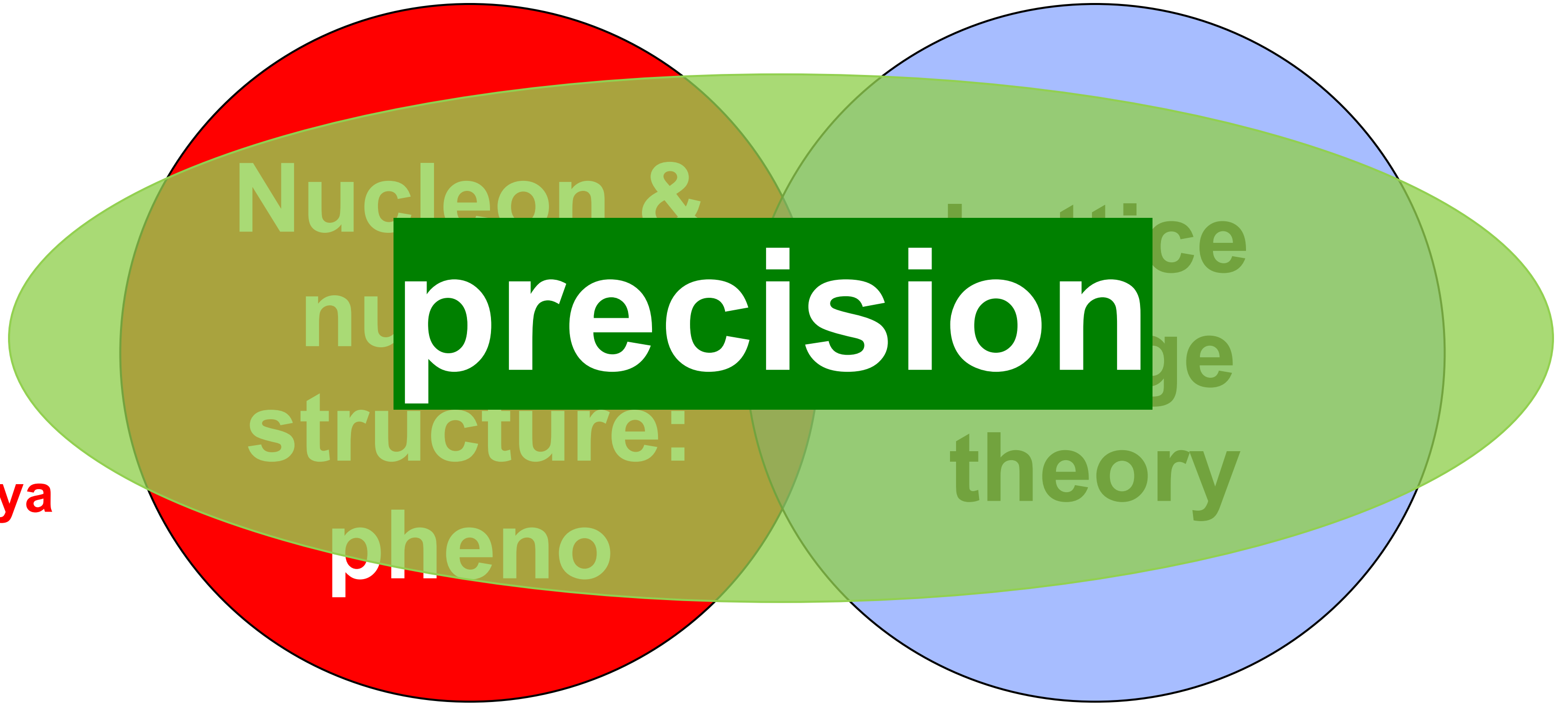

Bacchio
Koutsou
Pefkou
Zhang
Mukherjee
Constantinou
Pittler
Li

Disclaimers:

- “personal highlights”: will be selective
  -- apologies for talks not discussed in detail

- will make no attempt to do justice
  to wider literature (not a review of this field…)

- excellent introductions already by plenary talks

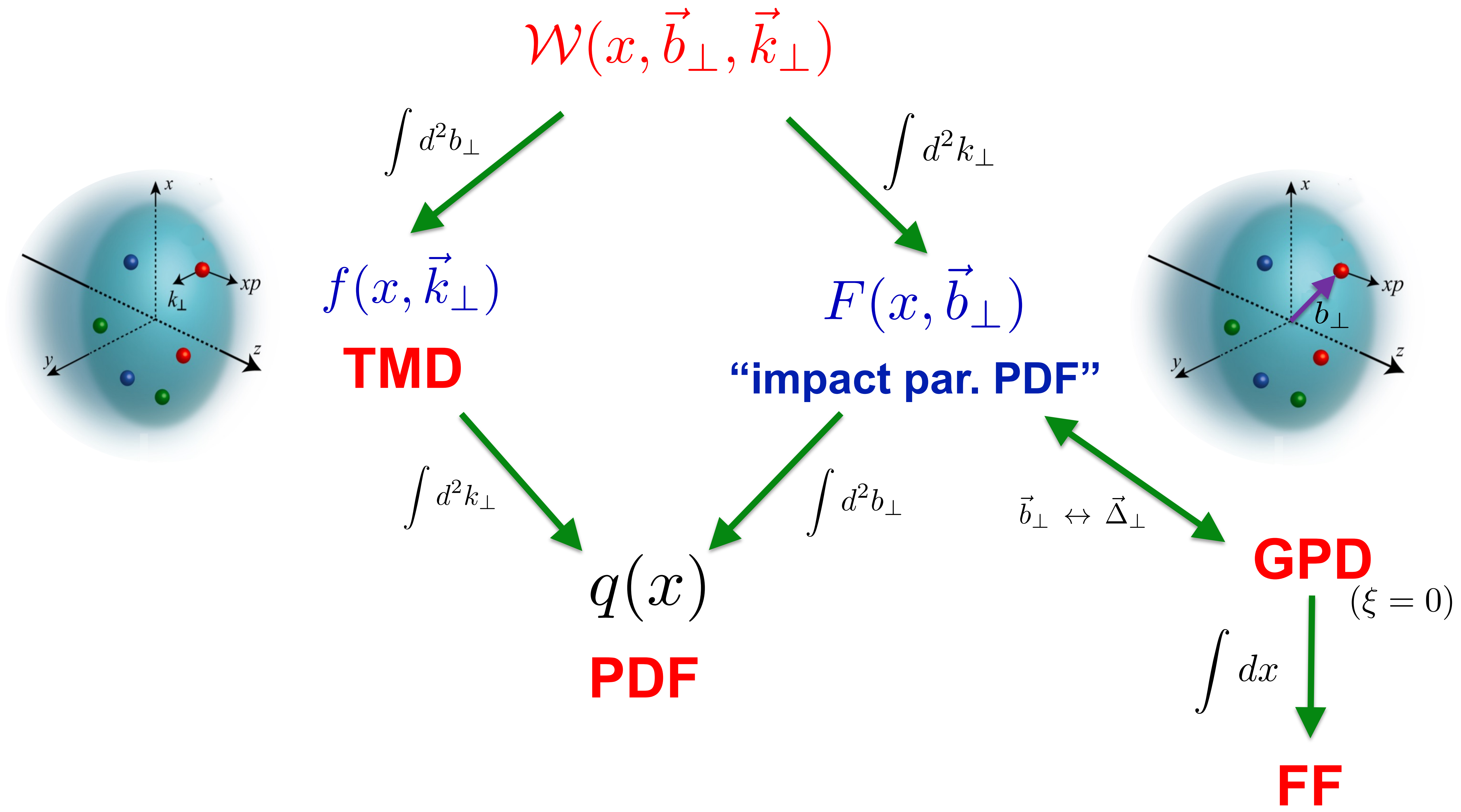

$\mathcal{W}(x, \vec{b}_\perp, \vec{k}_\perp)$
$\int d^2 b_\perp$
$\int d^2 k_\perp$
x
$k_\perp$
xp
y
z
$f(x, \vec{k}_\perp)$
TMD
$F(x, \vec{b}_\perp)$
"impact par. PDF"
x
$b_\perp$
xp
y
z
$\int d^2 k_\perp$
$\int d^2 b_\perp$
$\vec{b}_\perp \leftrightarrow \vec{\Delta}_\perp$
$q(x)$
PDF
GPD
$(\xi = 0)$
$\int dx$
FF

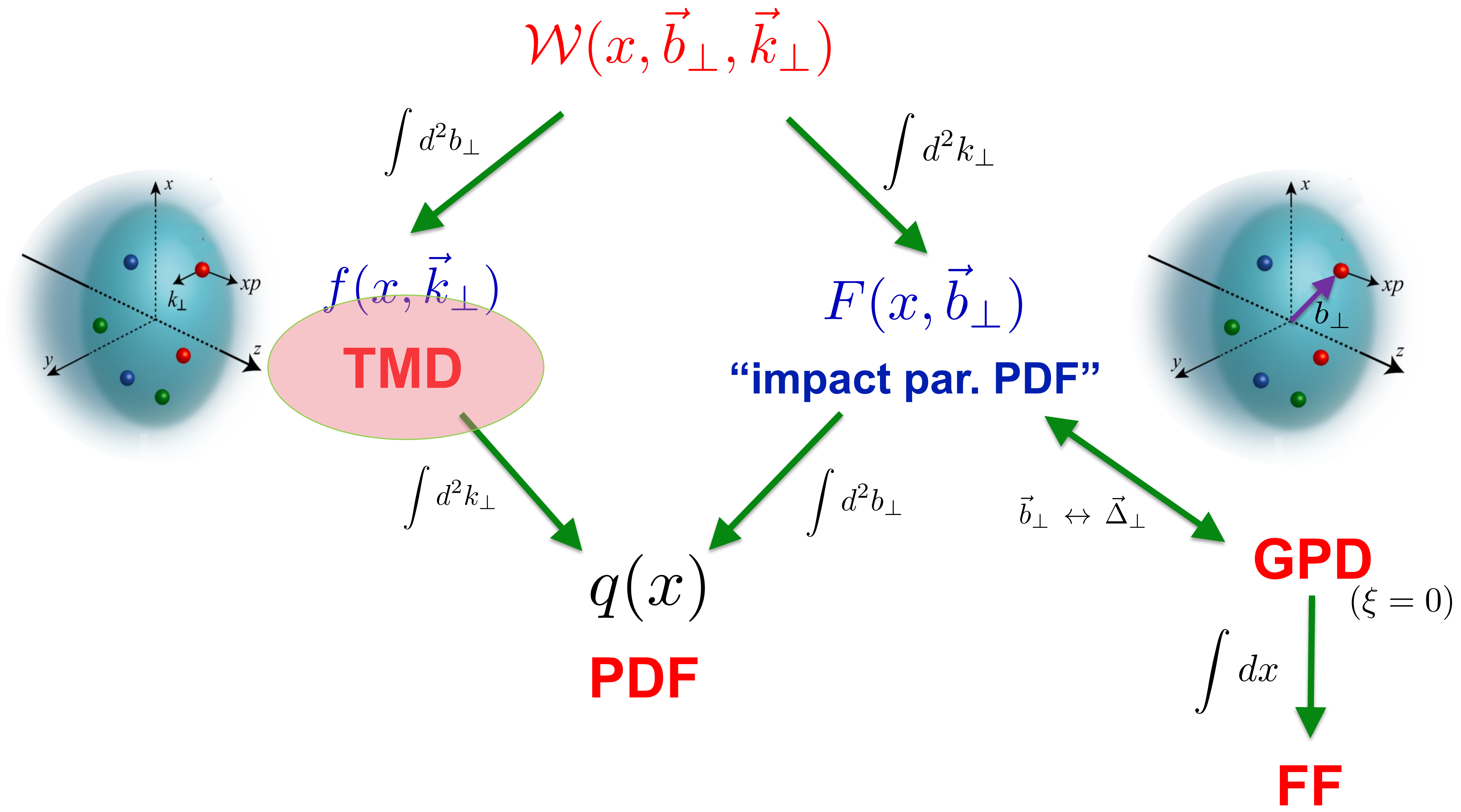
$\mathcal{W}(x, \vec{b}_\perp, \vec{k}_\perp)$
$\int d^2b_\perp$
$\int d^2k_\perp$
x
$k_\perp$
xp
y
z
$f(x, \vec{k}_\perp)$
TMD
$F(x, \vec{b}_\perp)$
"impact par. PDF"
$b_\perp$
$\int d^2k_\perp$
$\int d^2b_\perp$
$\vec{b}_\perp \leftrightarrow \vec{\Delta}_\perp$
GPD
$(\xi = 0)$
$\int dx$
$q(x)$
PDF
FF

N \ q	U	L	T
U	f_1		$h_1^\perp$
L		g_1	$h_{1L}^\perp$
T	$f_{1T}^\perp$	g_{1T}	h_1 $h_{1T}^\perp$

V. Moos

TMDPDF

CS

$$W^f_{f_1 f_1}(Q, q_T; x_1, x_2) \sim \int_0^\infty db\, b J_0(bq_T) f_{1,f\leftarrow h}(x_1, b) f_{1,\bar{f}\leftarrow h}(x_2, b) \left(\frac{Q^2}{\zeta_\mu(b)}\right)^{-2\mathcal{D}(b,\mu)}$$

$$\mu^2 \frac{d}{d\mu^2} f_{1,q\leftarrow h}(x, b; \mu, \zeta) = \frac{\gamma_F(\mu,\zeta)}{2} f_{1,q\leftarrow h}(x, b; \mu, \zeta)$$

$$\zeta \frac{d}{d\zeta} f_{1,q\leftarrow h}(x, b; \mu, \zeta) = -\mathcal{D}(b,\mu) f_{1,q\leftarrow h}(x, b; \mu, \zeta)$$

$$-\zeta \frac{d\gamma_F(\mu,\zeta)}{d\zeta} = \mu \frac{d\mathcal{D}(b,\mu)}{d\mu} = \Gamma_{\text{cusp}}(\mu)$$

FLAVOUR DEPENDENCE OF TMDS

P. Zurita

P. Zurita

$$f_{1,f}(x,b) = \int_x^1 \frac{dy}{y} \sum_{f'} C_{f\to f'}(y,\mathbf{L},a_s) q_{f'}\left(\frac{x}{y}\right) f_{\mathrm{NP}}^{f}(x,b)$$

$$f_{NP}^{f}(x,b) = \exp\left(- \frac{\lambda_1^f (1-x) + \lambda_2^f x}{\sqrt{1+\lambda_0 x^2 \mathbf{b}^2}} \mathbf{b}^2 \right)$$

$f = u, \bar{u}, d, \bar{d}, sea$

Black: final result.

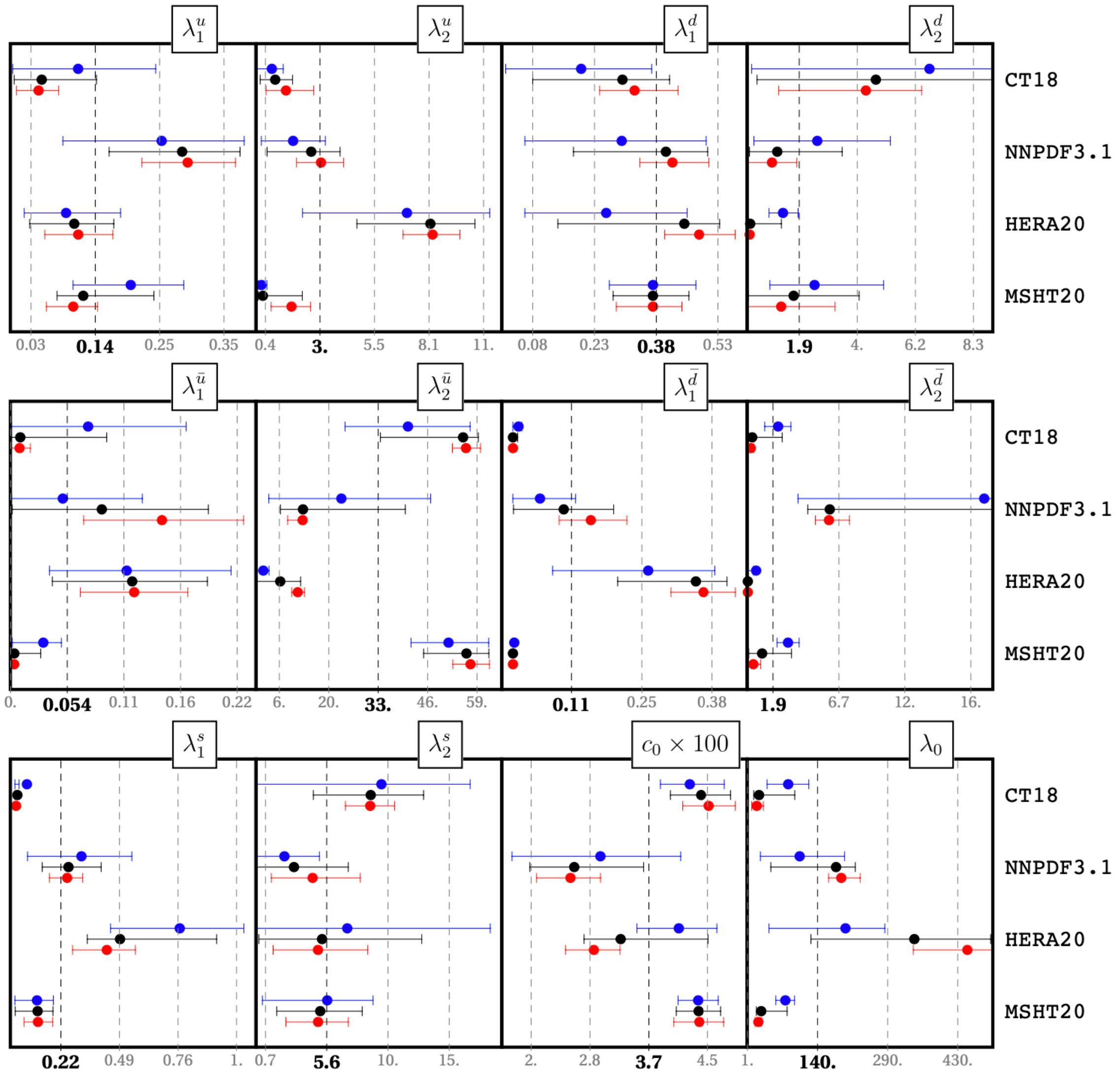

P. Zurita

We obtain more realistic uncertainty bands for the TMDPDFs:

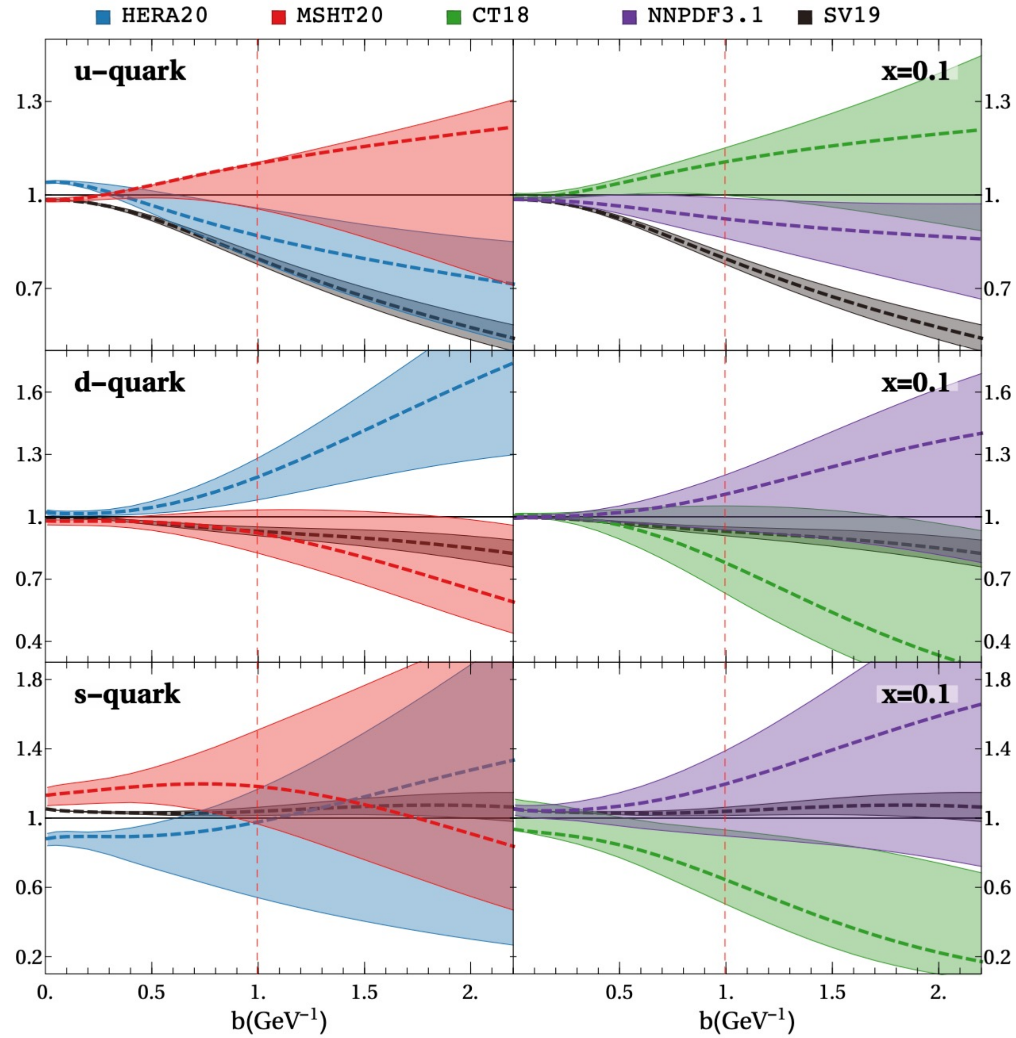

Now full analysis at N^{4}LL:

V. Moos

$$f_{1,f}(x,b) = \int_x^1 \frac{dy}{y} \sum_{f'} C_{f\to f'}(y,\mathbf{L},a_s) q_{f'}\left(\frac{x}{y}\right) f_{NP}^{f}(x,b)$$

$$f_{NP}^{f}(x,b) = \frac{1}{\cosh\left(\left(\lambda_1^f(1-x)+\lambda_2^f x\right) b\right)}$$

- $f \in \{u, \bar{u}, d, \bar{d}, sea\}$ $\rightarrow 2\times 5$ independent parameters!
- flavour dependent ansatz! **(=NEW feature!)**

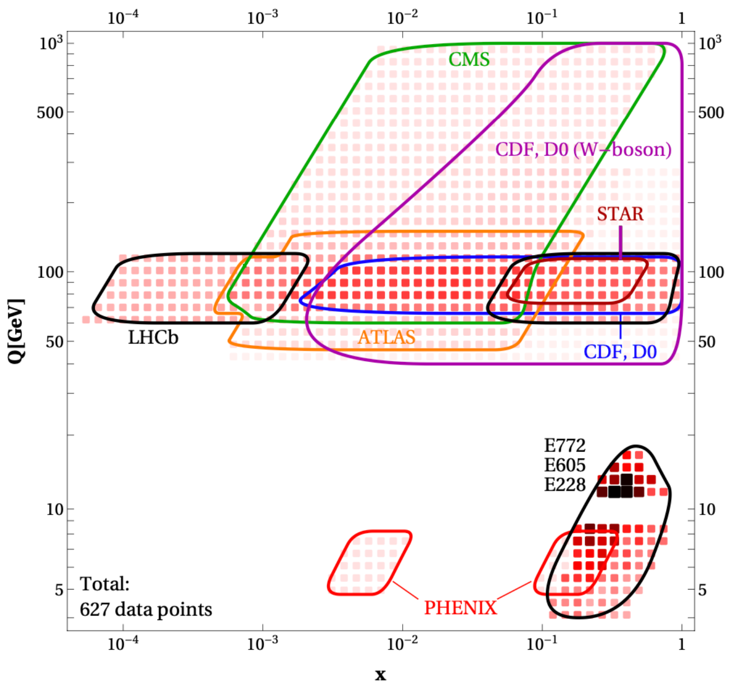

Features:

- large range of resolution scale: 4 GeV $\rightarrow$ 1 TeV
- including DY W production
- $\frac{q_T}{Q} < 0.25$ (TMD region!)
- 627 datapoints included in fit vs. 457 (SV19), vs. 484 (MAP22)

V. Moos

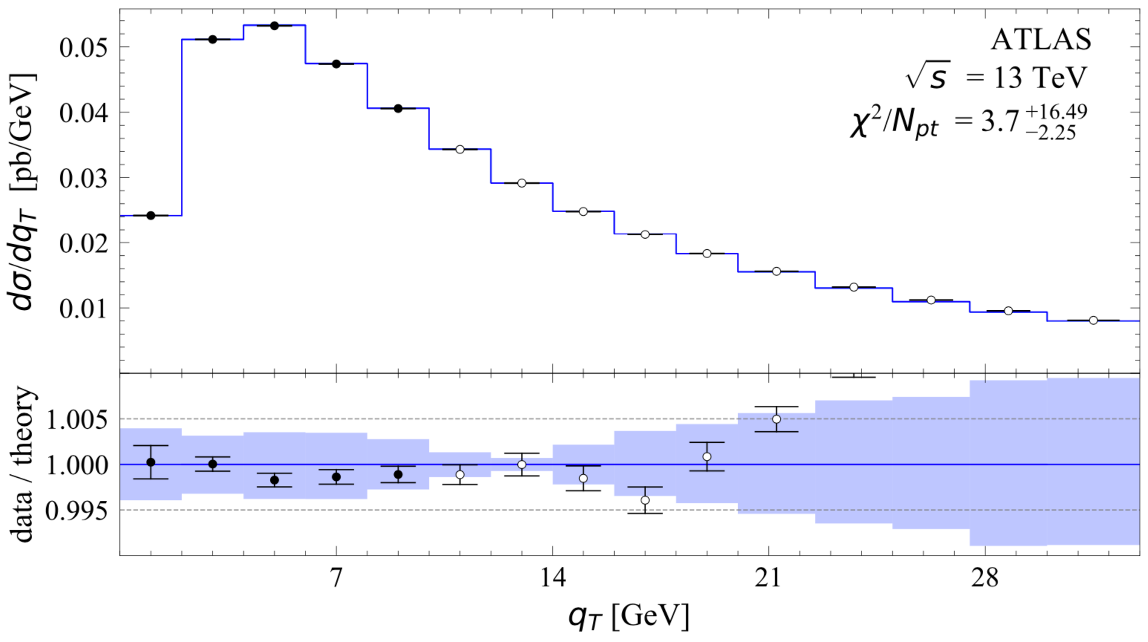

We can describe this VERY precise data!

overall $\chi^2/N_{pt} = 0.96^{+0.09}_{-0.01}$

...and also at very low Q for fixed target experiments.

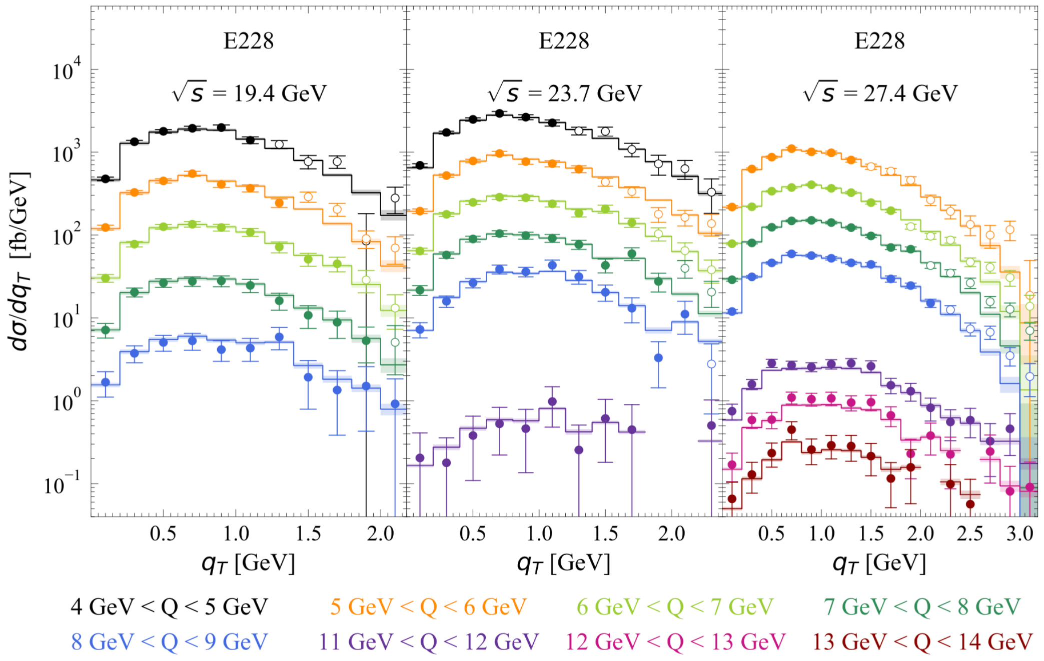

V. Moos

Still, rather large dependence on coll. PDF set and its uncertainty:

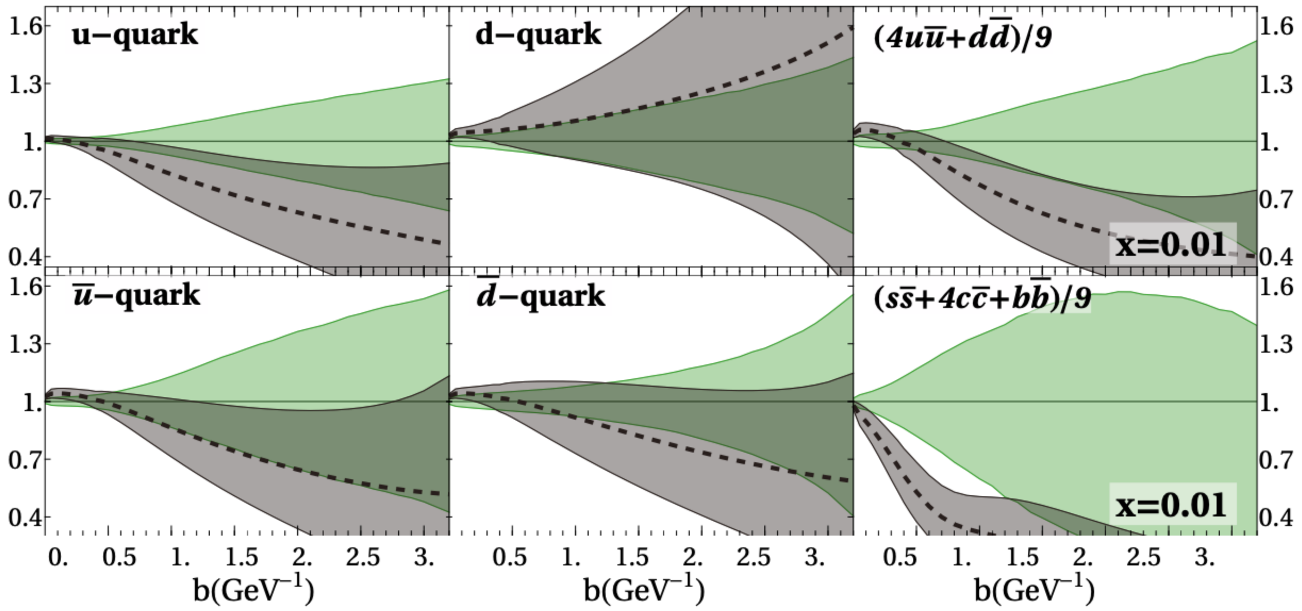

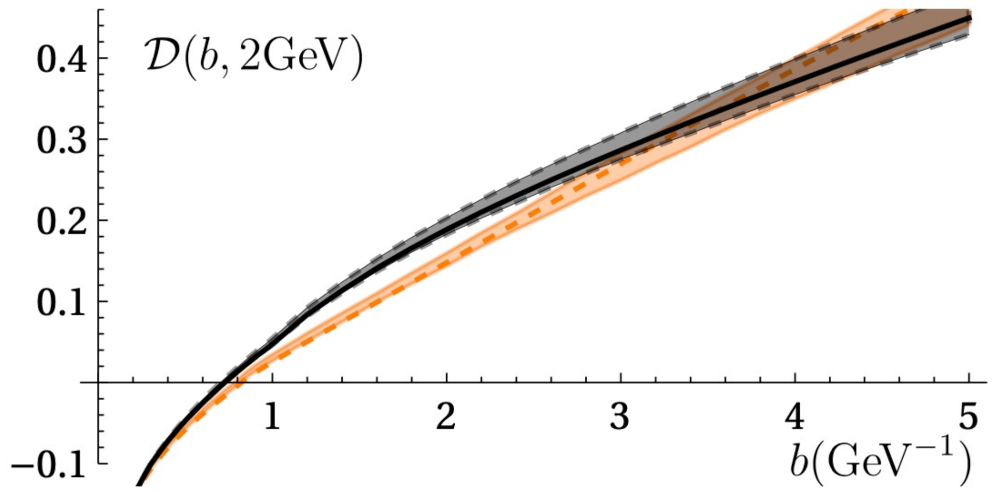

Wider ramifications of TMD flavor dependence? W mass?

Extractions using MSHT20 and NNPDF3.1

TMDs also exist beyond leading power.
Can one establish factorization?

L. Gamberg

- relevant as “background” to LP TMD analysis (often not small)
- interesting physics in itself (e.g., quark-gluon correlations)

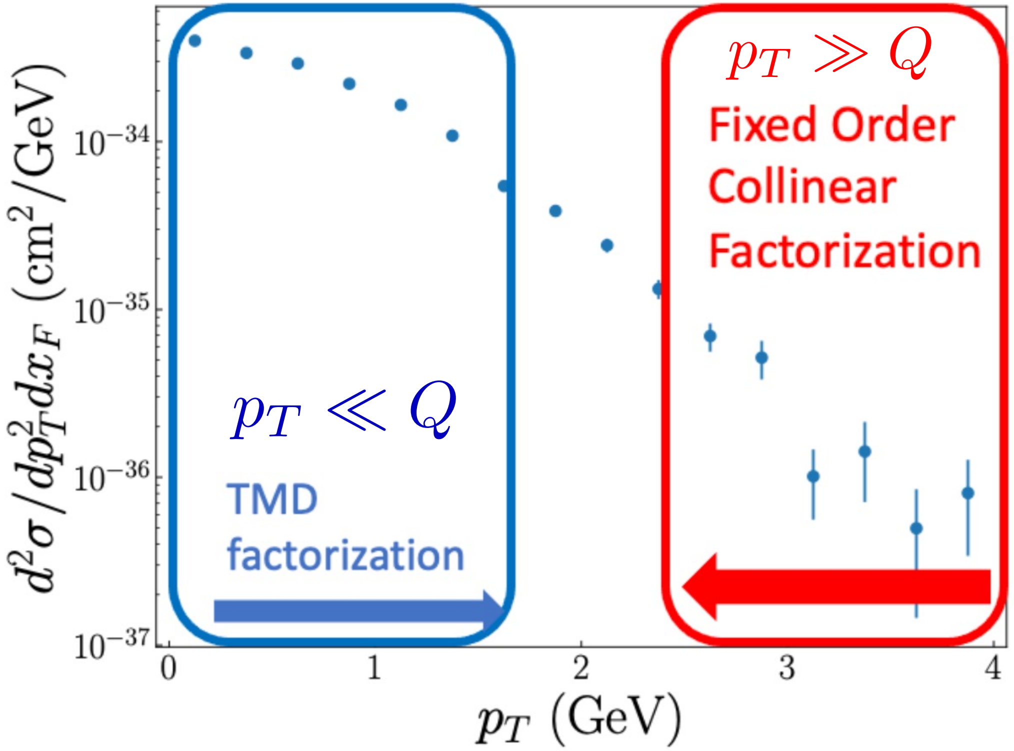

Various sources for power suppressed terms identified and discu

Tree level Studies, Mulders, Tangerman (1996), Bacchetta et al.

- This includes corrections associated to kinematic prefactors referred to as ***kinematic power corrections.***
- Another involve subleading terms in quark-quark correlators referred to as ***intrinsic power corrections*** — *e.g. Cahn function*
- Another from hadronic matrix elements of (interaction deper referred to ***dynamic power corrections*** multi-parton *qgq* corr

(linked by e.o.m.)

Cahn intrinsic k_T

Volume 78B, number 2,3 PHYSICS LETTERS 25 September 1978

AZIMUTHAL DEPENDENCE IN LEPTOPRODUCTION: A SIMPLE PARTON MODEL CALCULATION☆

Robert N. CAHN
Department of Physics, University of Michigan, Ann Arbor, MI 48109, USA

Received 5 June 1978

Semi-inclusive leptoproduction, $\ell + p \to \ell' + h + X$, is considered in the naive parton model. The scattered parton shows an azimuthal asymmetry about the momentum transfer direction. Simple derivations for the effects in ep, νp and $\bar{\nu}$p scattering are given. Reduction of the asymmetry due to fragmentation of partons into hadrons is estimated. The results cast doubt on the utility of such azimuthal asymmetry as a clean test of quantum chromodynamics.

parton model argument allowing for transverse momentum in Mandelstam variables...

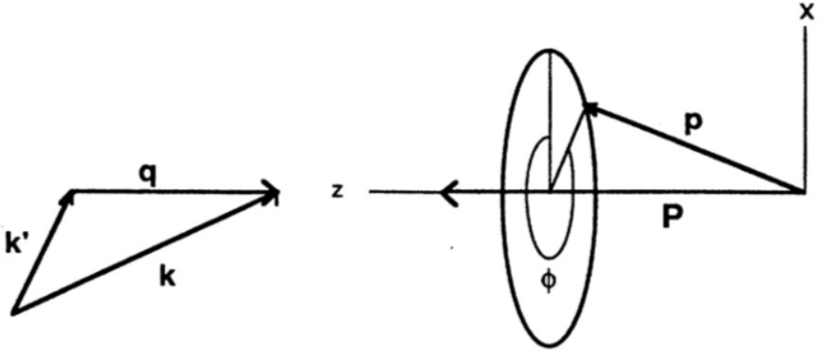

NLP

$$\langle \cos\phi \rangle_{ep} = -\left[\frac{2p_\perp}{Q}\right]\frac{(2-y)\sqrt{1-y}}{1+(1-y)^2}$$

L. Gamberg

TMD factorization at NLO and NLP

- We perform one loop calculation
- & attempt to establish renormalization group consistency: Regions hard,soft,collinear

$$
\begin{aligned}
F^3_{\rm DIS}(x,z,\boldsymbol{P}_{h\perp}) = & \; H^{\rm LP}_{\rm DIS}(Q;\mu)\,\mathcal{C}^{\rm DIS}\left[\frac{q_\perp}{Q} f_1\, D_1\, \mathcal{S}^{\rm LP}\right] \\
& - H^{\rm int}_{\rm DIS}(Q;\mu)\,\mathcal{C}^{\rm DIS}\left[\left(x\,\frac{\boldsymbol{k}_\perp\cdot\hat{x}}{Q} f^\perp\, D_1 - \frac{\boldsymbol{p}_\perp\cdot\hat{x}}{zQ} f_1\, D^\perp\right)\mathcal{S}^{\rm int}\right] \\
& - \int\frac{dx_g}{x_g} H^{\rm dyn}_{\rm DIS}(x_g,Q;\mu)\,\mathcal{C}^{\rm DIS}\left[x\,\frac{\boldsymbol{k}_\perp\cdot\hat{x}}{Q}\tilde{f}^\perp\, D_1\, \mathcal{S}^{\rm dyn}\right] \\
& + \int\frac{dz_g}{z_g} H^{\rm dyn}_{\rm DIS}(z_g,Q;\mu)\,\mathcal{C}^{\rm DIS}\left[\frac{\boldsymbol{p}_\perp\cdot\hat{x}}{zQ} f_1\, \tilde{D}^\perp \mathcal{S}^{\rm dyn}\right].
\end{aligned}
$$

NLO Ingredients collinear factor

L. Gamberg

Diagrams associated with the evolution of the collinear region

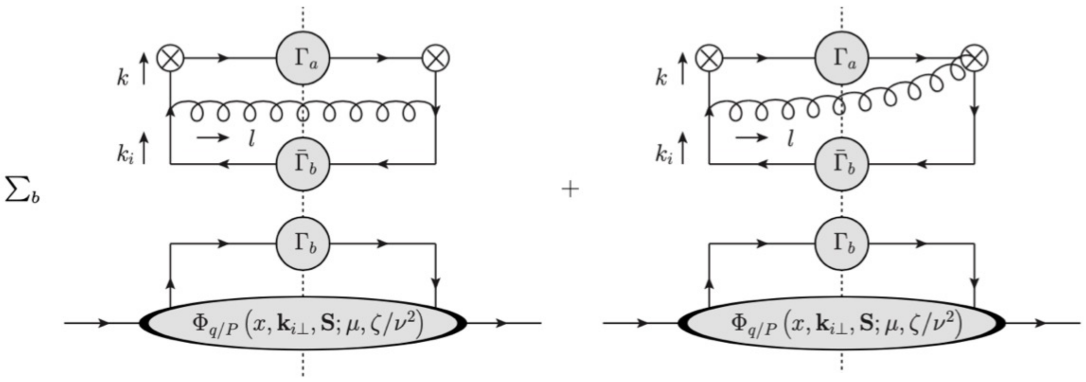

Renormalize TMDs: soft & UV subtraction

$$\hat{\Phi}^{[\Gamma^a]}\left(x,\boldsymbol{b},\boldsymbol{S};\mu,\zeta/\nu^2\right)=Z_{\Gamma^a\,\Gamma^b}\left(b,\mu,\zeta/\nu^2\right)\Phi^{[\Gamma^b]0}\left(x,\boldsymbol{b},\boldsymbol{S};xP^+\right)$$

Evolution equations naturally enter as matrices due to mixing

$$\frac{\partial}{\partial\ln\mu}\begin{bmatrix}\Phi^{[\not{n}]}\\ \Phi^{[\not{n}\gamma^5]}\\ \Phi^{[i\sigma^{i+}\gamma^5]}\\ \Phi^{[1]}\\ \Phi^{[\gamma^5]}\\ \Phi^{[\gamma^i]}\\ \Phi^{[\gamma^i\gamma^5]}\\ \Phi^{[i\sigma^{ij}\gamma^5]}\\ \Phi^{[i\sigma^{+-}\gamma^5]}\end{bmatrix}=\boldsymbol{\Gamma}^{\mu}\begin{bmatrix}\Phi^{[\not{n}]}\\ \Phi^{[\not{n}\gamma^5]}\\ \Phi^{[i\sigma^{l+}\gamma^5]}\\ \Phi^{[1]}\\ \Phi^{[\gamma^5]}\\ \Phi^{[\gamma^l]}\\ \Phi^{[\gamma^l\gamma^5]}\\ \Phi^{[i\sigma^{lm}\gamma^5]}\\ \Phi^{[i\sigma^{+-}\gamma^5]}\end{bmatrix}\qquad\frac{\partial}{\partial\ln\nu}\begin{bmatrix}\Phi^{[\not{n}]}\\ \Phi^{[\not{n}\gamma^5]}\\ \Phi^{[i\sigma^{i+}\gamma^5]}\\ \Phi^{[1]}\\ \Phi^{[\gamma^5]}\\ \Phi^{[\gamma^i]}\\ \Phi^{[\gamma^i\gamma^5]}\\ \Phi^{[i\sigma^{ij}\gamma^5]}\\ \Phi^{[i\sigma^{+-}\gamma^5]}\end{bmatrix}=\boldsymbol{\Gamma}^{\nu}\begin{bmatrix}\Phi^{[\not{n}]}\\ \Phi^{[\not{n}\gamma^5]}\\ \Phi^{[i\sigma^{l+}\gamma^5]}\\ \Phi^{[1]}\\ \Phi^{[\gamma^5]}\\ \Phi^{[\gamma^l]}\\ \Phi^{[\gamma^l\gamma^5]}\\ \Phi^{[i\sigma^{lm}\gamma^5]}\\ \Phi^{[i\sigma^{+-}\gamma^5]}\end{bmatrix}.$$

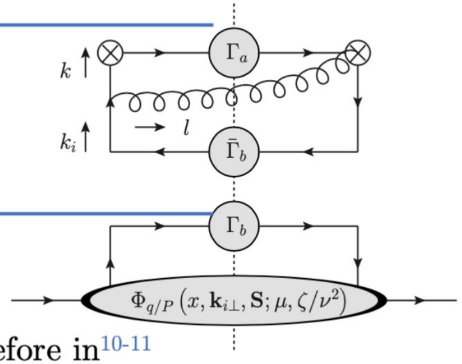

We find operator mixing in the Collins-Soper equation. Seen before in[10-11]

$$\boldsymbol{\Gamma}^{\mu}=\begin{bmatrix}\Gamma_2^{\mu}&0&0&0&0&0&0&0&0\\0&\Gamma_2^{\mu}&0&0&0&0&0&0&0\\0&0&\Gamma_2^{\mu}\delta_l^i&0&0&0&0&0&0\\0&0&0&\Gamma_3^{\mu}&0&0&0&0&0\\0&0&0&0&\Gamma_3^{\mu}&0&0&0&0\\0&0&0&0&0&\Gamma_3^{\mu}\delta_l^i&0&0&0\\0&0&0&0&0&0&\Gamma_3^{\mu}\delta_l^i&0&0\\0&0&0&0&0&0&0&\frac{1}{4}\Gamma_3^{\mu}\left(\delta_l^i\delta_m^j-\delta_l^j\delta_m^i\right)&0\\0&0&0&0&0&0&0&0&\Gamma_3^{\mu}\end{bmatrix}$$

$$\boldsymbol{\Gamma}^{\nu}=\frac{\alpha_s C_F}{2\pi}\begin{bmatrix}2L&0&0&0&0&0&0&0&0\\0&2L&0&0&0&0&0&0&0\\0&0&2L\delta_l^i&0&0&0&0&0&0\\0&0&0&L&0&0&0&0&0\\0&0&\frac{2ib_l}{xP^+}\frac{\partial L}{\partial b^2}&0&L&0&0&0&0\\\frac{2ib^i}{xP^+}\frac{\partial L}{\partial b^2}&0&0&0&0&L\delta_l^i&0&0&0\\0&\frac{2ib^i}{xP^+}\frac{\partial L}{\partial b^2}&0&0&0&0&L\delta_l^i&0&0\\0&0&\frac{i}{xP^+}\frac{\partial L}{\partial b^2}\left(b^j\delta_l^i-b^i\delta_l^j\right)&0&0&0&0&L\left(\delta_l^i\delta_m^j-\delta_l^j\delta_m^i\right)&0\\0&0&\frac{2ib_l}{xP^+}\frac{\partial L}{\partial b^2}&0&0&0&0&0&L\end{bmatrix}$$

LP to LP

LP to NLP

NLP to NLP

L. Gamberg

NLO Ingredients soft factor

The soft region

The soft function is generated through the emissions of soft gluons in the partonic cross section

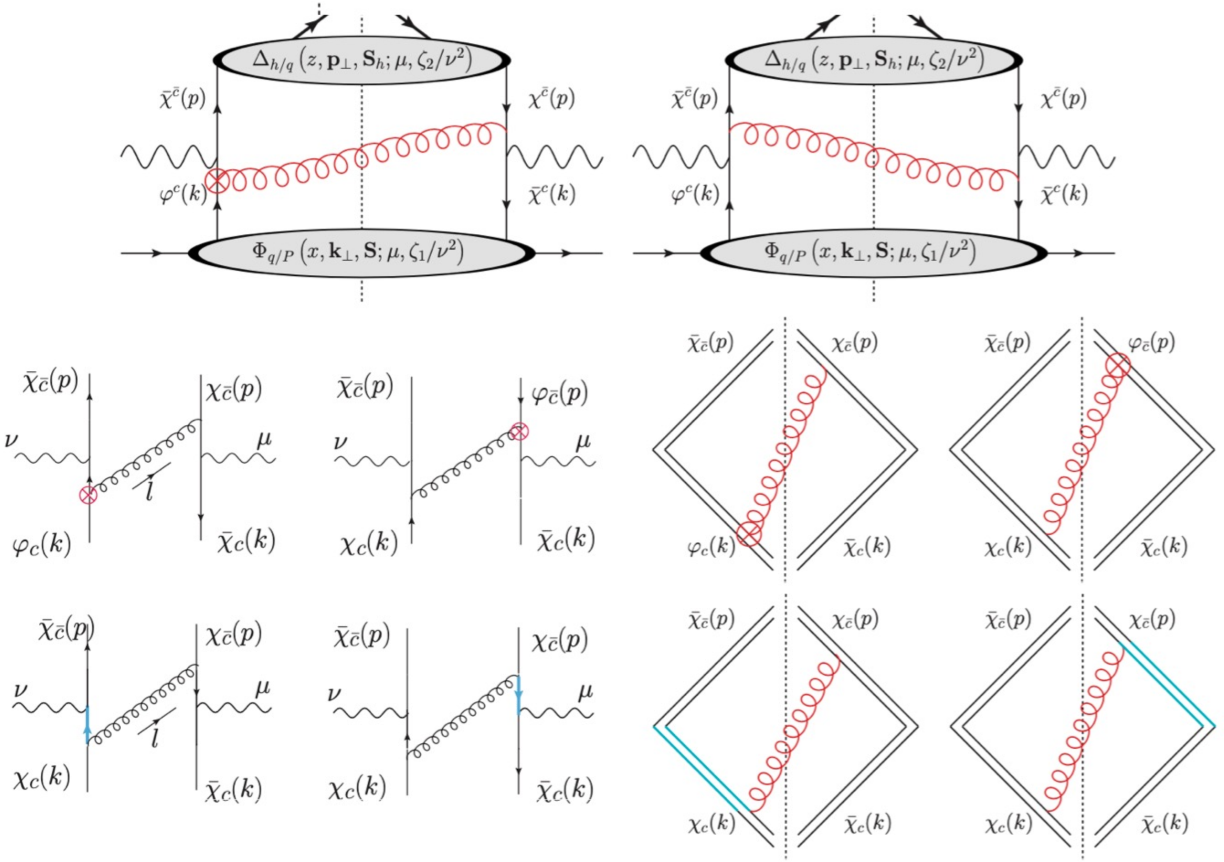

Progress Report
Stay tuned ...

Contributions to the soft factor after applying the eikonal approximation and including the effect from the transverse momentum contributions from the quark propagators.

M. Schlegel

- long-standing struggle to understand single-spin asymmetries

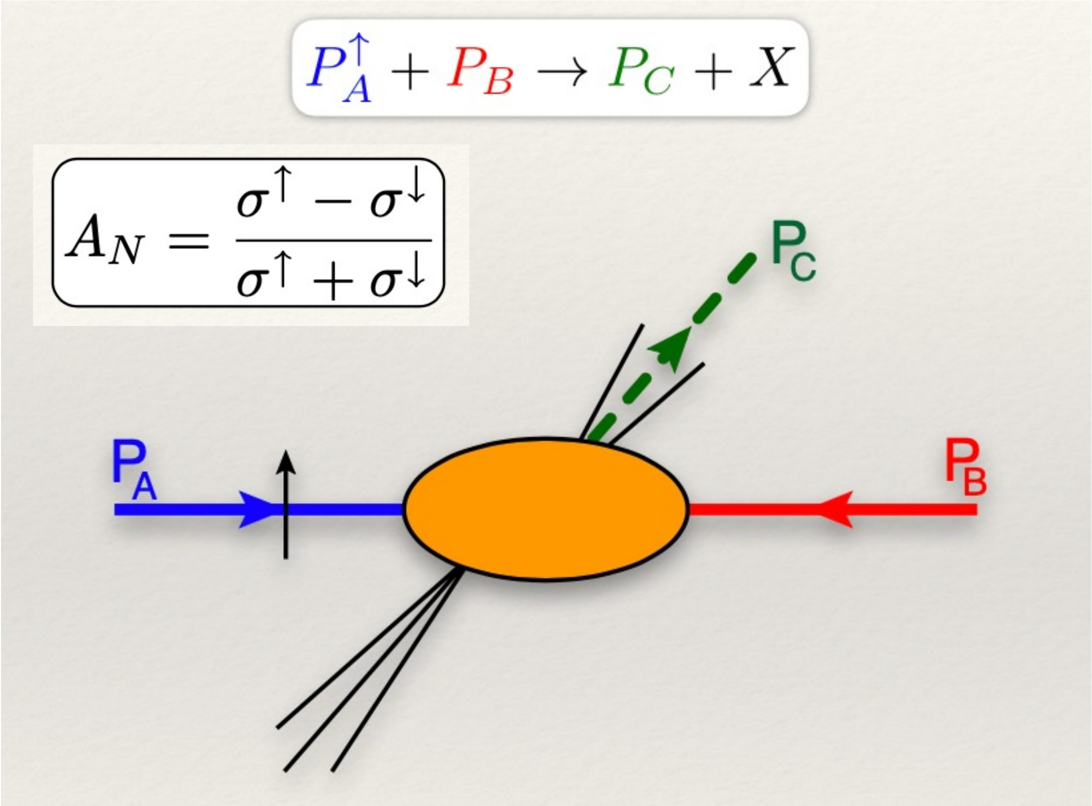

$e N^\uparrow \to \pi X$

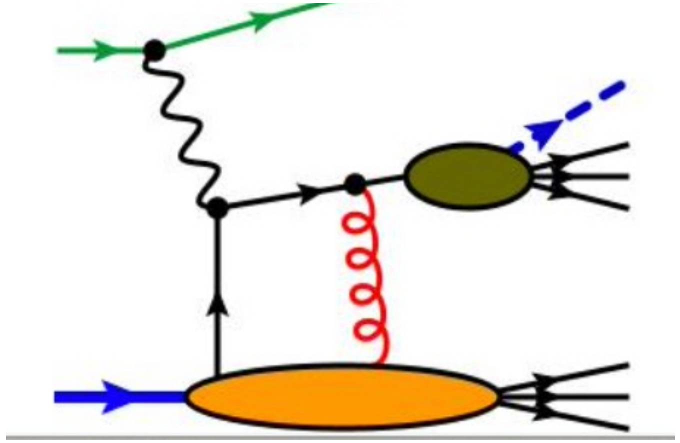

$$A_N \propto \sum_q e_q^2 \int dz \left(1 - x\frac{d}{dx}\right) F_{FT}^q(x,x)\, D_1^{\pi/q}(z)$$

M. Schlegel

Four partonic channels at NLO:

- **qg → g:** gluon fragmentation ✅

  The easiest channel:

  -12 real diagrams, no virtual contributions

  - no MS - subtraction of collinear divergences from SGP, but from FF

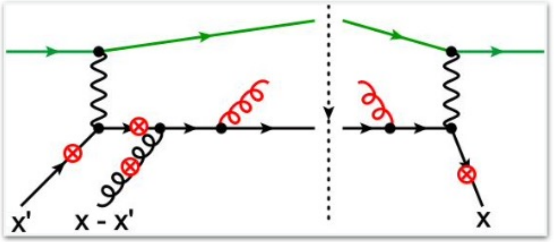

- **gg → q:** triple gluon correlations 🚫

  The next-to-easiest (?) channel:

  -12 real diagrams, no virtual contributions

  - MS - subtraction of collinear divergences from SGP (?)

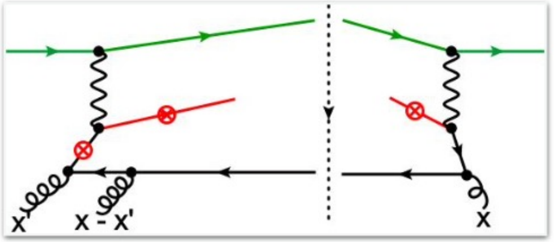

- **qq → q:** quark-antiquark correlations ✅

  The second most subtle channel: (suppressed in $1/N_c$)

  -12 real diagrams & virtual contributions (x' < 0)

  - MS - subtraction of collinear divergences from SGP needed

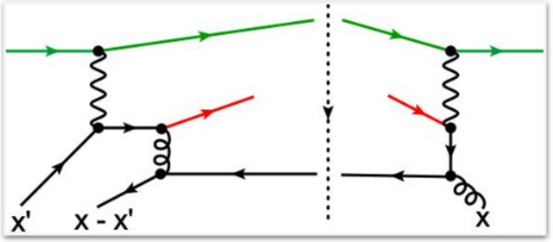

- **qg → q:** quark-antiquark correlations (partially ✅)

  The most difficult channel:

  -12 real diagrams & virtual contributions (x' > 0)

  - MS - subtraction of collinear divergences from SGP & FF needed

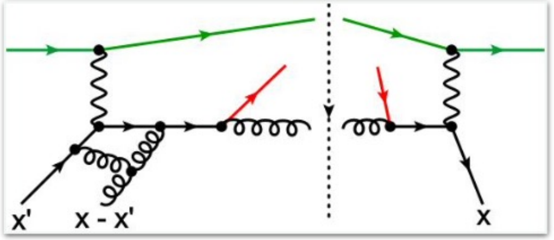

M. Schlegel

LO

$$E_\pi \frac{d\sigma}{d\mathbf{P}_\pi} = \sigma_0(S) \sum_q e_q^2 \int_{v_0}^{v_1} dv \, \frac{1+v^2}{(1-v)^4} \left[\left(F_{FT}^q - x_0 \, (F_{FT}^q)' \right) (x_0, x_0) \, D_1^q(z) \right]$$

Integral contribution

$$+\sigma_0(S) \frac{\alpha_s}{2\pi} \sum_q e_q^2 \int_{v_0}^{v_1} dv \int_{x_0}^{1} \frac{dw}{w} \int_0^1 d\zeta \, \left[C_F \, \hat{\sigma}_1^{\text{int}}(v,w,\zeta) + \tfrac{1}{2} N_c \, \hat{\sigma}_2^{\text{int}}(v,w,\zeta) \right] \, \frac{F_{FT}^q(x, x\zeta) - \zeta(2-\zeta) \, F_{FT}^q(x,x) + \zeta(1-\zeta) \frac{1}{2} x \frac{dF_{FT}^q}{dx}(x,x) - (1-\zeta)^2 \, F_{FT}^q(x,0)}{\zeta(1-\zeta)^2} D_1^q(z)$$

$$+\sigma_0(S) \frac{\alpha_s}{2\pi} \sum_q e_q^2 \int_{v_0}^{v_1} dv \int_{x_0}^{1} \frac{dw}{w} \int_0^1 d\zeta \, \left[C_F \, \hat{\sigma}_{5,1}^{\text{int}}(v,w,\zeta) + \tfrac{1}{2} N_c \, \hat{\sigma}_{5,2}^{\text{int}}(v,w,\zeta) \right] \, \frac{G_{FT}^q(x, x\zeta) + \zeta(1-\zeta) x \frac{\partial G_{FT}^q}{\partial x'}(x,x) - (1-\zeta)^2 \, G_{FT}^q(x,0)}{\zeta(1-\zeta)^2} D_1^q(z)$$

$$+\sigma_0(S) \frac{\alpha_s}{2\pi} \sum_q e_q^2 \int_{v_0}^{v_1} dv \int_{x_0}^{1} \frac{dw}{w} \left[C_F \, \hat{\sigma}_1^{\text{SGP}}(v,w,\tfrac{su}{t\mu^2}) + \tfrac{1}{2} N_c \, \hat{\sigma}_2^{\text{SGP}}(v,w,\tfrac{su}{tm_e^2}) \right] \, F_{FT}^q(x,x) D_1^q(z)$$

$$+\sigma_0(S) \frac{\alpha_s}{2\pi} \sum_q e_q^2 \int_{v_0}^{v_1} dv \int_{x_0}^{1} \frac{dw}{w} \left[C_F \, \hat{\sigma}_{5,1}^{\text{SGP}}(v,w) + \tfrac{1}{2} N_c \, \hat{\sigma}_{5,2}^{\text{SGP}}(v,w) \right] \, x \, \frac{\partial G_{FT}^q}{\partial x'}(x,x) \, D_1^q(z)$$

Soft-Gluon Pole

$$\ln\left(\frac{su}{t\,\mu^2}\right) \quad \ln\left(\frac{su}{t\,m_e^2}\right) \quad \frac{1}{(1-w)_+}$$

$$+\sigma_0(S) \frac{\alpha_s}{2\pi} \sum_q e_q^2 \int_{v_0}^{v_1} dv \int_{x_0}^{1} \frac{dw}{w} \left[C_F \, \hat{\sigma}_1^{\text{SFP}}(v,w,\tfrac{su}{tm_e^2}) + \tfrac{1}{2} N_c \, \hat{\sigma}_2^{\text{SFP}}(v,w,\tfrac{su}{tm_e^2}) \right] \, F_{FT}^q(x,0) D_1^q(z)$$

$$+\sigma_0(S) \frac{\alpha_s}{2\pi} \sum_q e_q^2 \int_{v_0}^{v_1} dv \int_{x_0}^{1} \frac{dw}{w} \left[C_F \, \hat{\sigma}_{5,1}^{\text{SFP}}(v,w,\tfrac{su}{tm_e^2}) + \tfrac{1}{2} N_c \, \hat{\sigma}_{5,2}^{\text{SFP}}(v,w,\tfrac{su}{tm_e^2}) \right] \, G_{FT}^q(x,0) D_1^q(z)$$

Soft-Fermion Pole

$$\ln\left(\frac{su}{t\,m_e^2}\right)$$

M. Schlegel

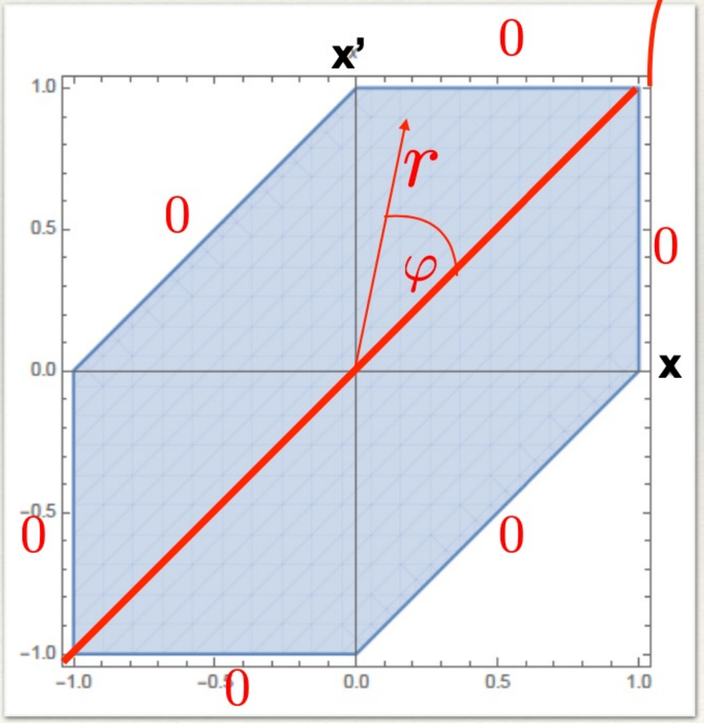

"Soft gluon pole" (SGP)

$$\pi F^q_{FT}(x,x) = f^{\perp(1),q}_{1T}(x)$$
$$G^q_{FT}(x,x) = 0$$

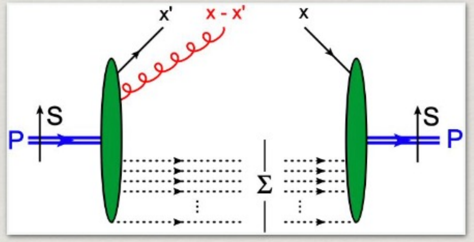

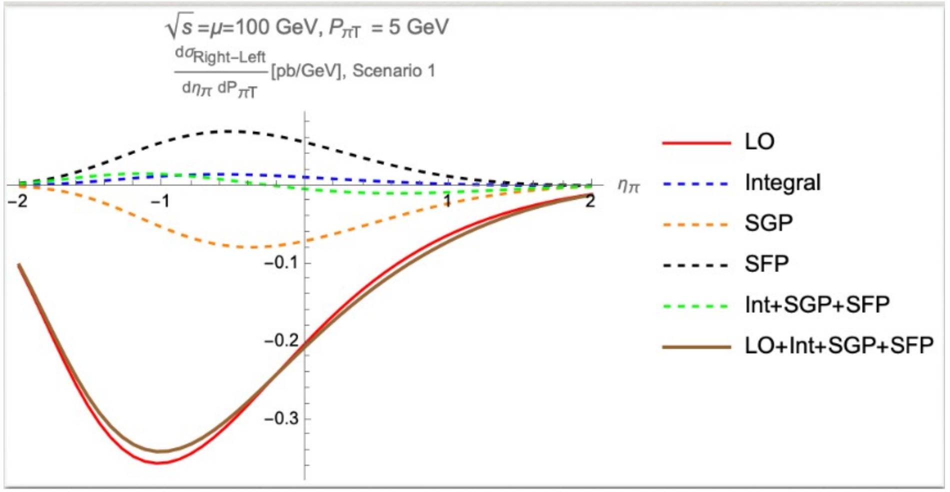

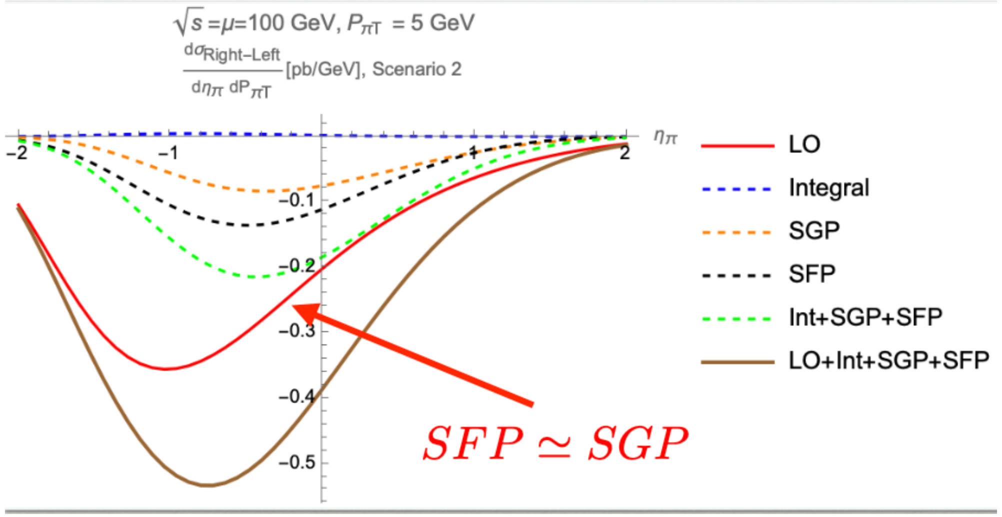

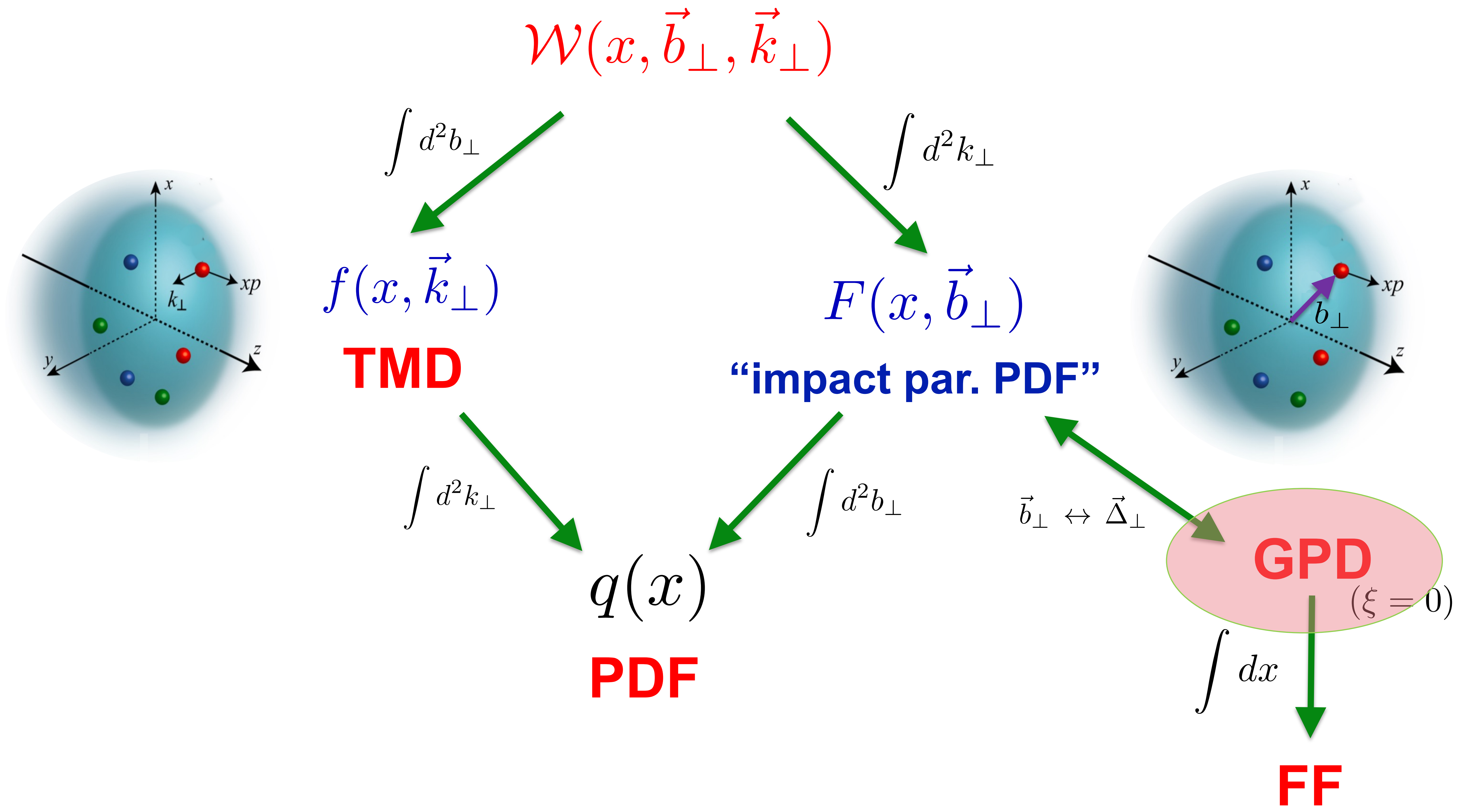

$\mathcal{W}(x, \vec{b}_\perp, \vec{k}_\perp)$
$\int d^2 b_\perp$
$\int d^2 k_\perp$
x
xp
$k_\perp$
y
z
$f(x, \vec{k}_\perp)$
TMD
$F(x, \vec{b}_\perp)$
"impact par. PDF"
x
xp
$b_\perp$
y
z
$\int d^2 k_\perp$
$\int d^2 b_\perp$
$\vec{b}_\perp \leftrightarrow \vec{\Delta}_\perp$
GPD
$(\xi = 0)$
$\int dx$
$q(x)$
PDF
FF

DVCS at the Precision Frontier

V. Braun

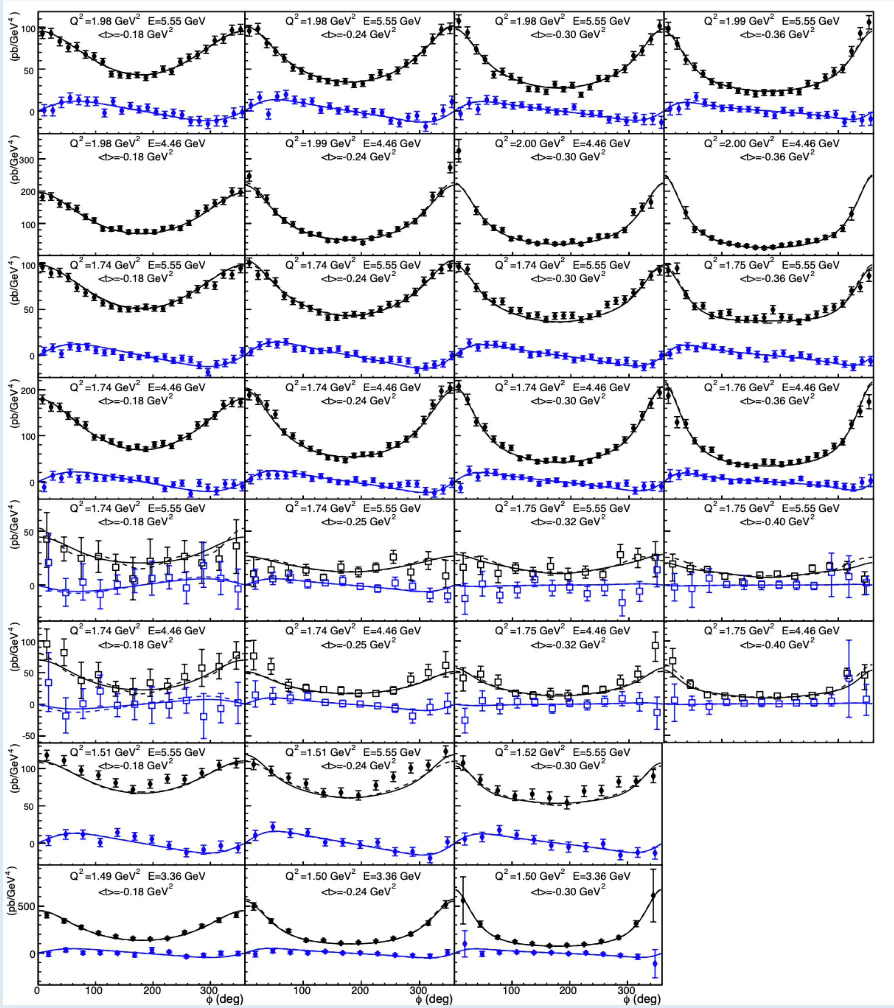

2010 data of E07-007 and E08-025 [2109.02076]

- High statistical accuracy
- Several beam energies
- Neutron/deuteron
- Coherent DVCS from ^{4}He

- Transverse polarization

@ leading tw.

V. Braun

$$\mathcal{A}^{\mathrm{DVCS}}_{\mu\nu} = -g^{\perp}_{\mu\nu} V + \epsilon^{\perp}_{\mu\nu} A + \dots$$

$$V(\xi, Q^2) = \sum_q e_q^2 \int_{-1}^{1} \frac{dx}{\xi} C_V(x/\xi, Q^2/\mu^2)\, F_q(x,\xi,t,\mu)\,.$$

$$F_q(x,\xi) = \frac{1}{2P_+}\left[H_q(x,\xi,t)\bar{u}(p')\gamma_+ u(p) + E_q(x,\xi,t)\bar{u}(p')\frac{i\sigma^{+\nu}\Delta_\nu}{2m_N}u(p)\right].$$

$$C(x/\xi, Q^2/\mu^2) = C^{(0)}(x/\xi) + a_s C^{(1)}(x/\xi, Q^2/\mu^2) + a_s^2 C^{(2)}(x/\xi, Q^2/\mu^2) + \dots$$

- Flavor-nonsinglet calculated using two different techniques

$C_V^{(2)}$: V.Braun, A.Manashov, S.Moch, J.Schönleber, JHEP **09**, 117 (2020)
J. Schönleber, unpublished

$C_A^{(2)}$: V.Braun, Manashov, Moch, Schönleber, 2106.01437
J.Gao, T.Huber, Y.Ji and Y.M.Wang, 2106.01390

- Flavor-singlet CFs:

$C_V^{(2)}$: V.Braun, Y. Ji, J. Schönleber, PRL **129** 172001 (2022)

$C_A^{(2)}$: Y. Ji, J. Schönleber, e-Print: 2310.05724

Example (flavor-nonsinglet)

$$C_V^{(2)}(x) = C_F^2 C_P^{(2)}(x) + \frac{C_F}{N_c} C_{NP}^{(2)}(x) + \beta_0 C_F C_\beta^{(2)}(x)$$

$$\begin{aligned}
C_{NP}^{(2)} = 6(1-2\omega)\Big\{ & \mathrm{H}_{20} - \mathrm{H}_3 + \mathrm{H}_{110} - \mathrm{H}_{12} + \zeta_2\Big(\mathrm{H}_0 + \mathrm{H}_1\Big) - 3\zeta_3 \Big\} \\
& + 12\Big(\mathrm{H}_{10} - \mathrm{H}_2 - \mathrm{H}_0 - \mathrm{H}_1 + \zeta_2\Big) + \frac{3}{\bar{\omega}}\mathrm{H}_0 + \frac{3}{\omega}\mathrm{H}_1 \\
& + \Big\{ \frac{1}{\omega}\Big(12\zeta_3 - \frac{3}{2}\zeta_2^2 - \frac{5}{2}\zeta_2 - \frac{73}{24}\Big) - \frac{3}{\omega}\mathrm{H}_{200} - \Big(\frac{2}{\omega} - \frac{1}{\bar{\omega}}\Big)\mathrm{H}_{30} + \Big(\frac{4}{\omega} - \frac{1}{\bar{\omega}}\Big)\mathrm{H}_4 \\
& - \Big(\frac{2}{\omega} - \frac{1}{\bar{\omega}}\Big)\mathrm{H}_{210} + \Big(\frac{3}{\omega} - \frac{2}{\bar{\omega}}\Big)\mathrm{H}_{22} - \Big(\frac{2}{\omega} - \frac{1}{\bar{\omega}}\Big)\mathrm{H}_{31} - \frac{5}{\bar{\omega}}\mathrm{H}_3 + \frac{5}{\bar{\omega}}\mathrm{H}_{20} \\
& + \Big(\frac{1}{\bar{\omega}}\Big(\zeta_2 - \frac{9}{2}\Big) + \frac{1}{\omega}\Big(\frac{4}{3} - 2\zeta_2\Big)\Big)\mathrm{H}_{00} - \Big(\frac{2}{\omega}\Big(\zeta_2 - 1\Big) - \frac{1}{\bar{\omega}}\Big(\zeta_2 + \frac{7}{6}\Big)\Big)\mathrm{H}_2 \\
& + \Big(\frac{1}{\bar{\omega}}\Big(\frac{19}{6} + 5\zeta_2 - 3\zeta_3\Big) + \frac{1}{\omega}\Big(7\zeta_3 - \frac{16}{9}\Big)\Big)\mathrm{H}_0 - (\omega \leftrightarrow \bar{\omega}) \Big\}
\end{aligned}$$

where $\omega = (1-x)/2$, $\bar{\omega} = (1+x)/2$, and $\mathrm{H}_{\vec{m}} \equiv \mathrm{H}_{\vec{m}}(\omega)$ are harmonic polylogarithms

CFF Im(H):

$t = -0.1\,\mathrm{GeV}^2$

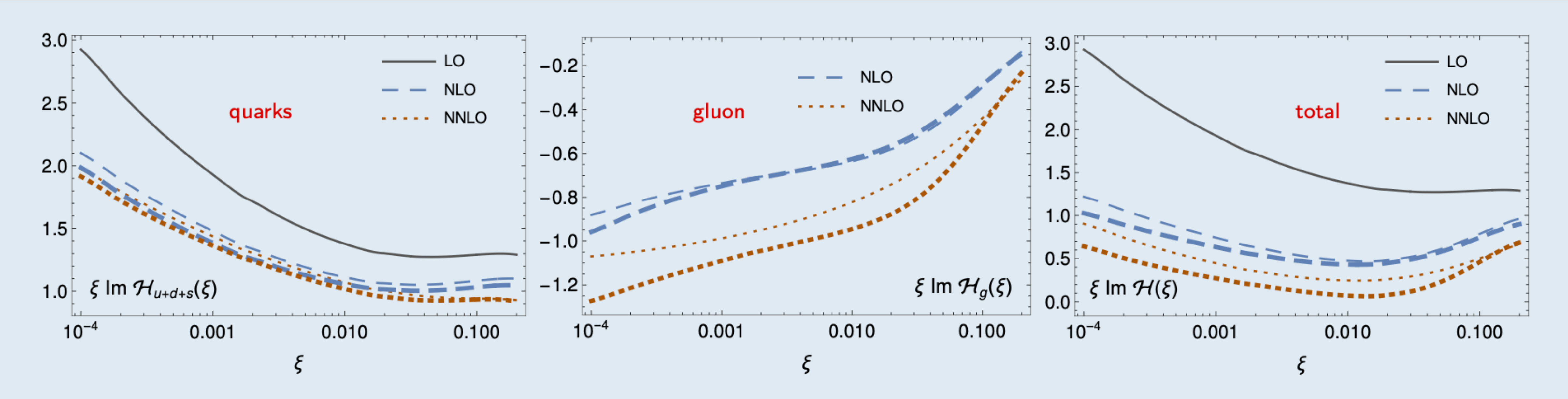

- even relevant for Jlab kinematics
- based on GK model → need to "retune"

Summary

V. Braun

1. **Towards NNLO accuracy**
   - Two-loop coefficient functions for DVCS

     — sizeable corrections, completed for light quarks
   - Three-loop evolution equations for GPDS

     — flavor nonsinglet in position space, singlet for the first few moments
     — pressing issue: numerical implementation, also in NLO

2. **Kinematic power corrections** $(\sqrt{-t}/Q)^k$, $(m/Q)^k$
   - Twist-four accuracy, $(\sqrt{-t}/Q)^2$, $(m/Q)^2$

     — complete results available, numerical code (B.Pirnay)
     — large effects for parts of phase space and in collider kinematics
     — Coherent DVCS from nuclei: Target mass corrections do not spoil factorization
   - Higher powers (work in progress)

     — all-order results on OPE level
     — cancellation of IR divergences checked up to twist-6
     — scalar target completed, nucleon in progress

Evolution equations

V. Bertone

- Defining the **anti-quark** distributions as:

$$F_{\bar{q}/H}^{[U,T]}(x,\xi,\Delta^2;\mu) = -F_{q/H}^{[U,T]}(-x,\xi,\Delta^2;\mu)$$

$$F_{\bar{q}/H}^{[L]}(x,\xi,\Delta^2;\mu) = +F_{q/H}^{[L]}(-x,\xi,\Delta^2;\mu)$$

- one can construct **non-singlet** and **singlet** combinations:

$$F^{[\Gamma],-} = F_{q/H}^{[\Gamma]} - F_{\bar{q}/H}^{[\Gamma]} \qquad F^{[\Gamma],+} = \begin{pmatrix} \sum_{q=1}^{n_f} F_{q/H}^{[\Gamma]} + F_{\bar{q}/H}^{[\Gamma]} \\ F_{g/H}^{[\Gamma]} \end{pmatrix}$$

- The evolution equations **decouple** and can be written in a **DGLAP-like** fashion:

$$\frac{dF^{[\Gamma],\pm}(x,\xi,\mu)}{d\ln\mu^2} = \frac{\alpha_s(\mu)}{4\pi}\int_x^\infty \frac{dy}{y}\mathcal{P}^{[\Gamma]\pm,[0]}\left(y,\frac{\xi}{x}\right)F^{[\Gamma],\pm}\left(\frac{x}{y},\xi,\mu\right)$$

$$\mathcal{P}^{[\Gamma]\pm,[0]}\left(y,\frac{\xi}{x}\right) = \theta(1-y)\mathcal{P}_1^{[\Gamma]\pm,[0]}\left(y,\frac{\xi}{x}\right) + \theta(\xi-x)\mathcal{P}_2^{[\Gamma]\pm,[0]}\left(y,\frac{\xi}{x}\right)$$

DGLAP region ERBL contribution

- $\mathscr{P}_{1,2}^{[\Gamma]\pm,[0]}$ are appropriate combinations of the functions $p_{i/j}^{\Gamma}$ presented before.

V. Bertone

Evolution and DGLAP limit [U]

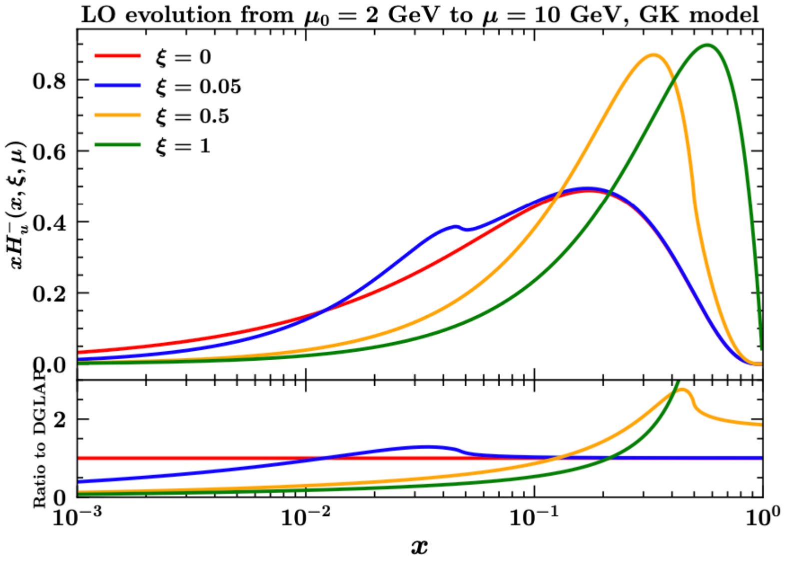

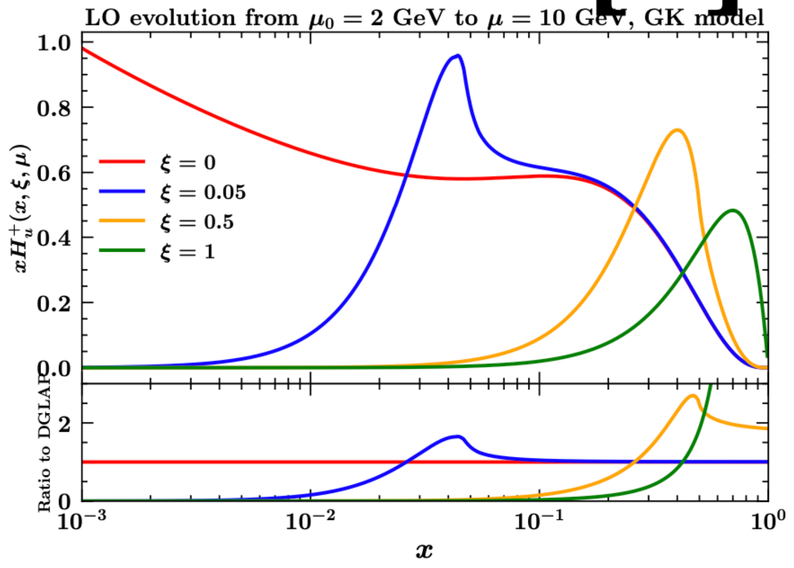

so far, LO

- **DGLAP limit** reproduced within 10^{-5} relative accuracy.
- GPD evolution may significantly deviate from DGLAP evolution.
- The evolution generates a cusp at $x = \xi$ but the distribution remains **continuous** at this point.

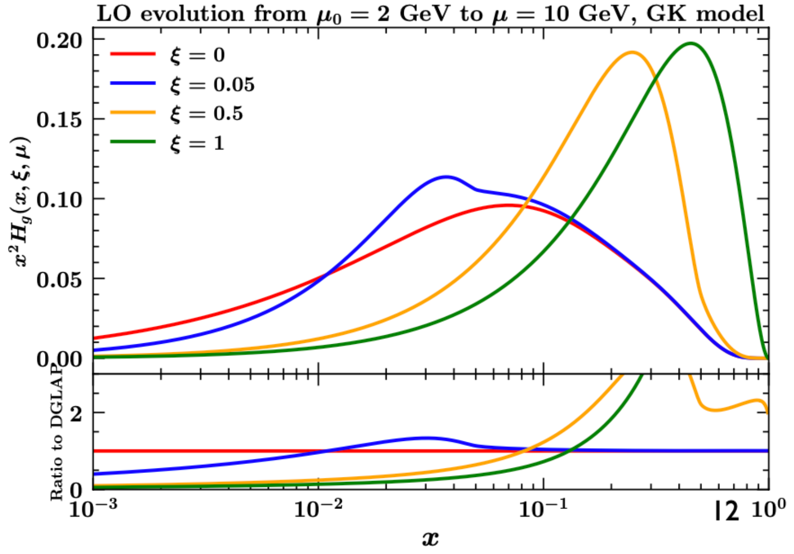

Polynomiality [U]

$$\int_0^1 dx\, x^{2n} F_q^{[\Gamma]-}(x,\xi,\mu) = \sum_{k=0}^{n} A_k^{[\Gamma]}(\mu)\xi^{2k}$$

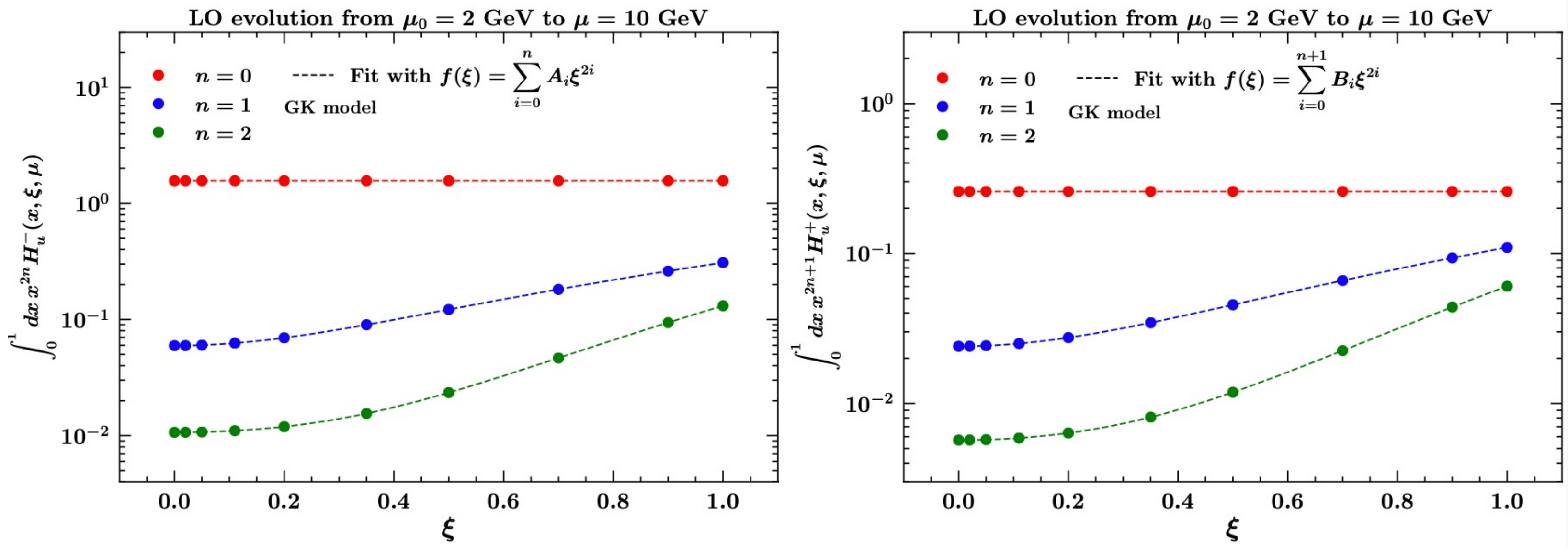

- **First moment** for both singlet and non-singlet is indeed **constant** in ξ:
  - this was expected and the expectation is very nicely fulfilled.
- **Second and third moments** follow the expected law:
  - including odd-power terms in the fit gives coefficients very close to zero.
  - B_{n+1} in the singlet is consistently found to be compatible with zero (no D-term).

V. Bertone

First-time measurement of nDVCS with detection of the active neutron

A. Hobart

CLAS12: nDVCS with an unpolarized deuterium target

Under internal review

- Observation of positive BSA for nDVCS
- Systematic errors include:
  - Error due to beam polarization
  - Error due to selection cuts
  - Error due to residual proton contamination
  - Error due to merging of data sets with different energies
- Statistics is expected to double with remaining schedualed beam time and improvements with reconstruction software

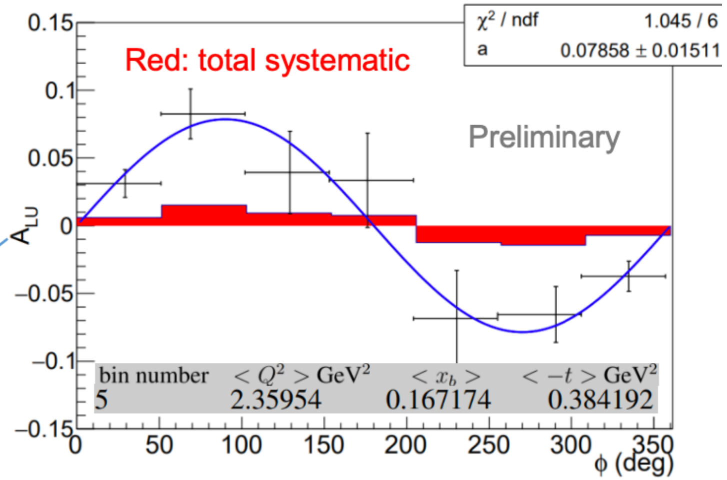

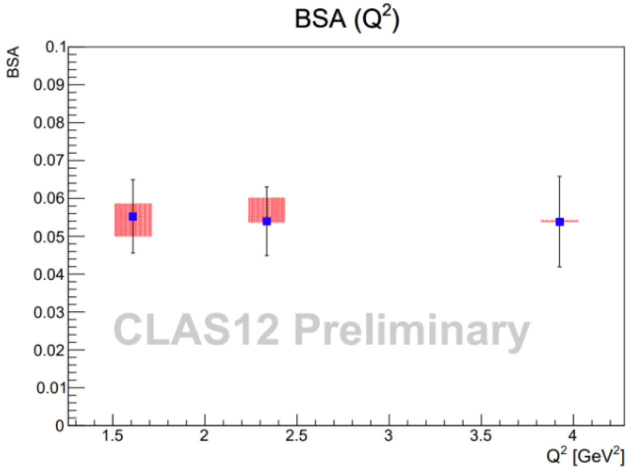

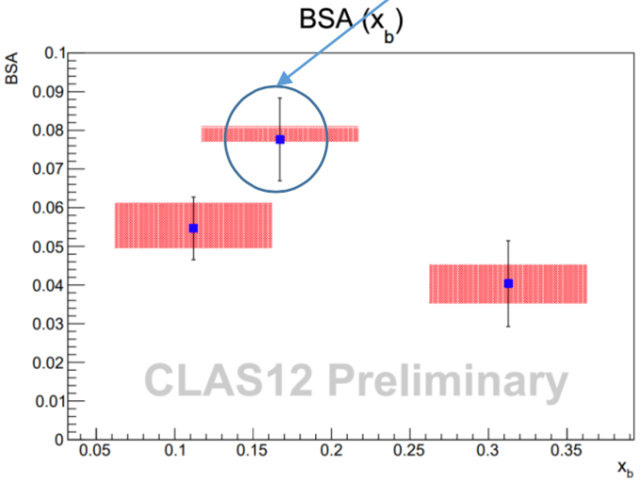

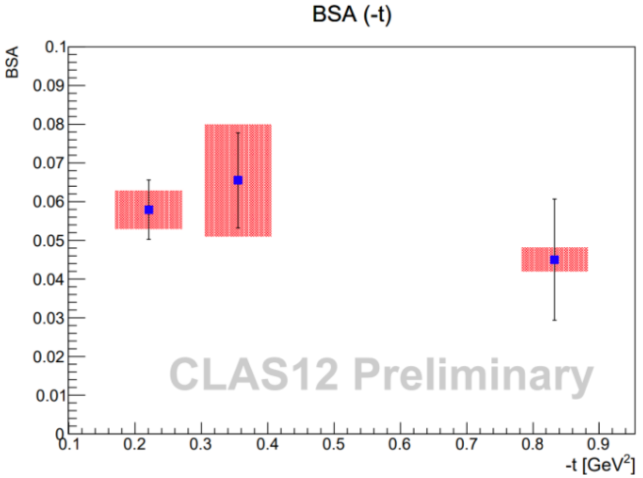

A. Hobart

- The exclusivity of the event is insured by:
  - Electron detection: Cerenkov detector, drift chambers and electromagnetic calorimeter
  - Photon detection: sampling calorimeter or a small PbWO4-calorimeter close to the beamline
  - Proton detection: Silicon and Micromegas detector OR Neutron detection: Central Neutron Detector
- For Neutron Detection:
  - Machine Learning techniques are applied to improve the Identification and reduce charged particle contamination

π^0 background subtraction

Under internal review

- Subtraction using simulations of the background channel
  - Monte Carlo simulations:
    - GPD-based event generator for DVCS/pi0 on deuterium
    - DVCS amplitude calculated according to the BKM formalism
    - Fermi-motion distribution evaluated according to Paris potential

1. Estimate the ratio of partially reconstructed eN π^0(1 photon) decay to fully reconstructed eN π^0 decays in MC
2. This is done for each kinematic bin to minimize MC model dependence
3. Multiply this ratio by the number of reconstructed eN π^0 in data to get the number of eN π^0(1 photon) in data
4. Subtract this number from DVCS reconstructed decays in data per each kinematical bin

$$\text{Simulations: R} = \frac{N(eN\pi^0_{1\gamma})}{N(eN\pi^0)}$$

$$\text{Data: } N(eN\pi^0_{1\gamma}) = R * N(eN\pi^0)$$

$$N(DVCS) = N(DVCS_{recon}) - N(eN\pi^0_{1\gamma})$$

- π^0 background subtraction is also performed by statistical unfolding of contribution to the missing mass spectrum

M. Pivk and F.R. Le Diberder, NIMA 555 1 2005

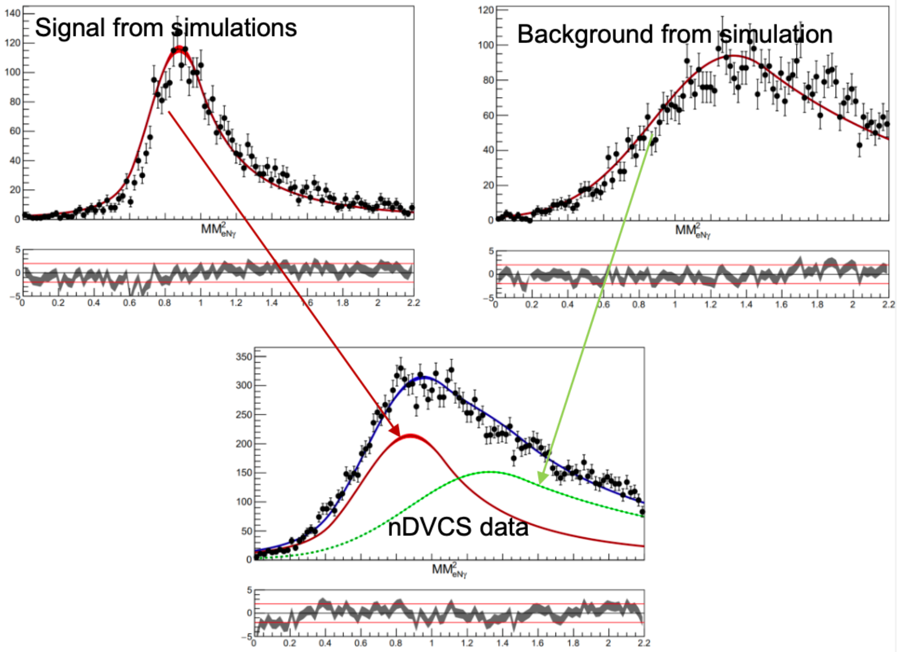

The difference between the estimations of background from both methods is considered as a systematic

CLAS12: pDVCS with an unpolarized deuterium target

Under internal review

- Systematic errors include:
  - Error due to beam polarization
  - Error due to selection cuts
  - Error due to merging of data sets with different energies
- Statistics is expected to triple with remaining schedualed beam time and improvements with reconstruction software

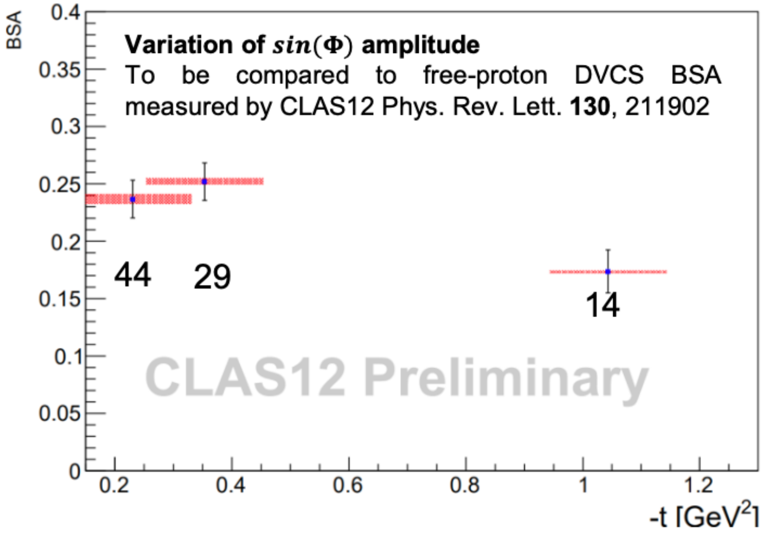

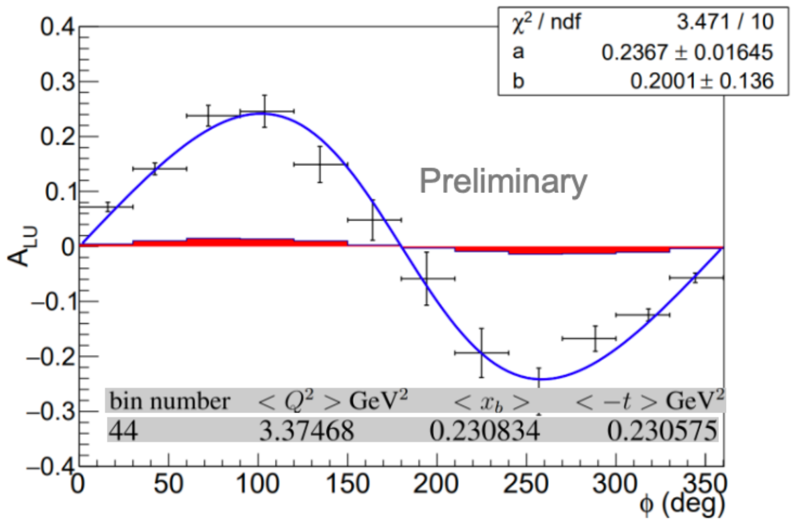

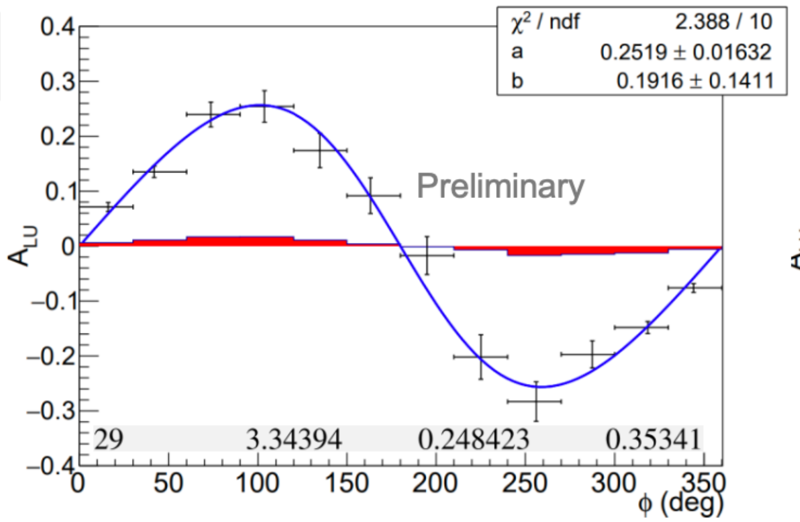

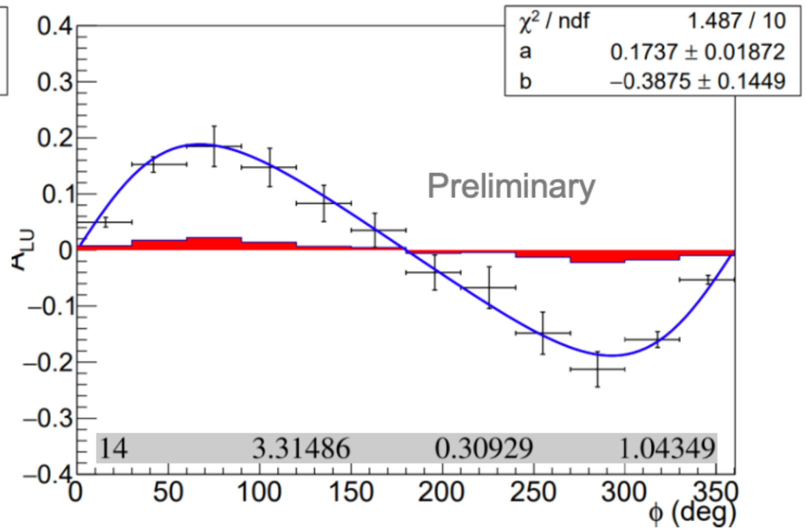

- Train new models with old JLab and new CLAS12 data
  - 40 NN trained on old data and another 40 NN trained on old JLAB pDVCS + new CLAS12 nDVCS data
  - separate models for u and d flavors of CFFs Im H and Im E
  - flavor agnostic (flavor summed) models for CFFs Re H and Im $\widetilde{H}$

Flavor separation of ImH is better than before

Less evident Flavor separation of Im E

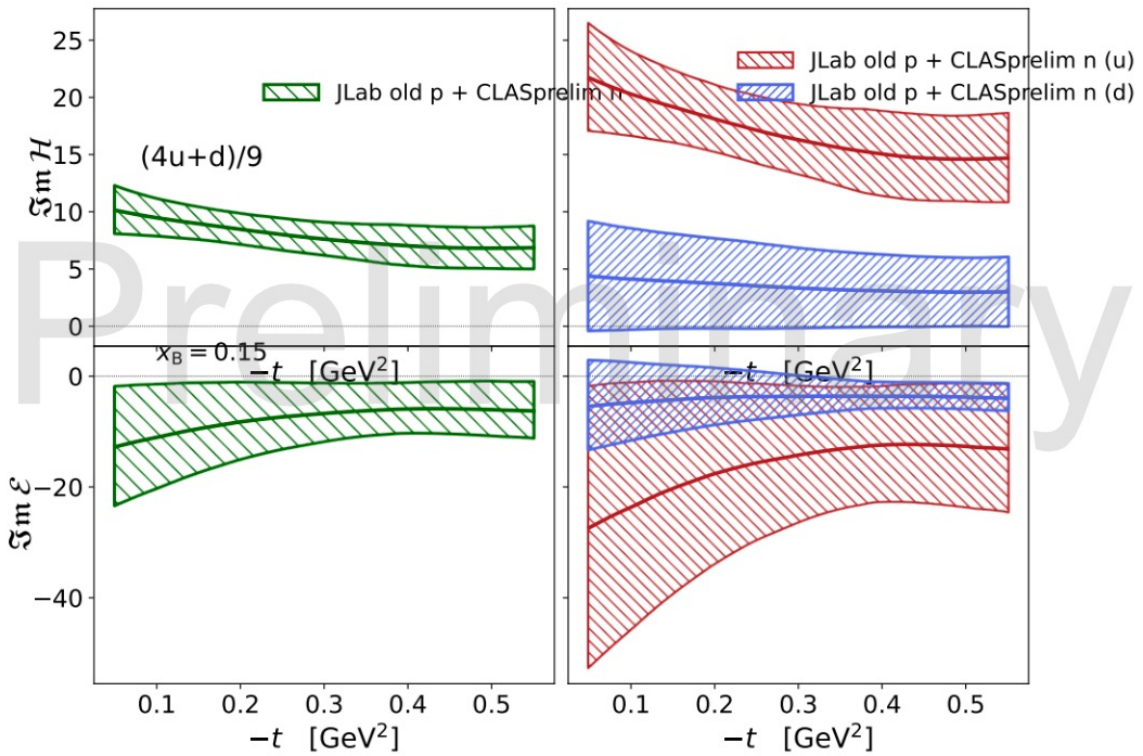

S. Bhattacharya

Imprint of Anomalies in QCD Compton scattering

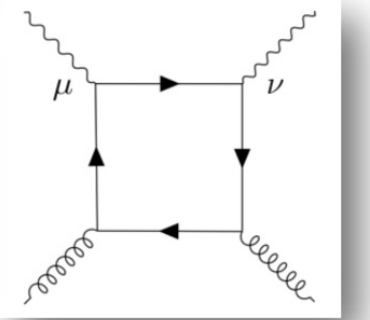

Antisymmetric part of Compton amplitude

Collinear singularity regularized by l^2

$$-\epsilon^{\alpha\beta\mu\nu}P_\beta \times T^{\text{asym}}_{\mu\nu} \approx \frac{1}{2}\frac{\alpha_s}{2\pi}\left(\sum_f e_f^2\right)\bar{u}(P_2)\left[\left(\tilde{\kappa}_{qg}\ln\frac{Q^2}{-l^2}+\delta\tilde{C}_g^{\text{off}}\right)\otimes\langle F^{+\mu}\tilde{F}^{+}_{\mu}\rangle\gamma^\alpha\gamma_5+\frac{l^\alpha}{l^2}\tilde{A}_g^{\text{anom}}\otimes\tilde{\mathcal{F}}(x_B)\gamma_5\right]u(P_1)$$

$l^2 \neq 0$

$$\tilde{\mathcal{F}}(x,l^2)=\frac{iP^+}{\bar{u}(P_2)\gamma_5 u(P_1)}\int\frac{dz^-}{2\pi}e^{ixP^+z^-}\langle P_2|F_a^{\mu\nu}(-z^-/2)\tilde{F}^a_{\mu\nu}(z^-/2)|P_1\rangle$$

Twist-4 GPD

But no suppression in $1/Q^2$!

The QCD factorization theorem: Collins, Freund; Ji, Osborne (1998)

$$-\epsilon^{\alpha\beta\mu\nu}P_\beta \times T^{\text{asym}}_{\mu\nu} = \frac{1}{2}\sum_f e_f^2\bar{u}(P_2)\left[\gamma^\alpha\gamma_5(\tilde{H}_f(x_B,\xi,l^2)+\tilde{H}_f(-x_B,\xi,l^2))+\frac{l^\alpha\gamma_5}{2M}(\tilde{E}_f^{\text{bare}}(x_B,\xi,l^2)+\tilde{E}_f^{\text{bare}}(-x_B,\xi,l^2))\right]u(P_1)$$
$$+\mathcal{O}(\alpha_s)+\mathcal{O}(1/Q^2)\,,$$

S. Bhattacharya

$$\tilde{E}_f(x_B, l^2) + \tilde{E}_f(-x_B, l^2) = \tilde{E}_f^{\text{bare}}(x_B, l^2) + \tilde{E}_f^{\text{bare}}(-x_B, l^2) + \frac{\alpha_s}{2\pi}\frac{2M}{l^2}\,\tilde{A}_g^{\text{anom}} \otimes \tilde{\mathcal{F}}(x_B, l^2)$$

"Bare GPD" (tree level)

Perturbative pole (one loop)

Postulate that the "renormalized" GPD integrates to $g_P(l^2)$:

$$g_P(l^2) = \sum_f \int_{-1}^{1} dx \tilde{E}_f(x, \xi, l^2) = \sum_f \int_0^1 dx(\tilde{E}_f(x, \xi, l^2) + \tilde{E}_f(-x, \xi, l^2))$$

obtain

$$\frac{g_P(\ell^2)}{2M} = -\frac{i}{\ell^2}\left(\frac{\langle P_2|\frac{n_f\alpha_s}{4\pi}F\tilde{F}|P_1\rangle}{\bar{u}(P_2)\gamma_5 u(P_1)}\bigg|_{\ell^2=0} - \frac{\langle P_2|\frac{n_f\alpha_s}{4\pi}F\tilde{F}|P_1\rangle}{\bar{u}(P_2)\gamma_5 u(P_1)}\right)$$

finite
at $\ell^2 = 0$

similarly, symmetric part / trace anomaly

S. Bhattacharya

Quark-channel diagrams in DVCS

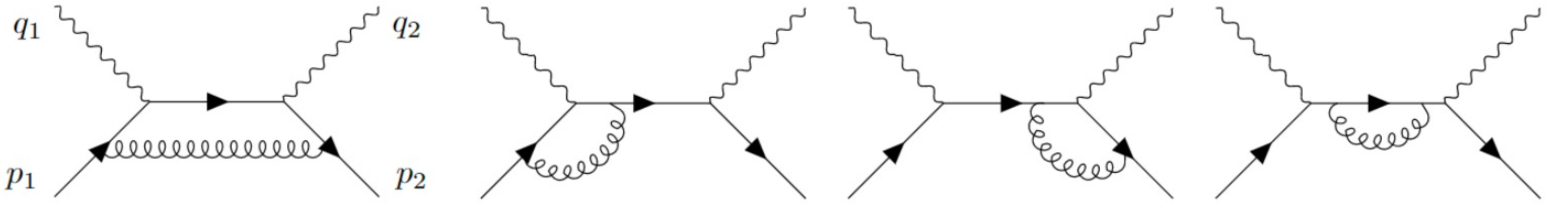

Example: Antisymmetric case

$$\sim \frac{1}{l^2} + \tilde{\kappa}_{qq}(\hat{x},\hat{\xi}) \ln \frac{Q^2}{-l^2} + \delta \tilde{C}_1^q(\hat{x},\hat{\xi})$$

Coefficient function

$$\delta \tilde{C}_1^q(\hat{x},\hat{\xi}) = -\frac{\left(\frac{Q^2}{-l^2}\right)^{\epsilon_{IR}}}{\epsilon_{IR}^2(1-\hat{x})} - \frac{3\left(\frac{Q^2}{-l^2}\right)^{\epsilon_{IR}}}{2\epsilon_{IR}(1-\hat{x})} + \frac{-1+2\hat{x}-4\hat{x}^2+3\hat{\xi}^2}{2(1-\hat{x})(1-\hat{\xi}^2)} \ln \frac{\hat{x}-1}{\hat{x}} + \frac{(\hat{x}-\hat{\xi})(1+2\hat{x}^2+3\hat{x}\hat{\xi})}{(1-\hat{x}^2)(1-\hat{\xi}^2)} \ln \frac{\hat{x}-\hat{\xi}}{\hat{x}}$$

Unexpected double IR pole

Unexpected single IR pole

$$\ldots \ln \frac{\hat{x}-\hat{\xi}}{\hat{x}} \ln \frac{\hat{x}+\hat{\xi}}{\hat{x}} + \frac{\pi^2-54}{12(1-\hat{x})}$$

Sudakov logs! $\ln\left(\frac{Q^2}{-l^2}\right), \ln^2\left(\frac{Q^2}{-l^2}\right)$

establishes factorization at one loop in regime $\Lambda_{\mathrm{QCD}}^2 \ll -t \ll Q^2$

M. Constantinou

★ Twist-3: poorly known, but very important:
- as sizable as twist-2
- contain information about quark-gluon correlations inside hadrons
- appear in QCD factorization theorems for various observables (e.g. g_2)
- certain twist-3 PDFs are related to the TMDs
- physical interpretation (e.g. average force on partons inside hadron)

While twist-3 $f_i^{(1)}$ share some similarities with twist-2 $f_i^{(0)}$ in their extraction, there are several challenges both experimentally and theoretically

Theoretical setup

★ Correlation functions in coordinate space

$$F^{[\Gamma]}(x,\Delta;P^3) = \frac{1}{2}\int \frac{dz^3}{2\pi} e^{ik\cdot z} \langle p_f,\lambda'|\bar\psi(-\tfrac{z}{2})\,\Gamma\,\mathcal{W}(-\tfrac{z}{2},\tfrac{z}{2})\psi(\tfrac{z}{2})|p_i,\lambda\rangle\Big|_{z^0=0,\vec{z}_\perp=\vec{0}_\perp}$$

★ Parametrization of coordinate-space correlation functions

[D. Kiptily and M. Polyakov, Eur. Phys. J. C37 (2004) 105] [F. Aslan et a., Phys. Rev. D 98, 014038 (2018)]

$$\begin{aligned}F^{[\gamma^\mu\gamma_5]}(x,\Delta;P^3) = \frac{1}{2P^3}\bar u(p_f,\lambda')\Big[&P^\mu\frac{\gamma^3\gamma_5}{P^0}F_{\widetilde H}(x,\xi,t;P^3) + P^\mu\frac{\Delta^3\gamma_5}{2mP^0}F_{\widetilde E}(x,\xi,t;P^3)\\ &+\Delta_\perp^\mu\frac{\gamma_5}{2m}F_{\widetilde E+\widetilde G_1}(x,\xi,t;P^3) + \gamma_\perp^\mu\gamma_5 F_{\widetilde H+\widetilde G_2}(x,\xi,t;P^3)\\ &+\Delta_\perp^\mu\frac{\gamma^3\gamma_5}{P^3}F_{\widetilde G_3}(x,\xi,t;P^3) + i\varepsilon_\perp^{\mu\nu}\Delta_\nu\frac{\gamma^3}{P^3}F_{\widetilde G_4}(x,\xi,t;P^3)\Big]u(p_i,\lambda)\end{aligned}$$

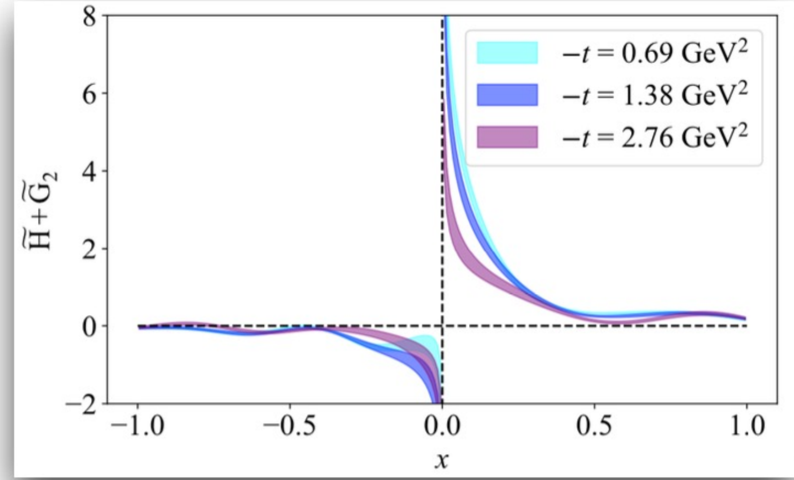

Isolating $\widetilde{G}_2$ using $\widetilde{H}$

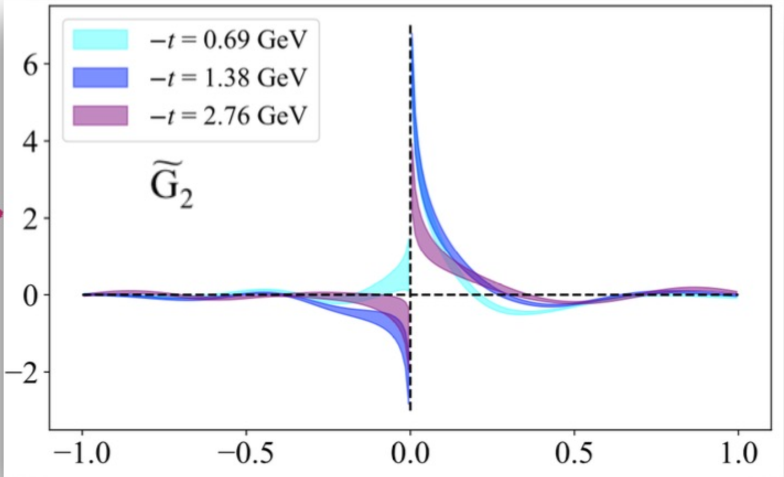

★ Direct access to $\widetilde{E}$-GPD not possible for zero skewness

$$P^\mu \frac{\Delta^3 \gamma_5}{2mP^0} F_{\widetilde{E}}(x,\xi,t;P^3)$$

★ Glimpse into $\widetilde{E}$-GPD through twist-3 :

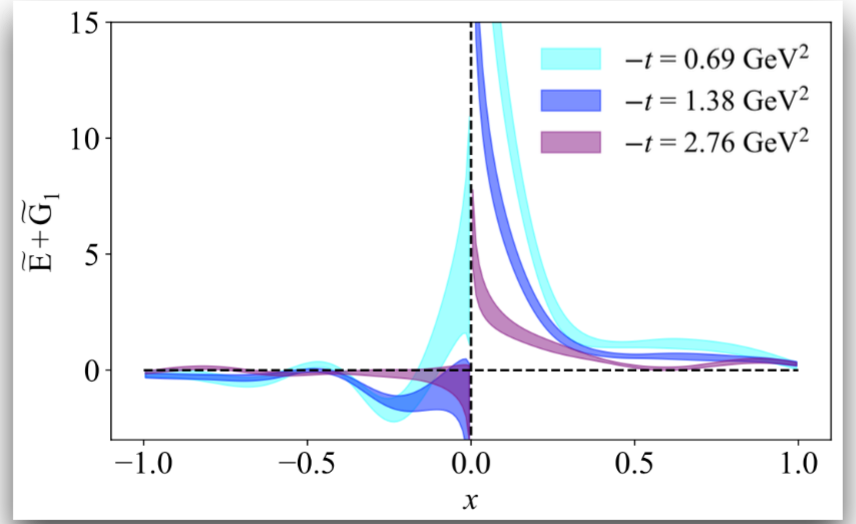

★ LaMET formalism is applicable beyond leading twist. However, several improvements needed, e.g., mixing with quark-gluon-quark correlator

M. Constantinou

★ **New proposal for Lorentz invariant decomposition has great advantages:**

- significant reduction of computational cost
- access to a broad range of t and ξ

M. Constantinou

$$F^{\mu}_{\lambda,\lambda'} = \bar{u}(p',\lambda')\left[\frac{P^\mu}{M}A_1 + z^\mu MA_2 + \frac{\Delta^\mu}{M}A_3 + i\sigma^{\mu z}MA_4 + \frac{i\sigma^{\mu\Delta}}{M}A_5 + \frac{P^\mu i\sigma^{z\Delta}}{M}A_6 + \frac{z^\mu i\sigma^{z\Delta}}{M}A_7 + \frac{\Delta^\mu i\sigma^{z\Delta}}{M}A_8\right]u(p,\lambda)$$

- symmetric frame: $\vec{p}^{\,s}_f = \vec{P} + \frac{\vec{Q}}{2}, \quad \vec{p}^{\,s}_i = \vec{P} - \frac{\vec{Q}}{2} \qquad -t^s = \vec{Q}^2 = 0.69\, GeV^2$

- asymmetric frame: $\vec{p}^{\,a}_f = \vec{P}, \qquad \vec{p}^{\,a}_i = \vec{P} - \vec{Q} \qquad t^a = -\vec{Q}^2 + (E_f - E_i)^2 = 0.65\, GeV^2$

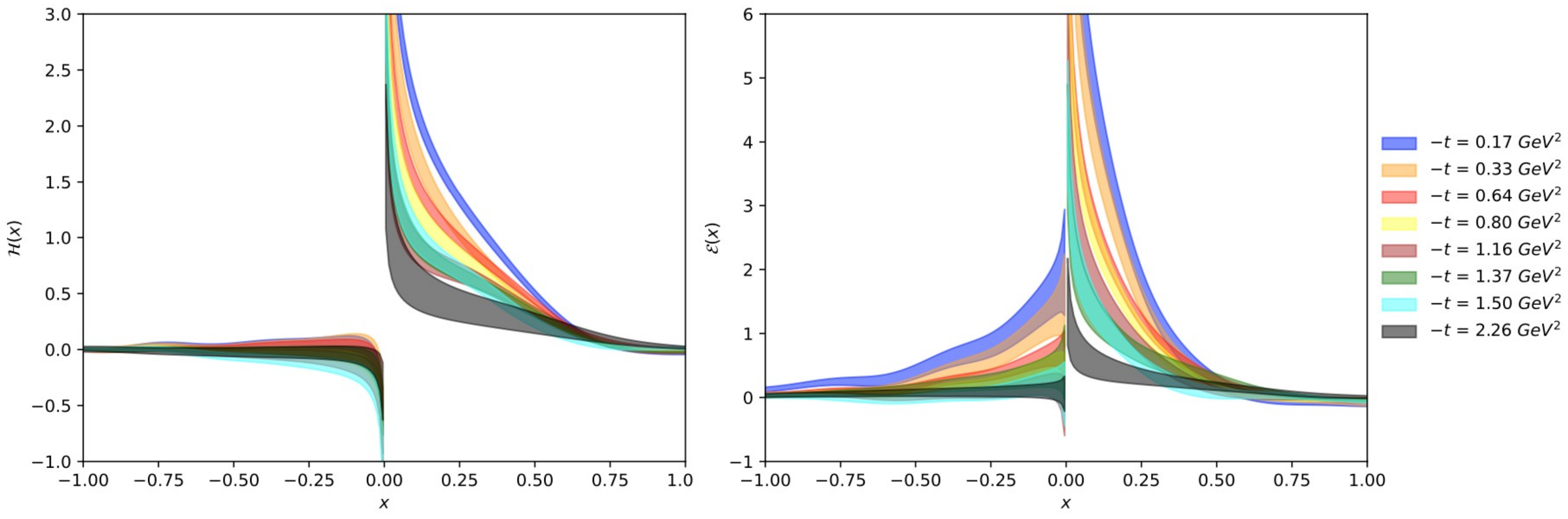

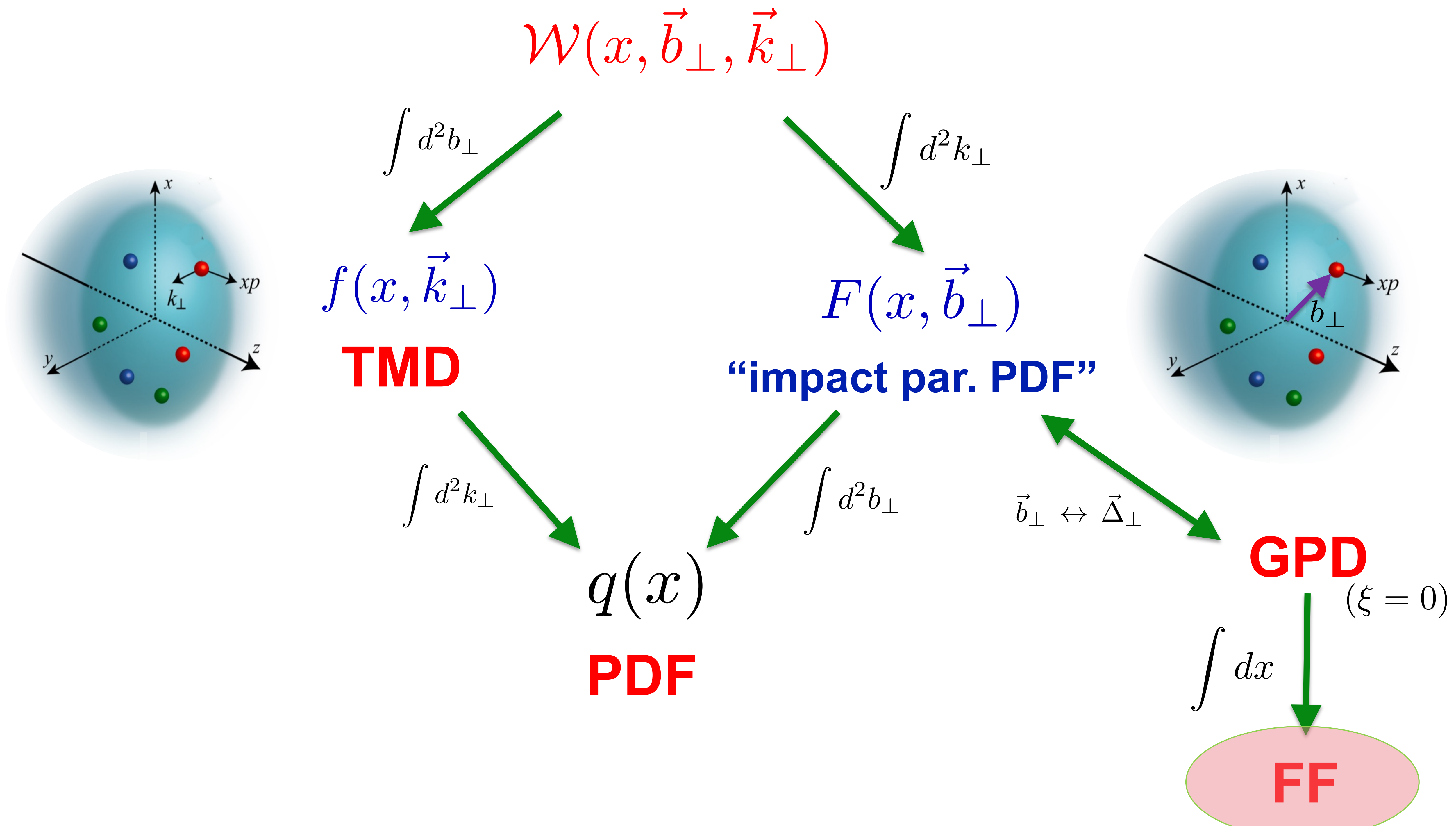

$\mathcal{W}(x, \vec{b}_\perp, \vec{k}_\perp)$
$\int d^2 b_\perp$
$\int d^2 k_\perp$
$f(x, \vec{k}_\perp)$
TMD
$F(x, \vec{b}_\perp)$
“impact par. PDF”
$\int d^2 k_\perp$
$\int d^2 b_\perp$
$\vec{b}_\perp \leftrightarrow \vec{\Delta}_\perp$
$q(x)$
PDF
GPD
$(\xi = 0)$
$\int dx$
FF
x
xp
$k_\perp$
y
z
x
xp
$b_\perp$
y
z

S. Bacchio

Nucleon axial and pseudoscalar form factors from Lattice QCD simulations at the physical point

Dr. Simone Bacchio

Computational Scientist
CaSToRC, The Cyprus Institute
National Competence Center in HPC

31/10/23 - EINN

Extended Twisted Mass Collaboration

- Three physical point ensemble
- Thorough excited state analysis
- Combined fit of Q^2-dependence and continuum limit

$$\langle N(p', s')|A_\mu|N(p, s)\rangle = \bar{u}_N(p', s') \left[\gamma_\mu G_A(Q^2) - \frac{Q_\mu}{2m_N} G_P(Q^2)\right] \gamma_5 u_N(p, s)$$

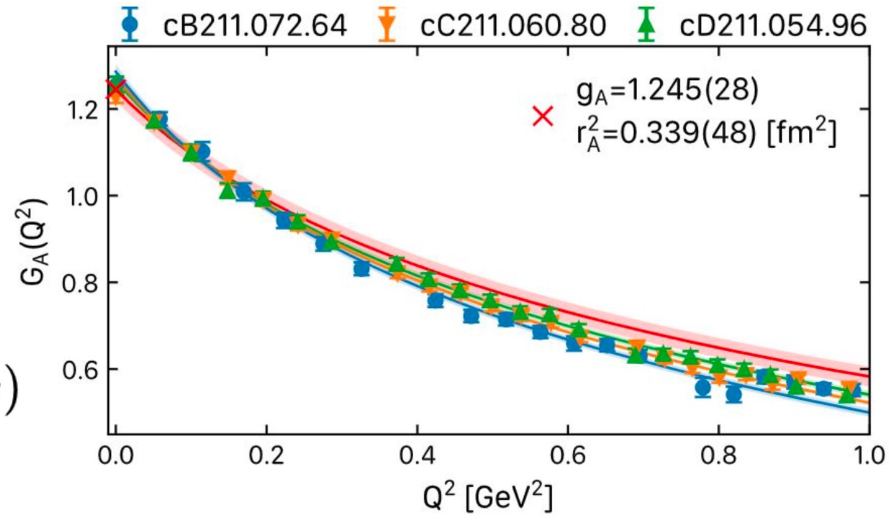

Conclusions

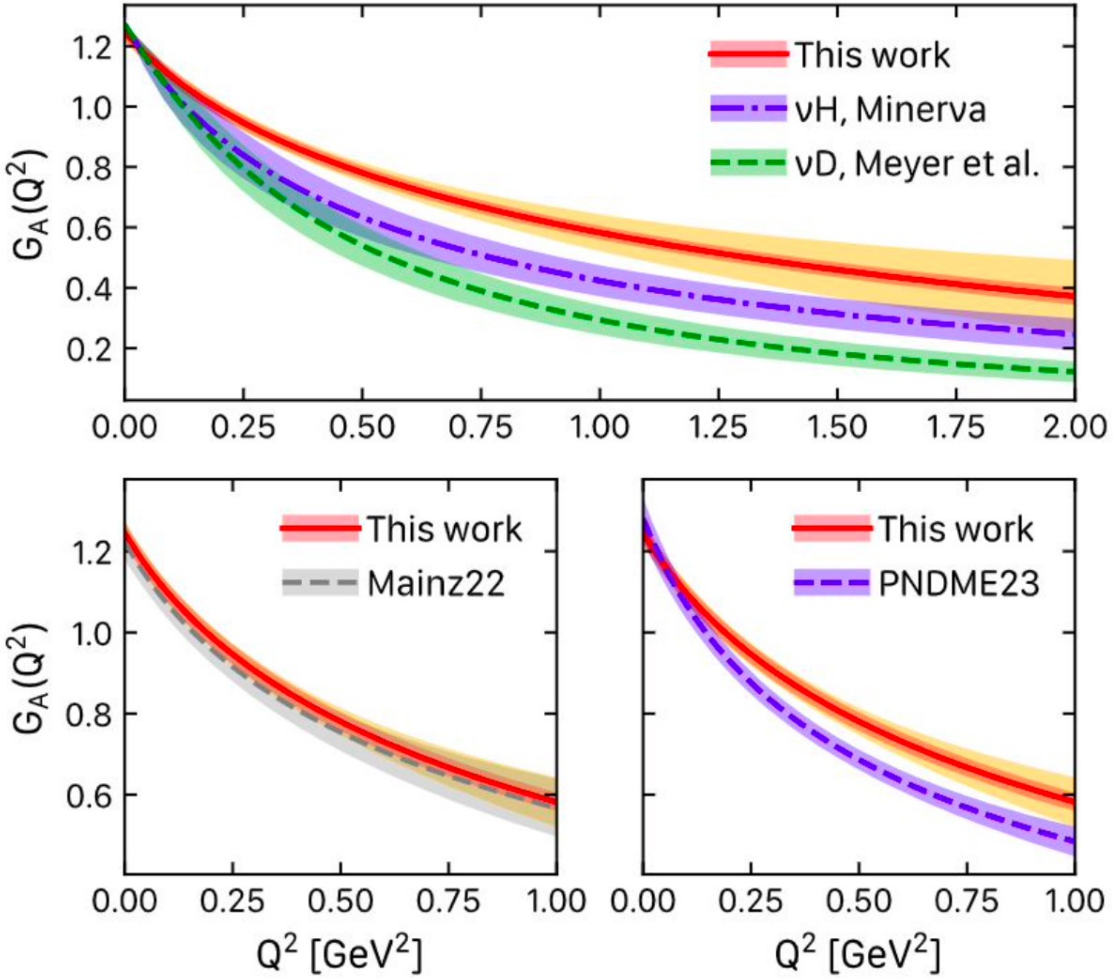

- Overall good agreement between recent lattice results and better agreement with the very recent results from Minerva

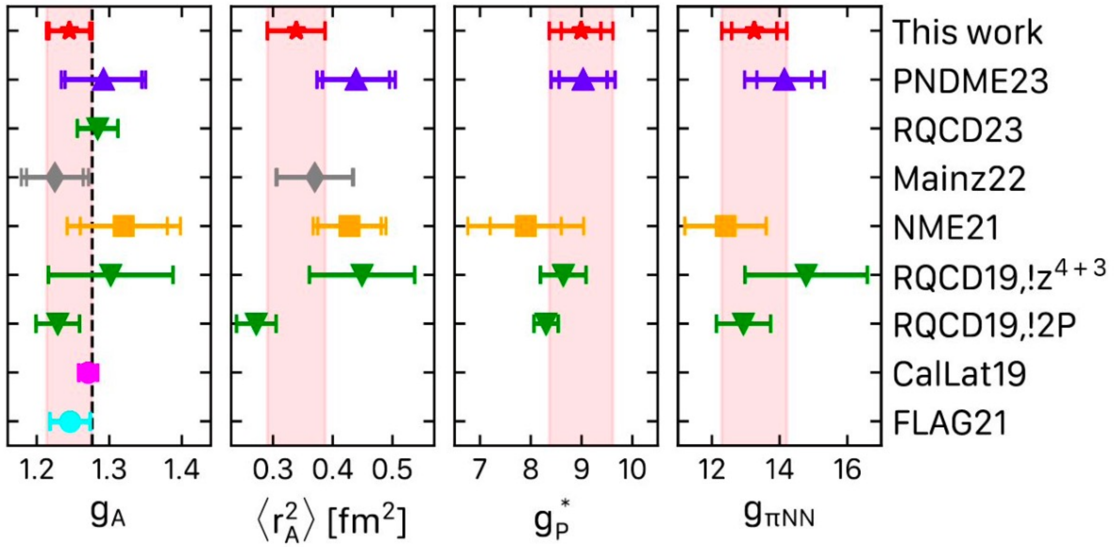

Interaction mechanisms

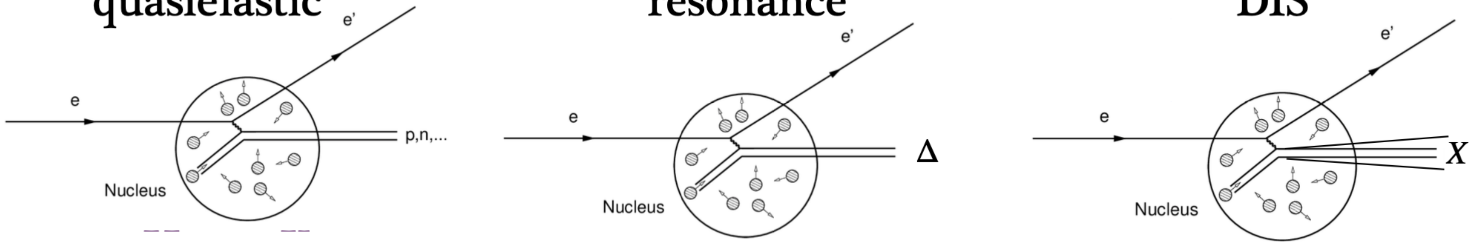

O. Tomalak

CCQE scattering on free nucleon

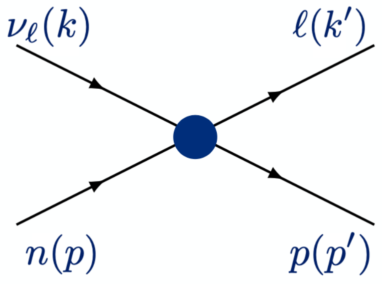

$$\nu = E_\nu/M - \tau - r^2$$

$$r = \frac{m_\ell}{2M} \qquad \tau = \frac{Q^2}{4M^2}$$

unpolarized cross section

$$\frac{d\sigma}{dQ^2} \sim \frac{M^2}{E_\nu^2}\left(\left(\tau + r^2\right) A(Q^2) - \nu B(Q^2) + \frac{\nu^2}{1+\tau} C(Q^2)\right)$$

Llewellyn Smith (1972)

- structure-dependent functions

$$A = \tau \left(G_M^V\right)^2 - \left(G_E^V\right)^2 + (1+\tau) F_A^2 - r^2\left(\left(G_M^V\right)^2 + F_A^2 - 4\tau F_P^2 + 4F_A F_P\right)$$

$$B = \pm 4\tau F_A G_M^V \qquad C = \tau \left(G_M^V\right)^2 + \left(G_E^V\right)^2 + (1+\tau) F_A^2$$

- pseudoscalar form factor contribution is suppressed by lepton mass
- cross section is sensitive to both vector and axial contributions

Lattice QCD vs MINERvA

O. Tomalak

- PNDME 2023 axial-vector form factor as representative of lattice QCD

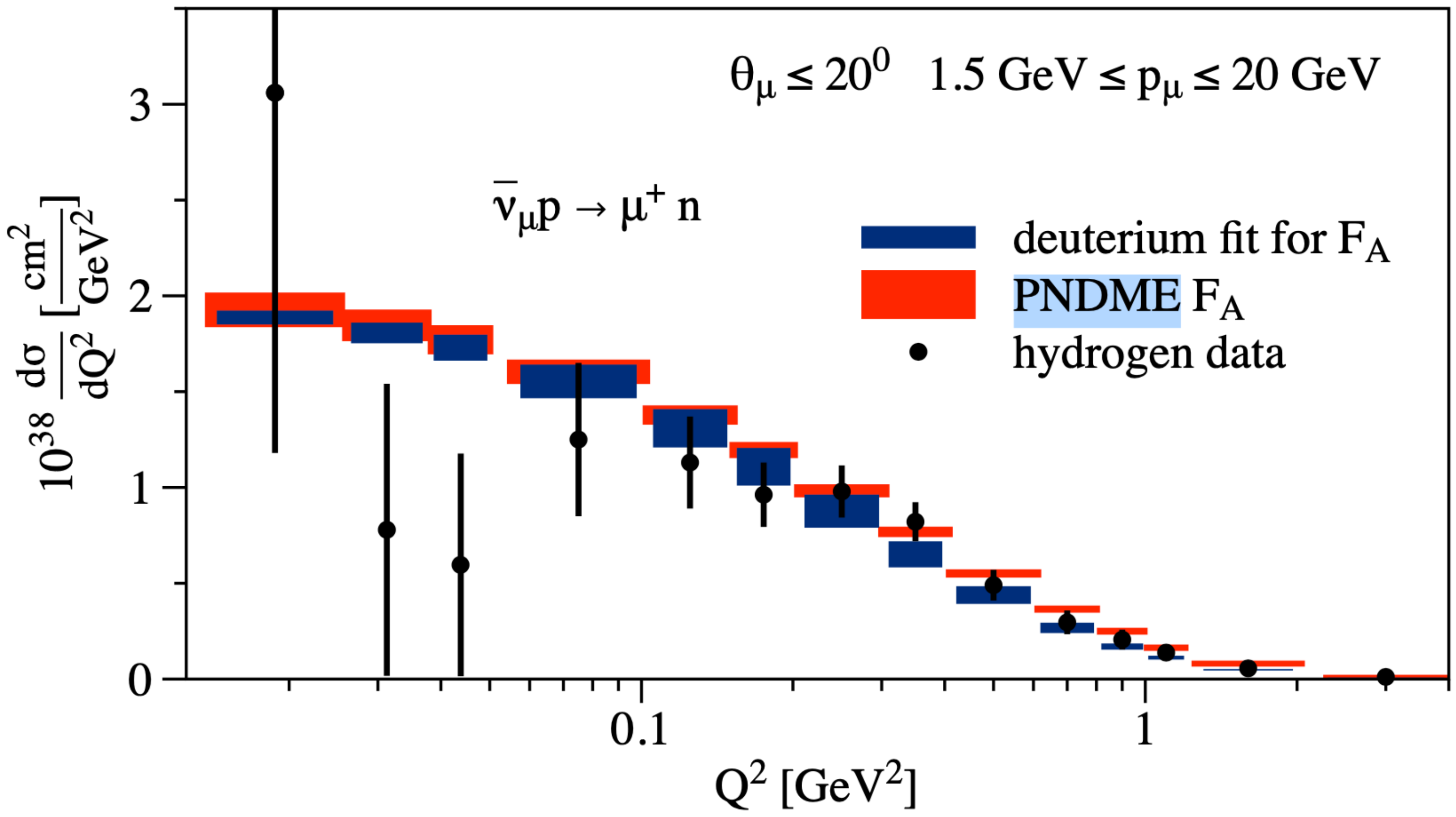

- $\lesssim 1\sigma$ agreement for each bin besides two at small Q^2

- 2-3σ tension between lattice QCD and deuterium data
- MINERvA hydrogen data consistent with LQCD and deuterium

O. T., Rajan Gupta, and Tanmoy Bhattacharya, Phys.Rev.D 108 (2023) 7, 074514

Ensembles

G. Koutsou

Landscape of ensembles used for nucleon structure

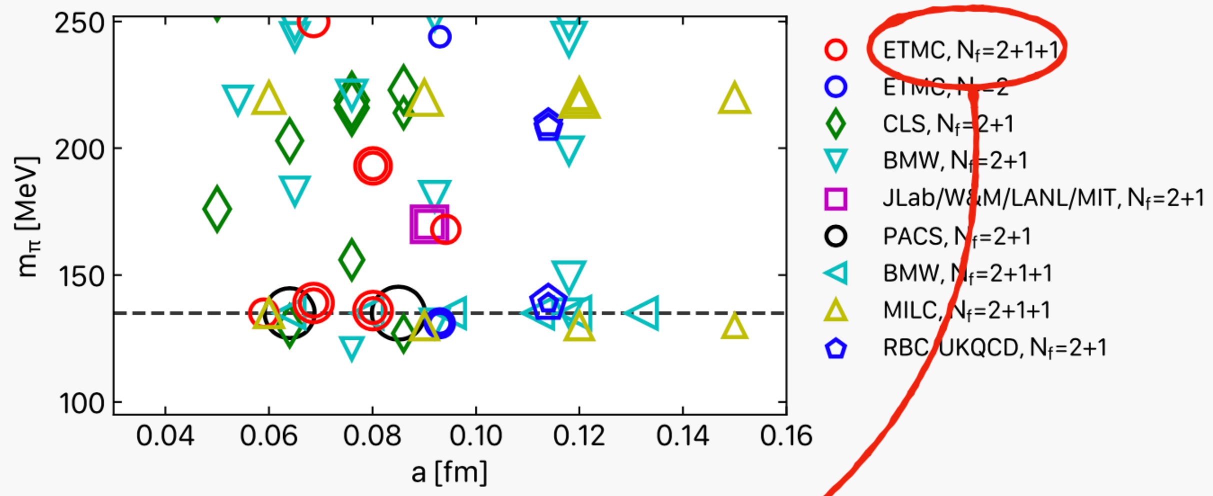

ETMC: three $N_f=2+1+1$ ensembles at physical pion mass

Ens. ID (abbrv.)	Vol.	a [fm]
cB211.072.64 (cB64)	64×128	0.080
cC211.060.80 (cC80)	80×160	0.068
cD211.054.96 (cD96)	96×192	0.057

- Three lattice spacings at physical point
- Ongoing generation of finer ensembles and larger volumes
- ***This talk:*** 3 ensembles with: $a = 0.057 - 0.068$ fm

Nucleon axial charge

G. Koutsou

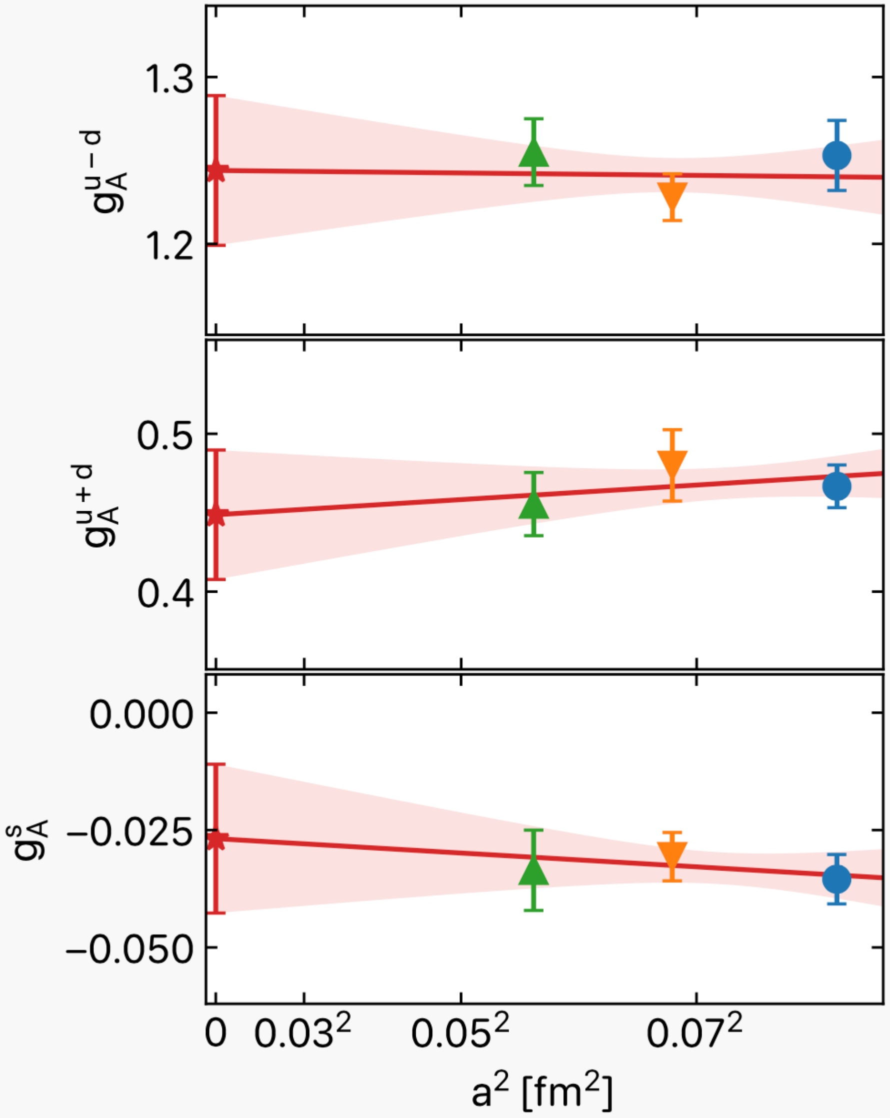

See arXiv:2309.05774 [hep-lat]; Includes isovector axial form-factors

- Errors for each ensemble include *statistical* and *systematic* due to excited state contamination
- Model averaged based on AIC (see e.g. arXiv:2208.14983)

Preliminary!

Complete analysis for flavour separated charges ongoing

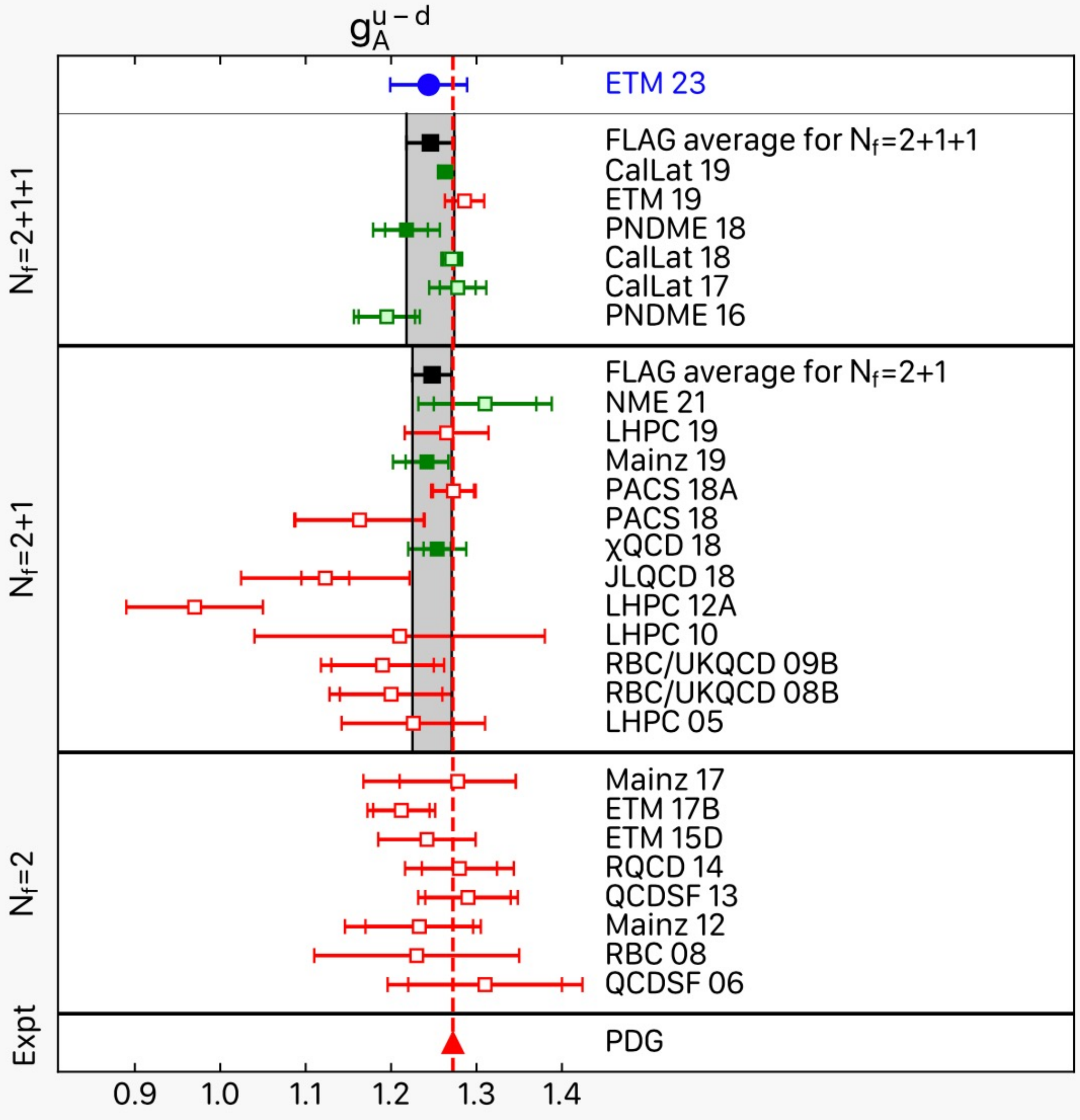

G. Koutsou

Latest FLAG21 values

- ETM23 consistent with FLAG average
- Only result with three physical point ensembles
- Agreement for g_A means confidence for more challenging quantities
- E.g.

tensor charge

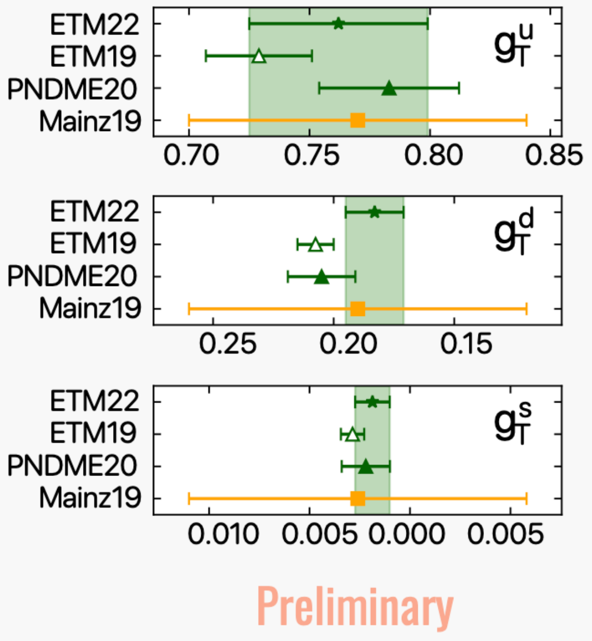

Investigation of two-particle contributions to nucleon matrix elements

Yan Li

- Nucleon structure: nucleon matrix elements

$$\frac{\langle 0|O_N(t_{\rm sink})J(t_{\rm ins})\bar{O}_N(0)|0\rangle}{\langle 0|O_N(t_{\rm sink})\bar{O}_N(0)|0\rangle} \xrightarrow{\text{all } t \text{ well-separated}} \langle N|J|N\rangle$$

- Time-dependence indicates contamination from excited states

$\mathcal{J} = S^{u+d} = \bar{u}u + \bar{d}d, \quad \vec{q} = (0,0,0)$

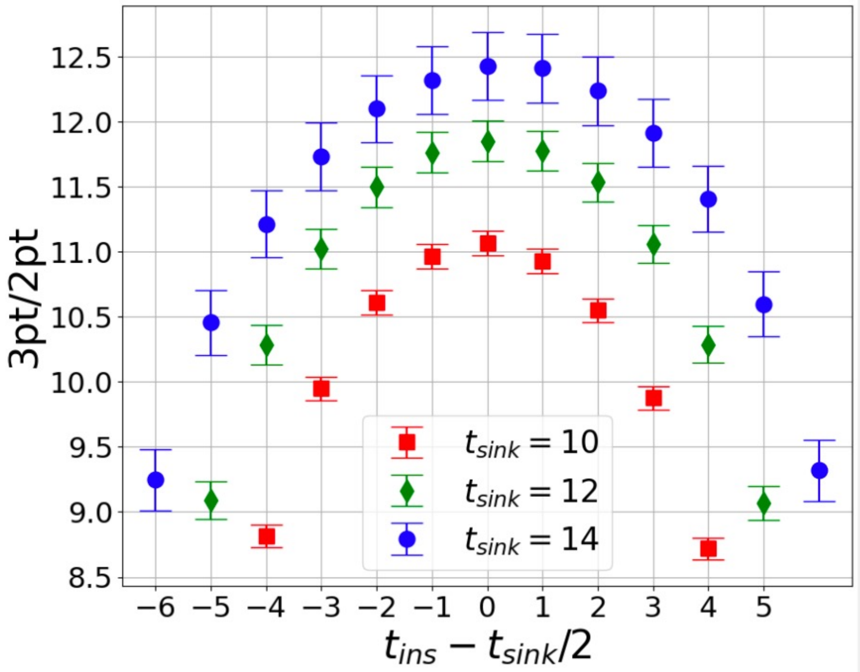

- Lowest excited state is a Nucleon-Pion state

Diagrams: 2pt functions

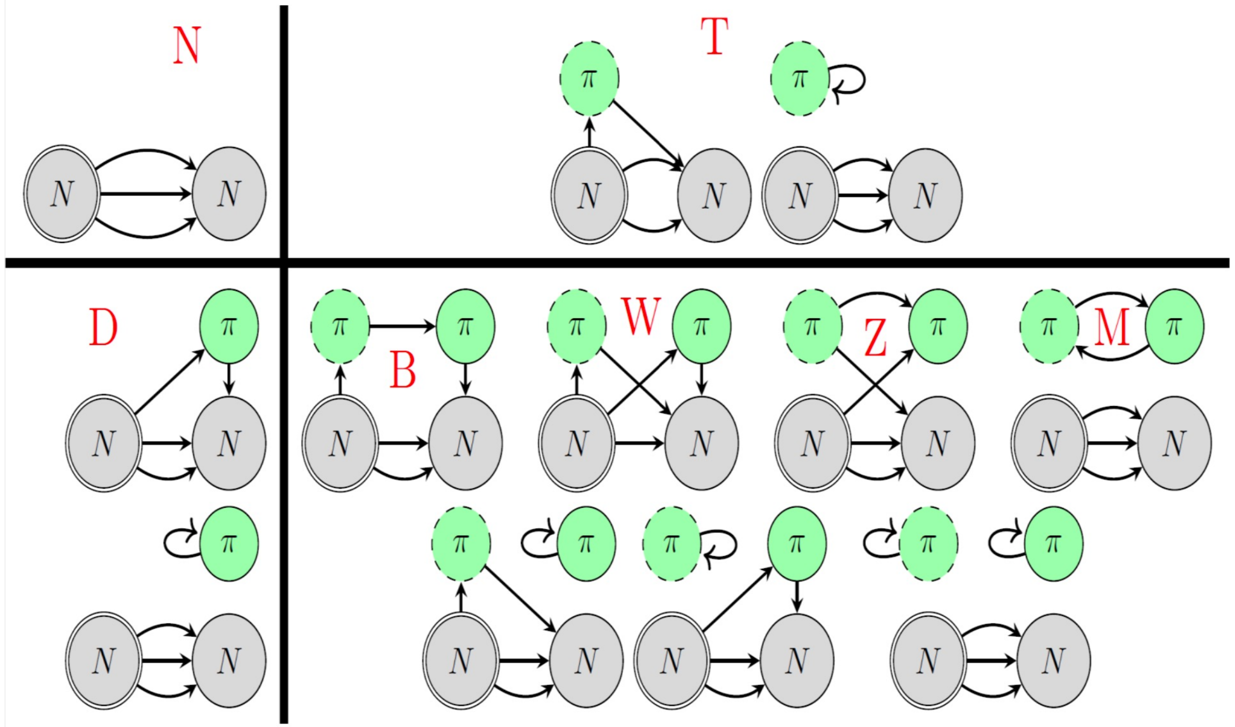

Diagrams: 3pt functions

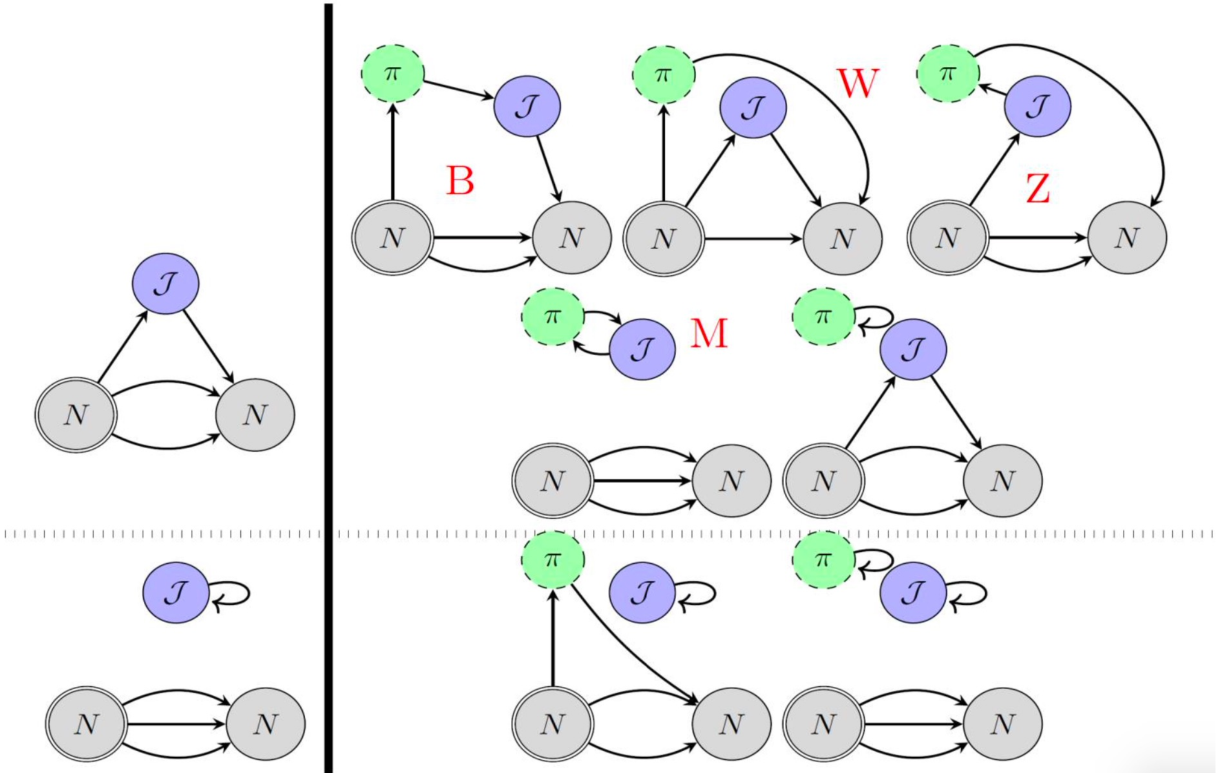

Generalized eigenvalue problem (GEVP)

GEVP improvement on 3pt functions:

$$J = A_4^{u-d} = \bar{u}\gamma_5\gamma_4 u - \bar{d}\gamma_5\gamma_4 d;\ \vec{q} = (0,0,1)$$

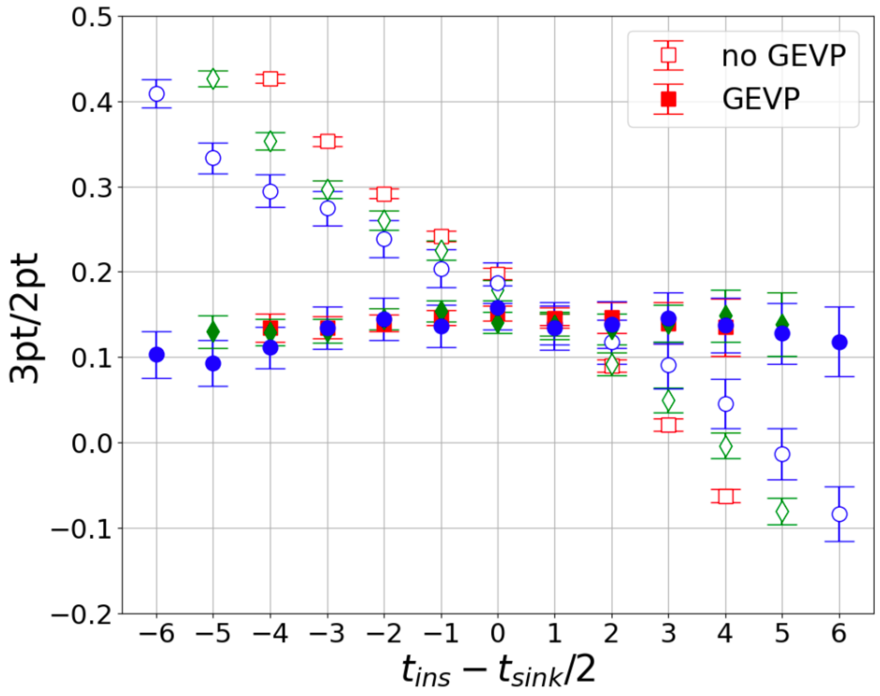

$m_\pi = 346$ MeV

Gravitational form factors - proton

D. Pefkou

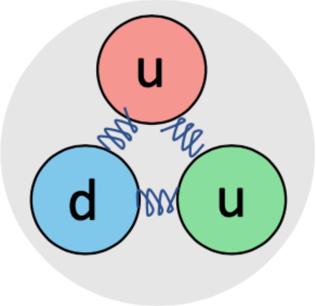

EMT

$$\langle N(p',s')|T_{\mu\nu}|N(p,s)\rangle = \frac{1}{m_N}\bar{u}(\boldsymbol{p}',s')\begin{bmatrix} P_\mu P_\nu A^N(t) \\ iP_{\{\mu}\sigma_{\nu\}\rho}\Delta^\rho J^N(t) \\ \frac{1}{4}(\Delta_\mu\Delta_\nu - g_{\mu\nu}\Delta^2)D^N(t)\end{bmatrix}u(\boldsymbol{p},s)$$

P_μ: $(p'_\mu + p_\mu)/2$; Δ_μ: $p'_\mu - p_\mu$; $t = \Delta^2$

t –dependence: much less is known

$$A^N(t) = A_g^N(t) + A_q^N(t),\ A^N(0) = 1$$
$$J^N(t) = J_g^N(t) + J_q^N(t),\ J^N(0) = 1/2$$
$$D^N(t) = D_g^N(t) + D_q^N(t),\ D^N(0) = ?$$

Lattice A+J+D for q + g : Hackett **DAP** Shanahan 2310.08484 → this talk

Experiment (A+D): Duran Meziani et al Nature 2023

Lattice (A+J+D): Shanahan Detmold PRL 2018, **DAP** Hackett Shanahan PRD 2022

Lattice (A+J+D): ETMC PRD 2020, LHPC PRD 2008

Experiment (D): Burkert Elouadrhiri Girod Nature 2018

Dispersive (D): Pasquini et al 2014

+ more from theory and models (see 2023 Colloquium Burkert et al for review)

Renormalized nucleon GFFs

D. Pefkou

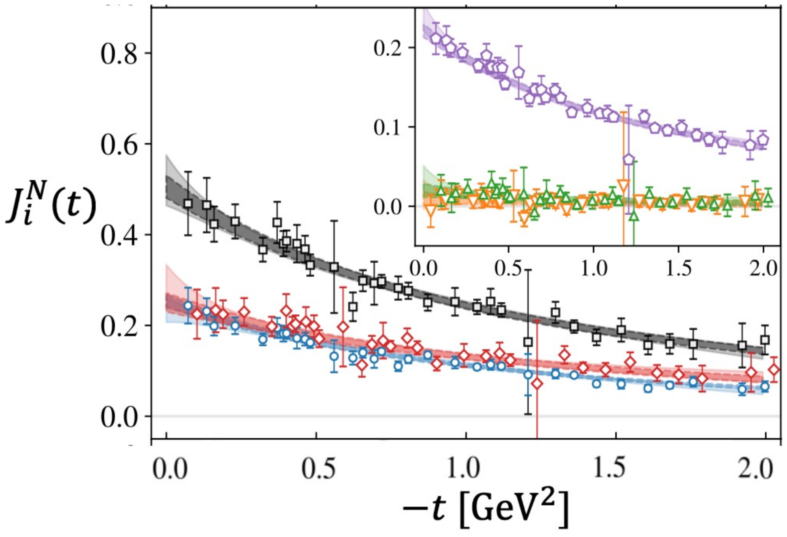

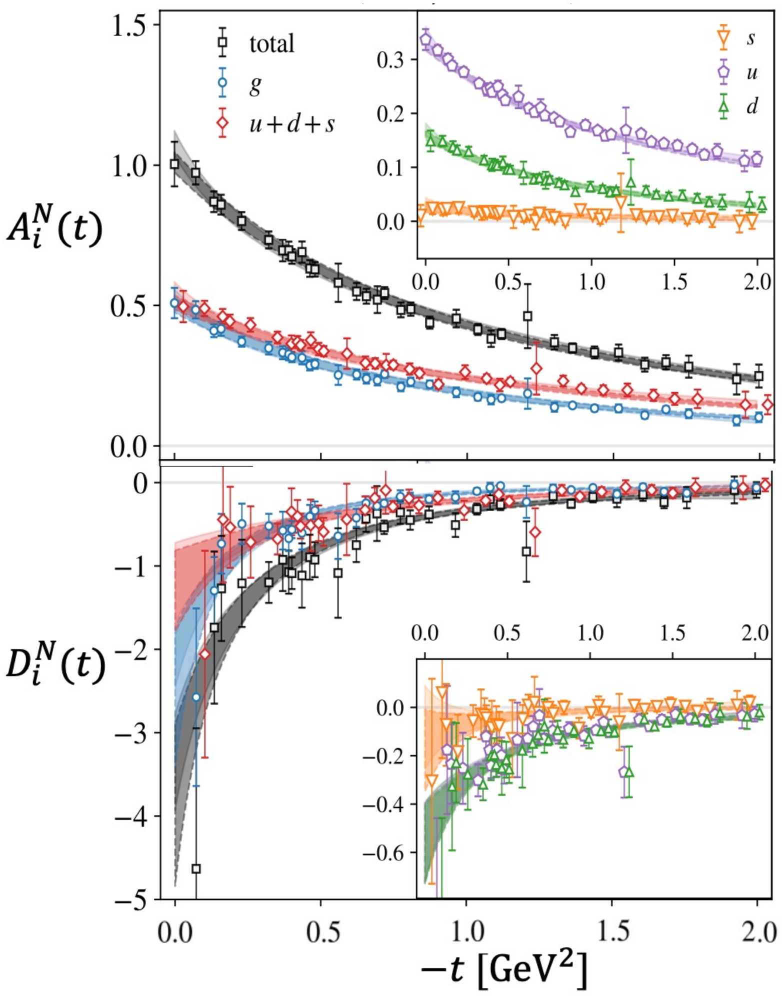

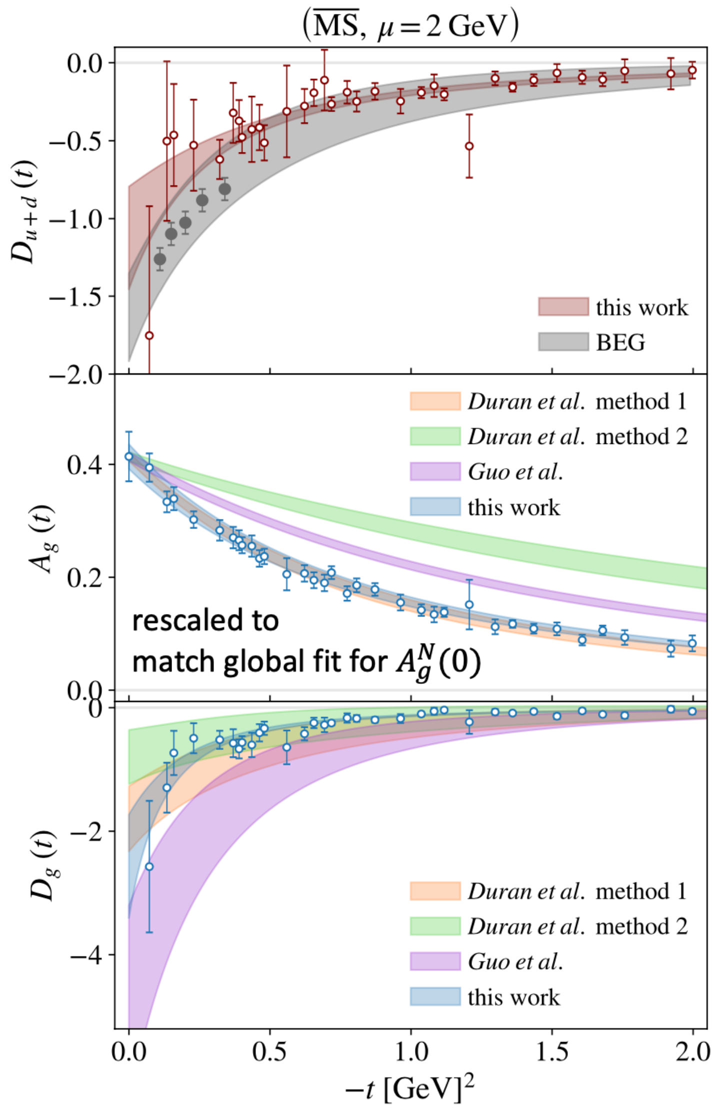

The Δ resonance at different physical parameters

F. Pittler

Delta resonance

- $\Delta(1232)$
- Lightest baryonic resonance
- Dominant in the p wave $N\pi$ scattering
- Simplest resonance: 3 quark and $N\pi$ contribution
- Resonances are not eigenstates of the QCD Hamiltonian

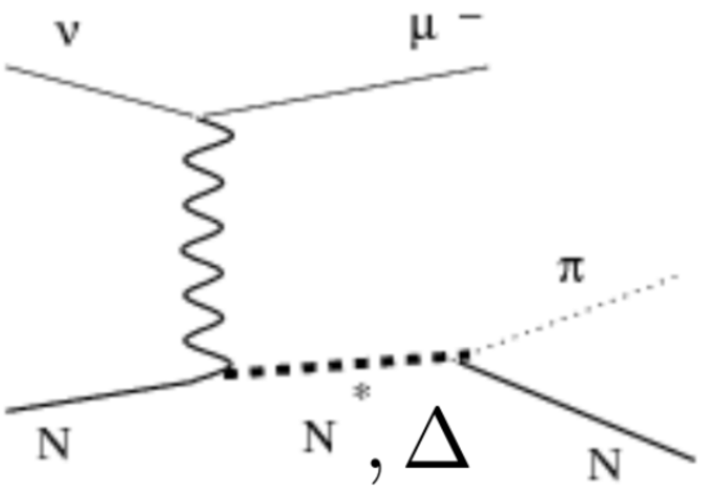

- They decay via strong interactions
- Finite volume influences the two-hadron spectrum

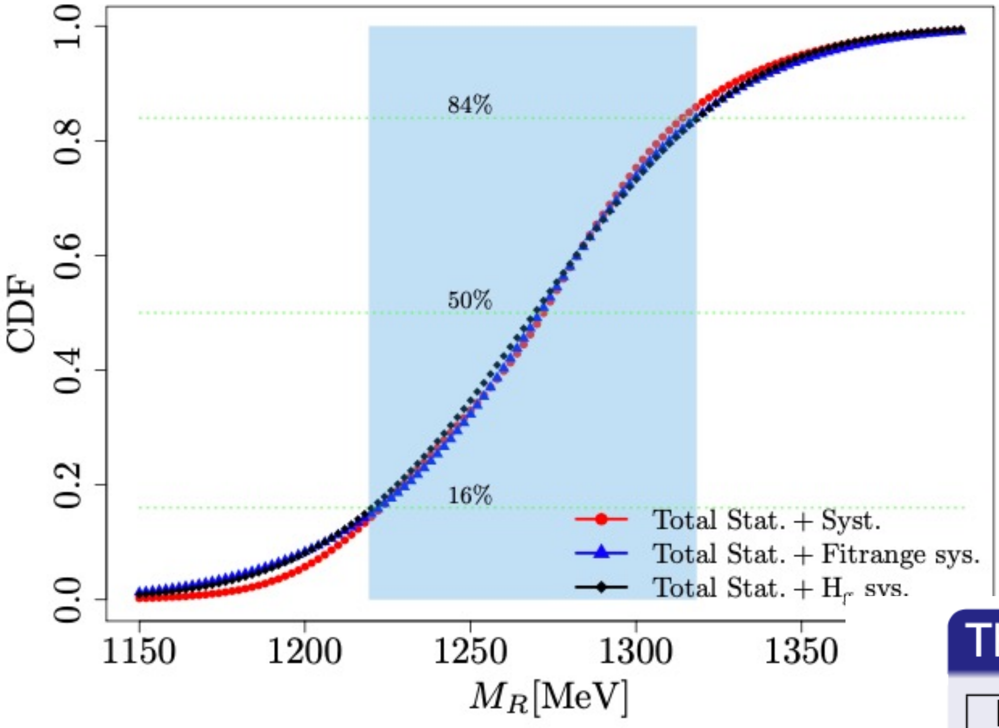

F. Pittler

This work (Details [arXiv:2307.12846])

Ensemble	m_π[MeV]	L	m_Δ[MeV]	$g_{\Delta-\pi N}$
Twisted-Clover	139 MeV	5.12 fm	1267(46) MeV	
Nf2+1 Clover	200 MeV	3.7 fm	1320(10) MeV	17.6(2.7)
Nf2+1 Clover	250 MeV	2.8 fm	1380(7) MeV	13.6(5)
Nf2+1 Clover	250 MeV	3.7 fm	1373(6) MeV	10.3(1.6)

Collaboration	m_π[MeV]	Methodology	m_Δ[MeV]	$g_{\Delta-\pi N}$
Verduci(2014)	266	Distillation, Lüscher	1396(19)	19.9(8)
Alexandrou et.al. (2013)	360	LO pert., Michael & McNeile	1535(25)	26.7(1.5)
Alexandrou et.al. (2015)	180	LO pert., Michael & McNeile	1350(50)	23.7(1.3)
Andersen et.al. (2017)	280	Stoch. distillation, Lüscher	1344(20)	37.1(9.2)
Morningstar et.al.(2022)	200	Stoch. distillation, Lüscher	1290(7)	$14.41(53)_{\mathrm{BW}}$
Silvi et.al. (2021)	255	Smeared sources, Lüscher	$1380(7)(9)_{\mathrm{BW}}$	$13.6(5)_{\mathrm{BW}}$

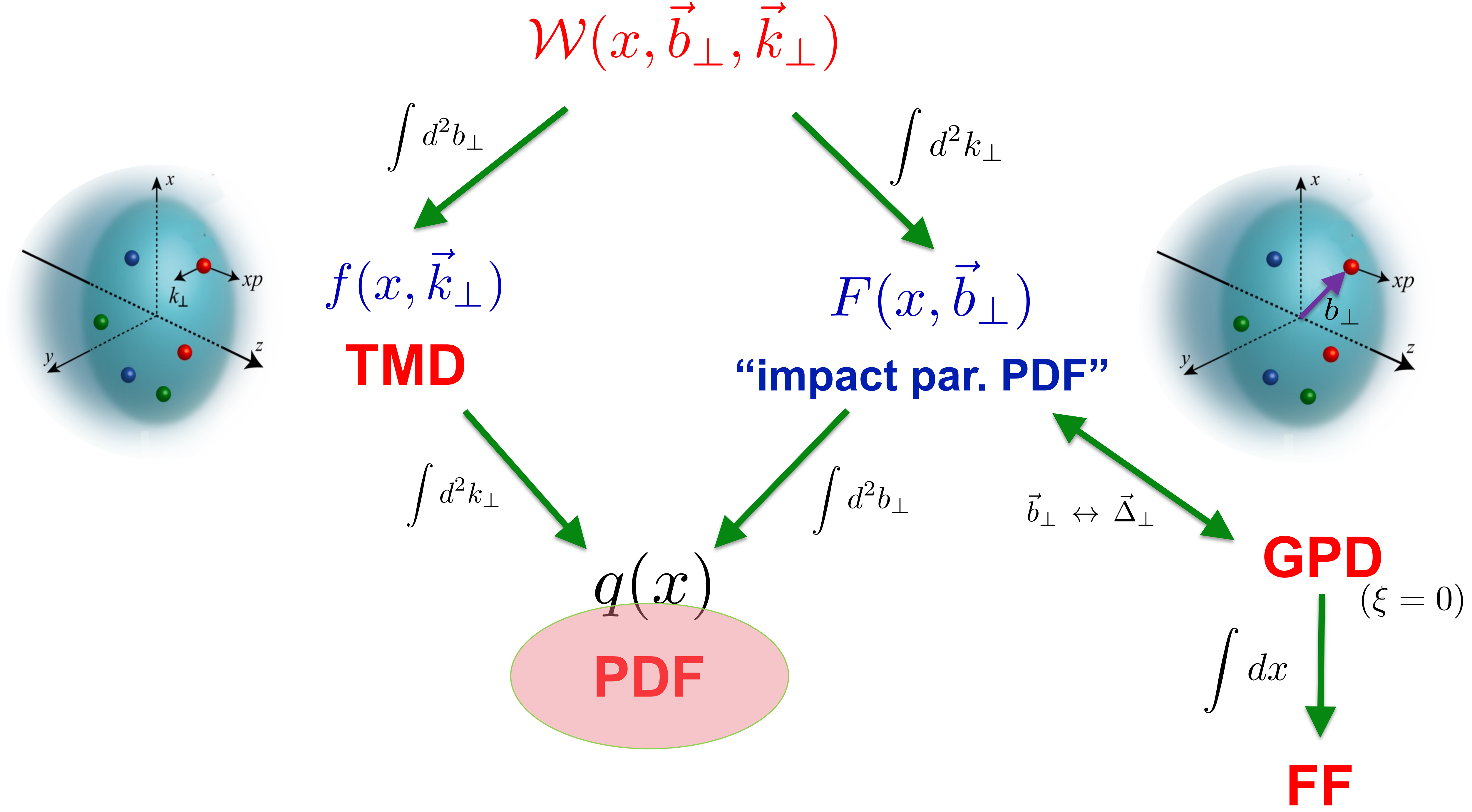

$\mathcal{W}(x, \vec{b}_\perp, \vec{k}_\perp)$
$\int d^2b_\perp$
$\int d^2k_\perp$
$f(x, \vec{k}_\perp)$
TMD
$F(x, \vec{b}_\perp)$
“impact par. PDF”
$\int d^2k_\perp$
$\int d^2b_\perp$
$\vec{b}_\perp \leftrightarrow \vec{\Delta}_\perp$
GPD
$(\xi = 0)$
$\int dx$
$q(x)$
PDF
FF
x
xp
$k_\perp$
y
z
$b_\perp$

S. Mukherjee

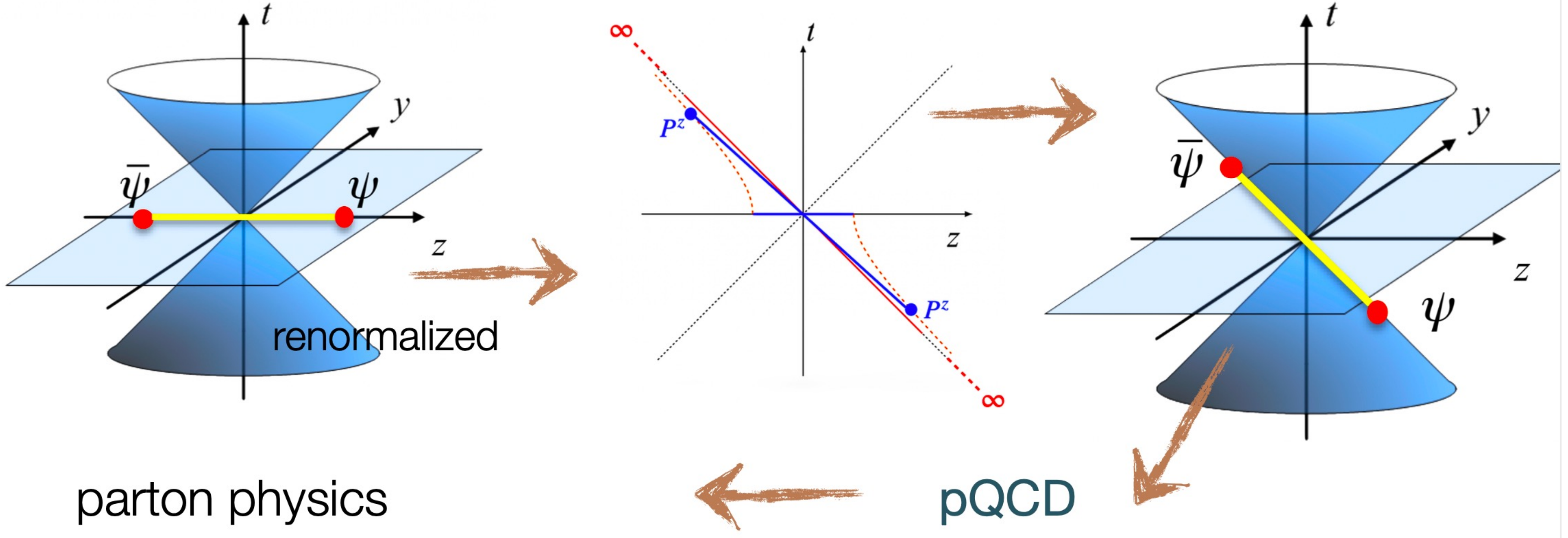

- difference is UV physics, can be taken care of through pQCD matching

$$+\mathcal{O}\left[\frac{\Lambda^2_{\mathrm{QCD}}}{x^2P_z^2}, \frac{\Lambda_{\mathrm{QCD}}}{(1-x)P_z}, \frac{M_H^2}{P_z^2}, \ldots\right]$$

$$+\mathcal{O}\left[z^2\Lambda^2_{\mathrm{QCD}}, z^2M_H^2, \ldots\right]$$

$C(x, P_z, \mu) \otimes$ momentum space

$C(\alpha, z^2, \mu) \otimes$ position space

S. Mukherjee

pion valance PDF

Yong Zhao *et al.*, *Phys.Rev.Lett.* 128 (2022) 14, 142003

NNLO momentum matching

valance pion mass 300 MeV

lattice spacing 0.04 fm

pion momenta up to 2.4 GeV

first LQCD PDF at NNLO

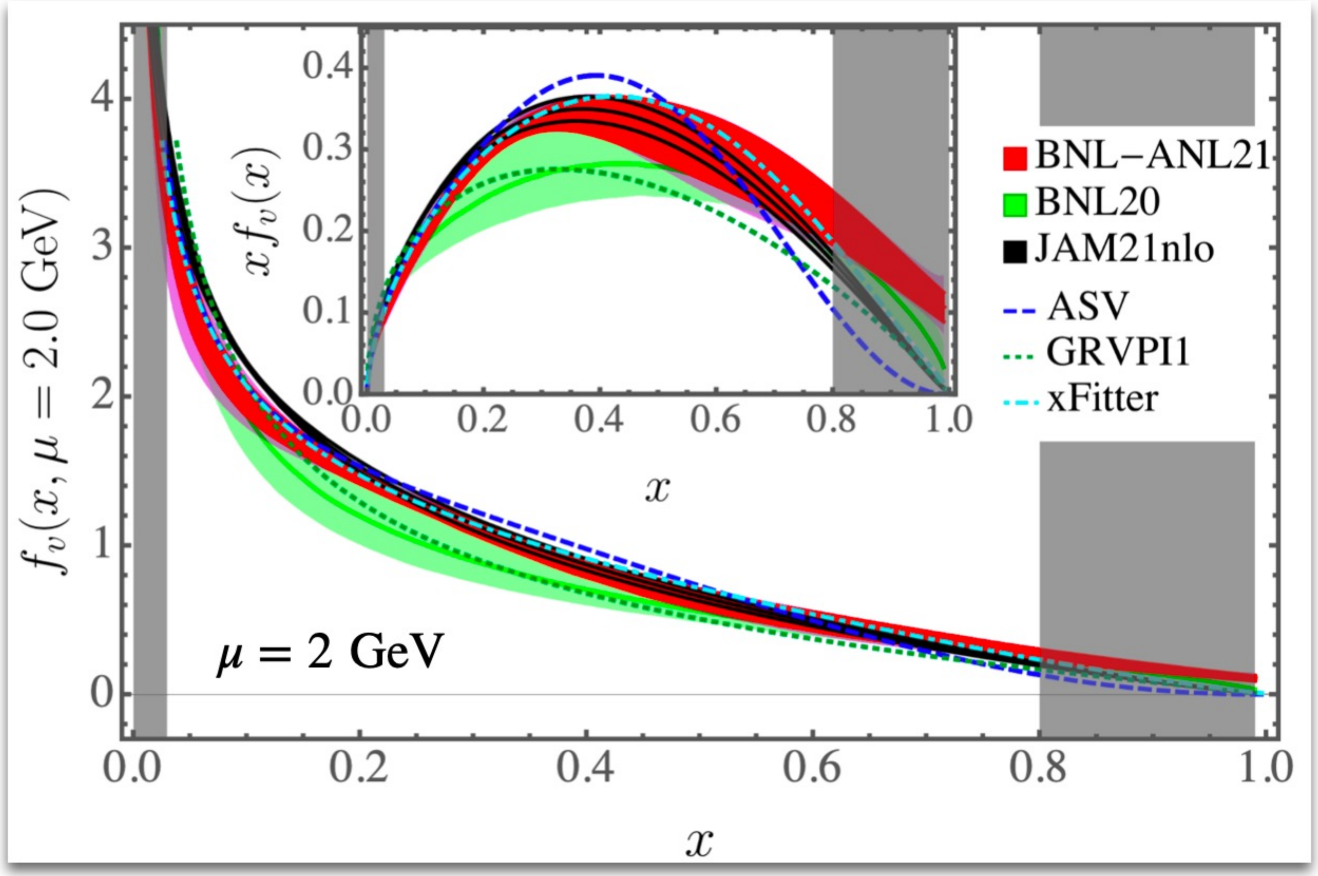

proton unpolarized isovector PDF

S. Mukherjee

NNLO momentum matching

physical pion mass

lattice spacing 0.075 fm

proton momenta ≲ 1.53 GeV

Andrew Hanlon *et al.*, *Phys.Rev.D* 107 (2023) 7, 074509

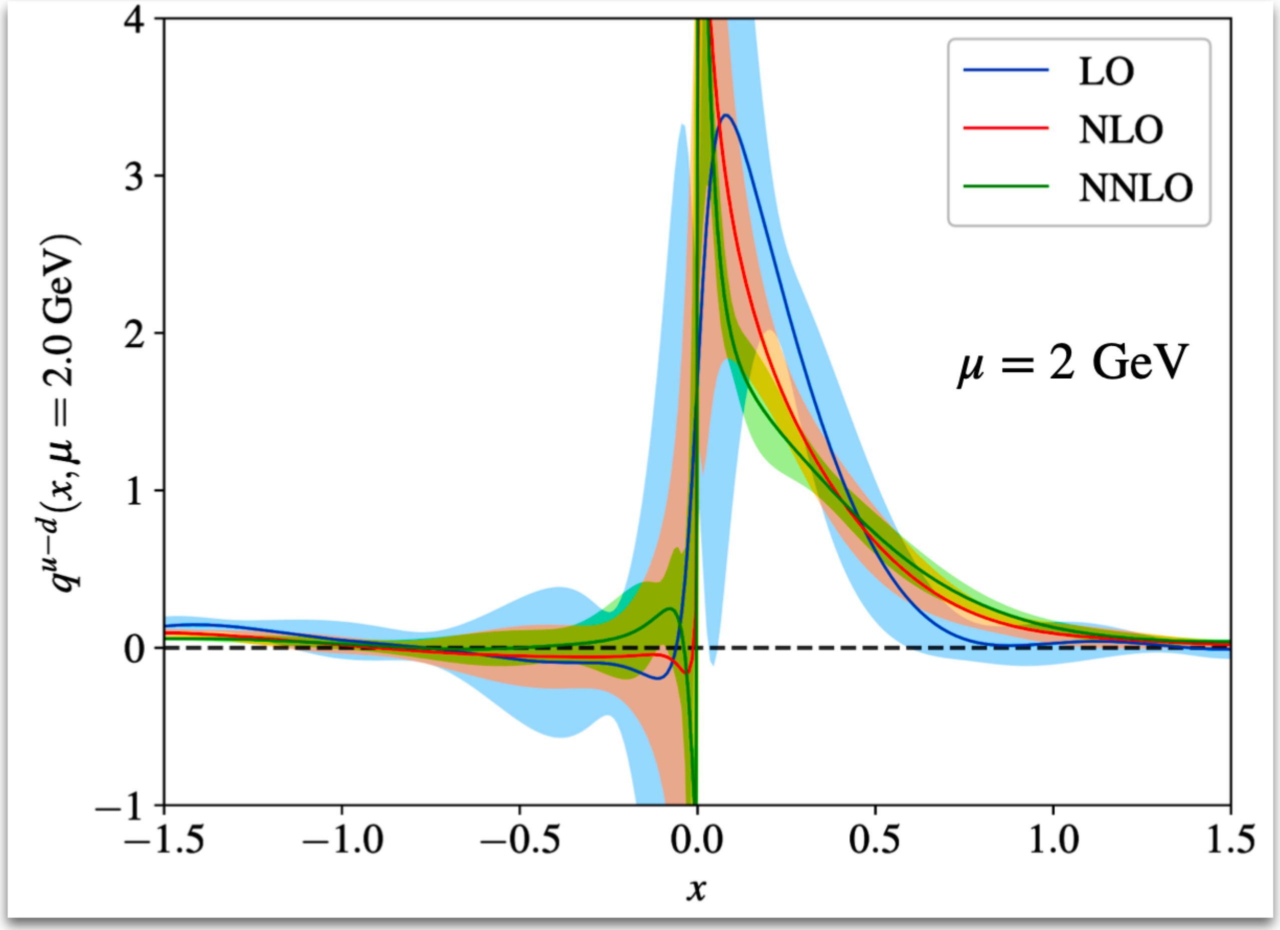

S. Mukherjee

$$C(\mathcal{S},\mu) \sim \alpha_s^0(\mu) + \alpha_s(\mu) f\left(\ln[\mathcal{S}\mu]\right) + \alpha_s^2(\mu) f\left(\ln[\mathcal{S}\mu]\right) + \cdots$$

$\mathcal{S} \sim 1/\mu$ ⟶ $\ln[\mathcal{S}\mu]$ large $\qquad \mathcal{S} = 2xP_z\,,\, z^2$

proton transversity PDF

Andrew Hanlon *et al.*, arXiv:2310.19047

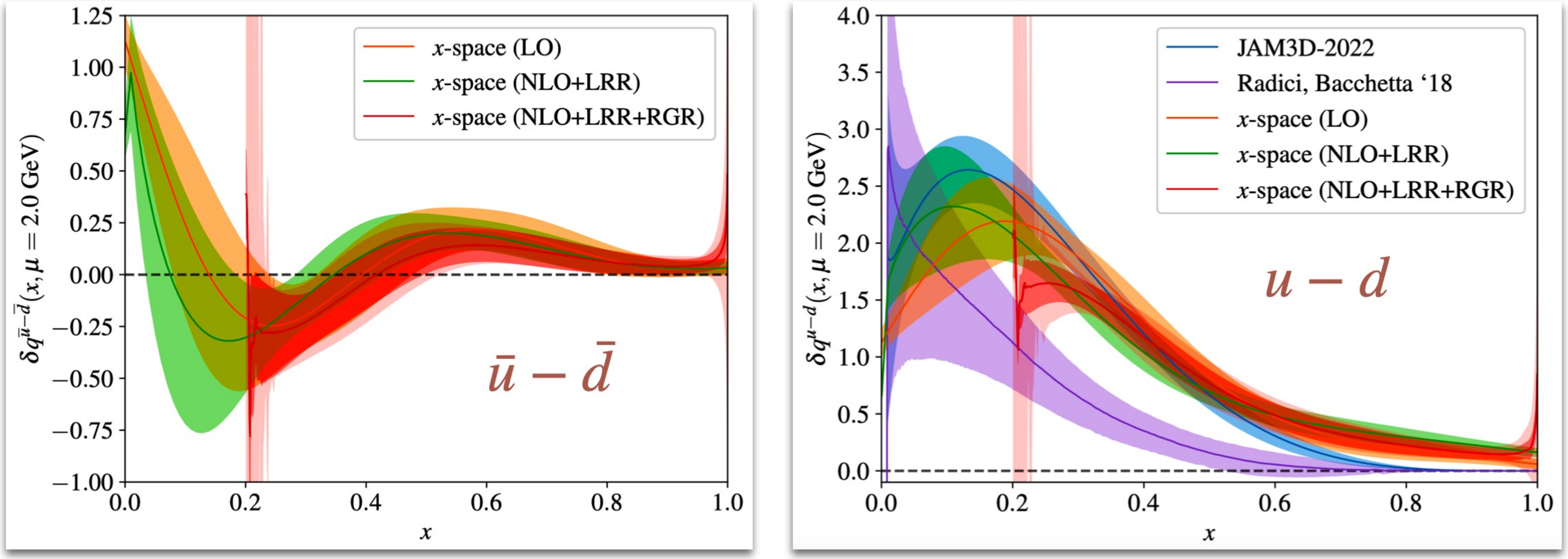

NLO+LRR+NLL(RGR) momentum matching

lattice spacing 0.075 fm, proton momenta 1.53 GeV, physical pions

QUARK-GLUON TOMOGRAPHY COLLABORATION

R. Zhang

Pion Distribution Amplitude (DA)

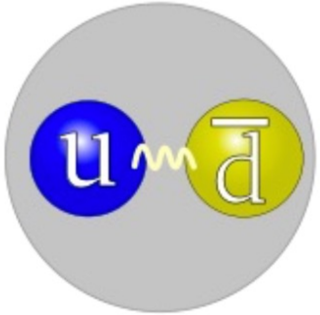

Pion lightfront DA $\phi(x)$: probability amplitude of pion in the bound state's minimal Fock component $|q\bar{q}\rangle$

$$\phi(x,\mu)=\frac{1}{if_\pi}\int\frac{d\xi^-}{2\pi}e^{i\left(\frac{1}{2}-x\right)\xi^- p^+}\langle 0|\bar{q}\left(\frac{\xi^-}{2}\right)\gamma^-\gamma_5 U\left(\frac{\xi^-}{2},-\frac{\xi^-}{2}\right)q\left(-\frac{\xi^-}{2}\right)|\pi(p)\rangle$$

DA as important input to hard exclusive process at $Q^2 \gg \Lambda_{\mathrm{QCD}}^2$: Beneke, et al. NPB(2001)

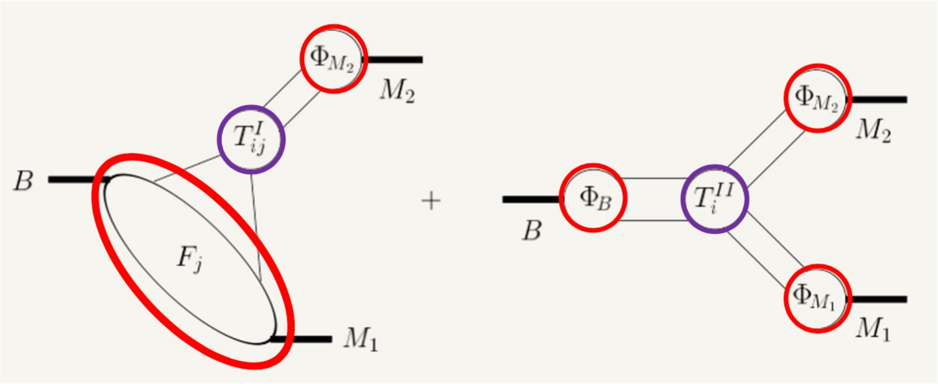

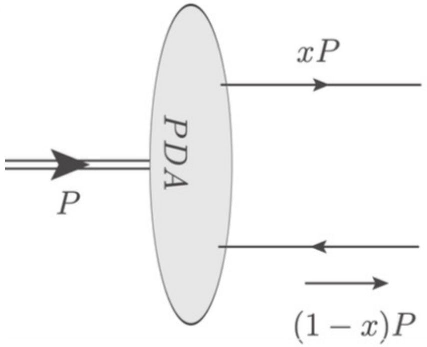

Argonne NATIONAL LABORATORY

R. Zhang

Comparison with previous results

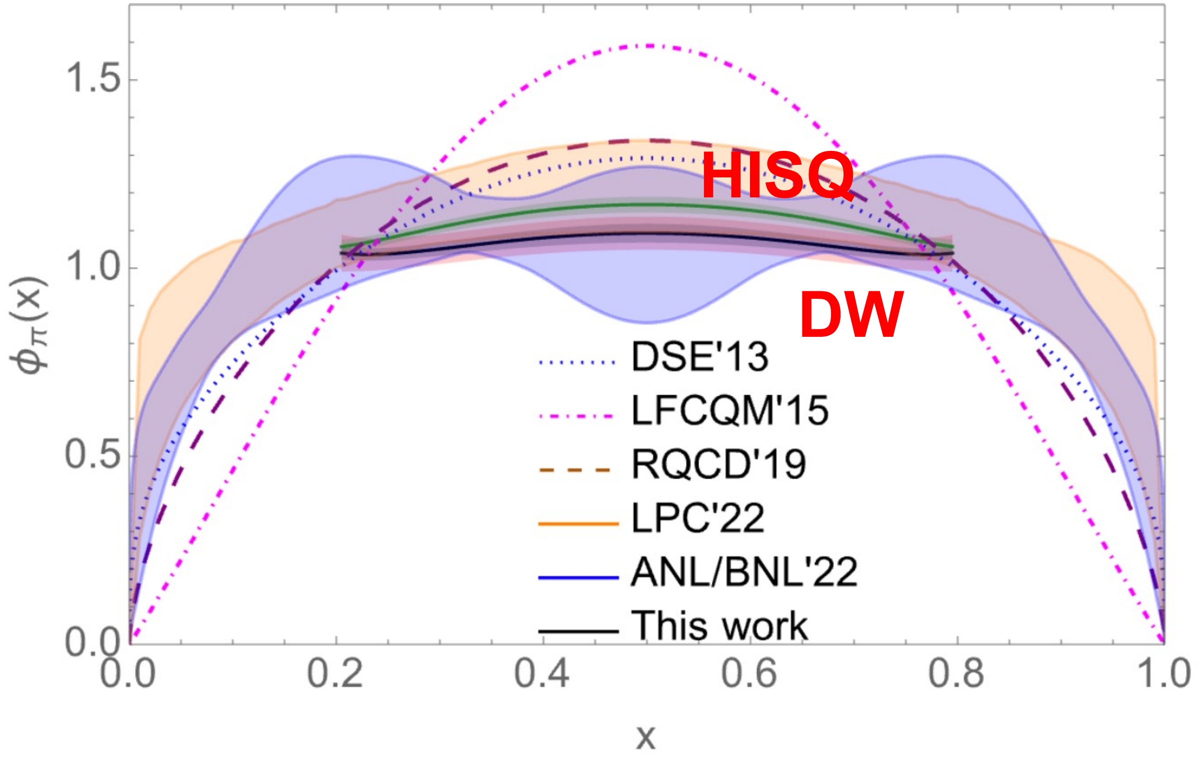

- One possible explanation is that the explicit chiral-symmetry breaking term in HISQ action has a similar effect as making the meson heavier (thus has a more narrow distribution)

❑A continuum limit study is needed for a more conclusive comparison

❑Threshold resummation is needed for more exact matching

The Intrinsic Charm hypothesis

G. Magni

- We define the charm content of the proton for $Q < m_c$ in the $n_f = 3$ flavour scheme as **Intrinsic Charm (IC)**.

- To determine IC we will need to **separate the perturbative component** of the charm PDF. Results are based on:

Allowing for **Intrinsic Charm** means:

$$f_c^{(3)}(x) \neq 0 \;\rightarrow\; f_c^{(4)}(x, m_c^2) = A_{cc} \otimes f_c^{(3)}(x) \;+ \sum_{i=g,q} A_{c,i} \otimes f_i^{(3)}(x, m_c^2)$$

$f_c^{(4)}(x, Q)$ has to treated as the other light flavour and **fitted to the data**.

Probing Intrinsic Charm

G. Magni

- Starting from the fitting scale we **evolve** the NNPDF4.0 baseline **to** $Q^2 = m_c^2$.
- When passing the heavy quark threshold we need to **invert the matching conditions** A_{ij}.
- The **remaining part** of the charm PDF **is the intrinsic component**, which is scale independent for $Q^2 < m_c^2$.

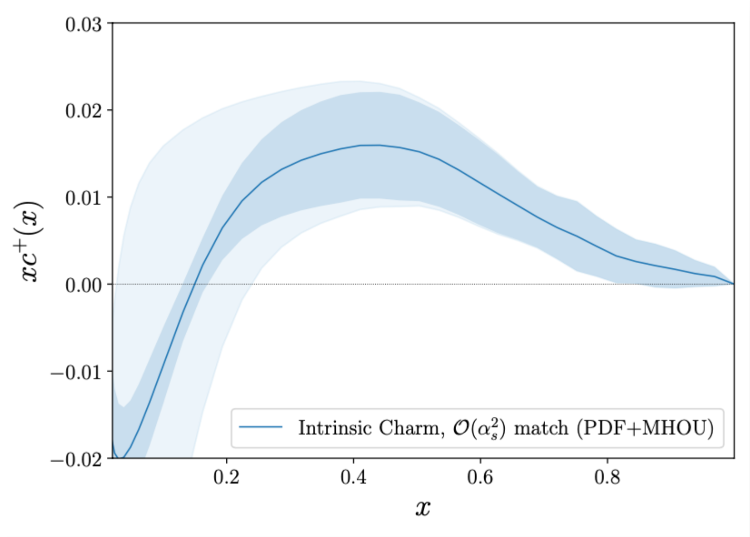

The resulting **IC** in the $n_f = 3$ scheme:

✔ Still contains ***valence-like*** peak.

✔ For $x \leq 0.2$ the perturbative uncertainties are quite large.

✔ The carried **momentum fraction** is within **1%.**

$Z + c$ @ LHCb

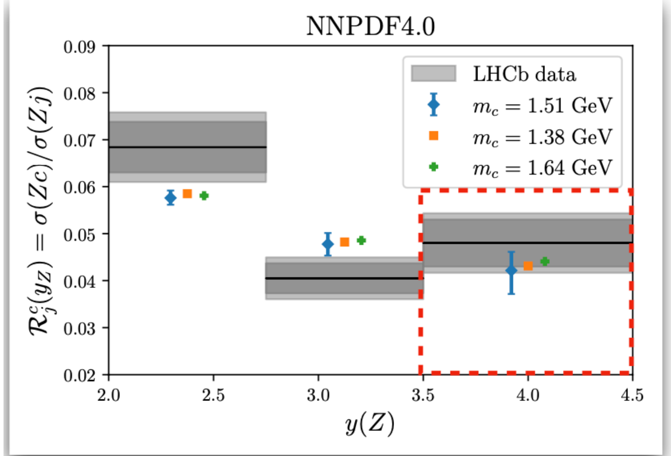

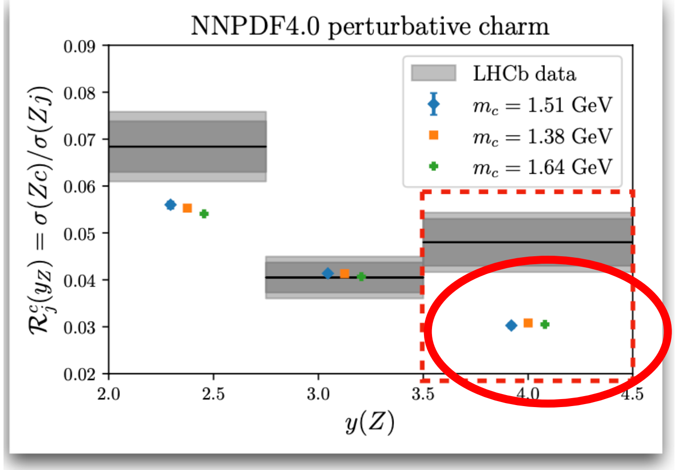

Current status of jets in polarized DIS

Status on jet production in polarized DIS:

- Not much interest in fixed-target
- 1jet at NLO (N-jetiness)
  Boughezal, Petriello, Xing ('18)
- 2jets at NLO (dipoles)
  Photon - Borsa, de Florian, **IP** ('20)
  NC & CC - Borsa, de Florian, **IP** ('21)
- 1jet at NNLO (dipoles + P2B)
  Photon - Borsa, de Florian, **IP** ('20)
  NC & CC - Borsa, de Florian, **IP** ('23)

Status on polarized inclusive DIS:

Structure function coefficients available at

- NNLO (photon - g1)
  van Neerven, Zijlstra ('94)
- NNLO (NC & CC - g1, g4, g5)
  Borsa, de Florian, **IP** ('22)
- N3LO (photon – g1)*
- Blumlein, Marquard, Schneider, Schönwald ('22)

I. Pedron

NNLO – Projection-to-Born method (P2B)

Obtain the **fully differential** cross section from

- The **inclusive** cross section at the desired order
- The exclusive cross section of the **observable + 1 jet at one lower order**

In our case...

Born kinematics mapping:

$$p_B = xP$$
$$p'_B = p_B + q$$

Not possible in the Breit-frame!!

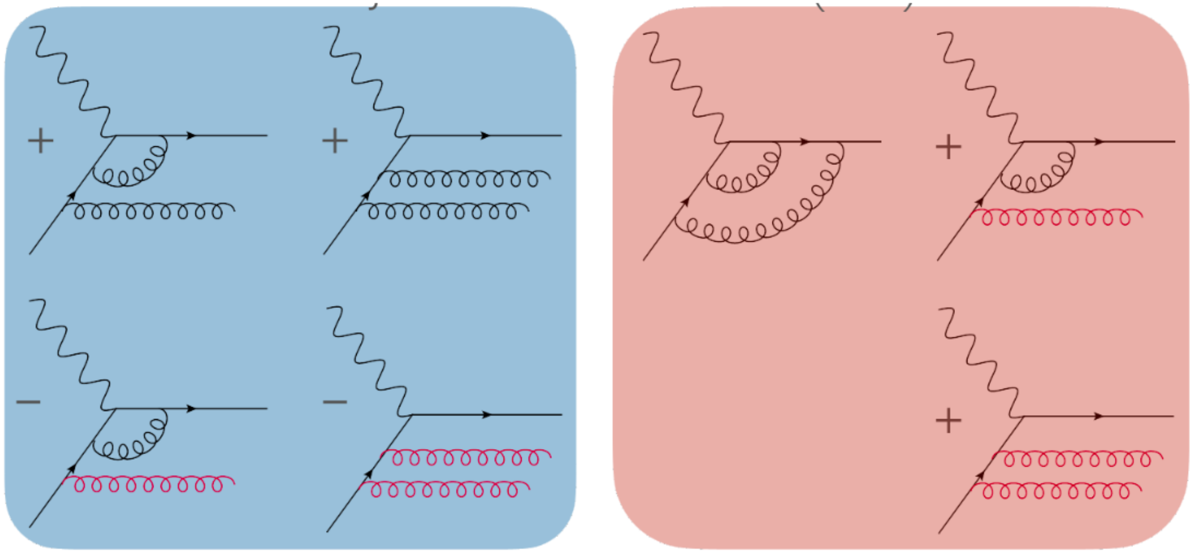

$$d\sigma^{\mathrm{NNLO}}_{1jet} = d\sigma^{\mathrm{NLO}}_{2jet} - d\sigma^{\mathrm{NLO}}_{2jet,\mathrm{P2B}} + d\sigma^{\mathrm{NNLO,\ incl}}_{1jet}$$

Dipoles

Structure Functions

NC

I. Pedron

CC

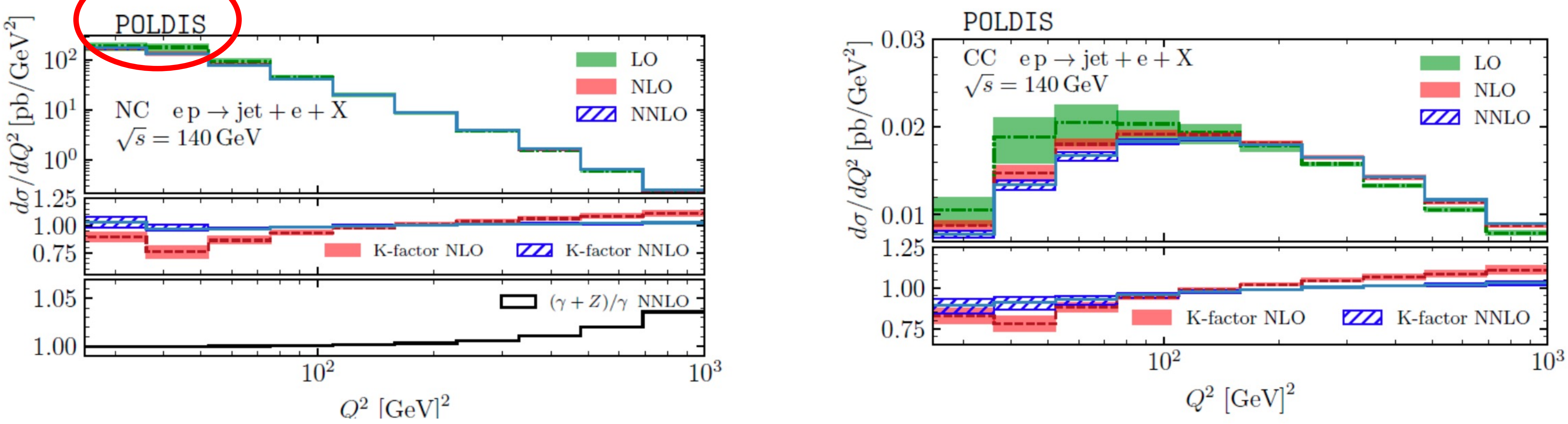

A_{LL}

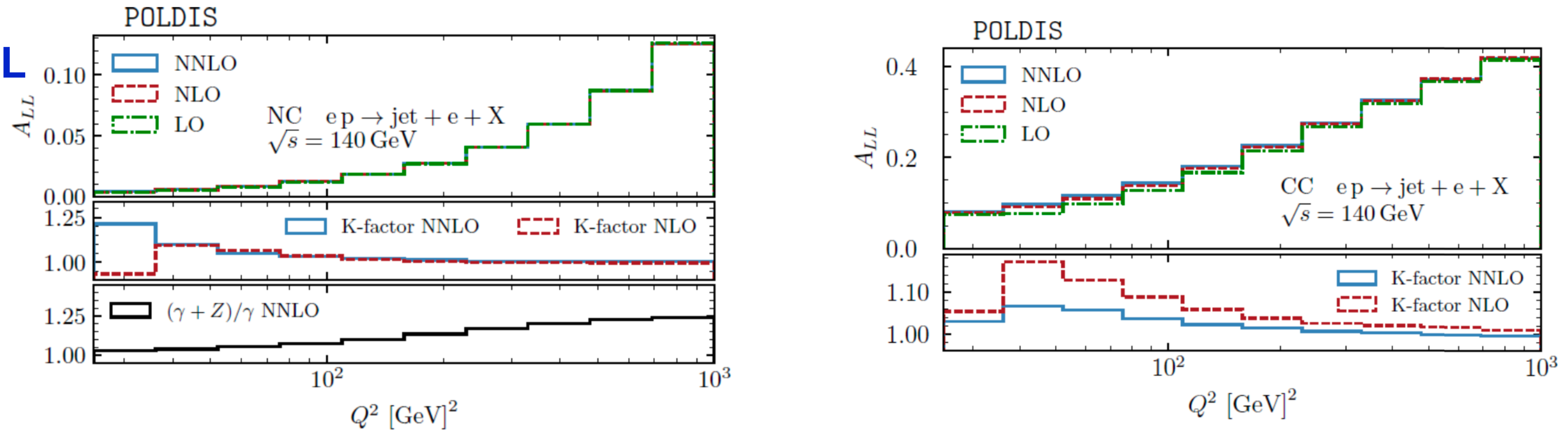

Nucleon helicity structure at NNLO

I. Borsa (WV)

- PDF evolution: $$\Delta\mathcal{P}_{ij} = \frac{\alpha_s}{2\pi}\Delta P_{ij}^{\mathrm{LO}} + \left(\frac{\alpha_s}{2\pi}\right)^2 \Delta P_{ij}^{\mathrm{NLO}} + \left(\frac{\alpha_s}{2\pi}\right)^3 \Delta P_{ij}^{\mathrm{NNLO}} + \ldots$$

Moch, Vogt, Vermaseren
Blümlein, Marquard, Schneider, Schönwald

- Partonic hard scattering: $$\Delta\hat{\sigma}_{ab} = \Delta\hat{\sigma}_{ab}^{\mathrm{LO}} + \frac{\alpha_s}{\pi}\Delta\hat{\sigma}_{ab}^{\mathrm{NLO}} + \left(\frac{\alpha_s}{\pi}\right)^2 \Delta\hat{\sigma}_{ab}^{\mathrm{NNLO}} + \ldots$$

Zijlstra, van Neerven

Boughezal, Li, Petriello

+ soft-gluon techniques for SIDIS, pp

Why NNLO ?

- need per cent accuracy for EIC and JLab (cf. LHC experience)
- reduce theory uncertainty

$$\frac{\sigma(\mu) - \sigma(Q)}{\sigma(Q)}$$

$$Q/2 \leq \mu_{R,F} \leq 2Q$$

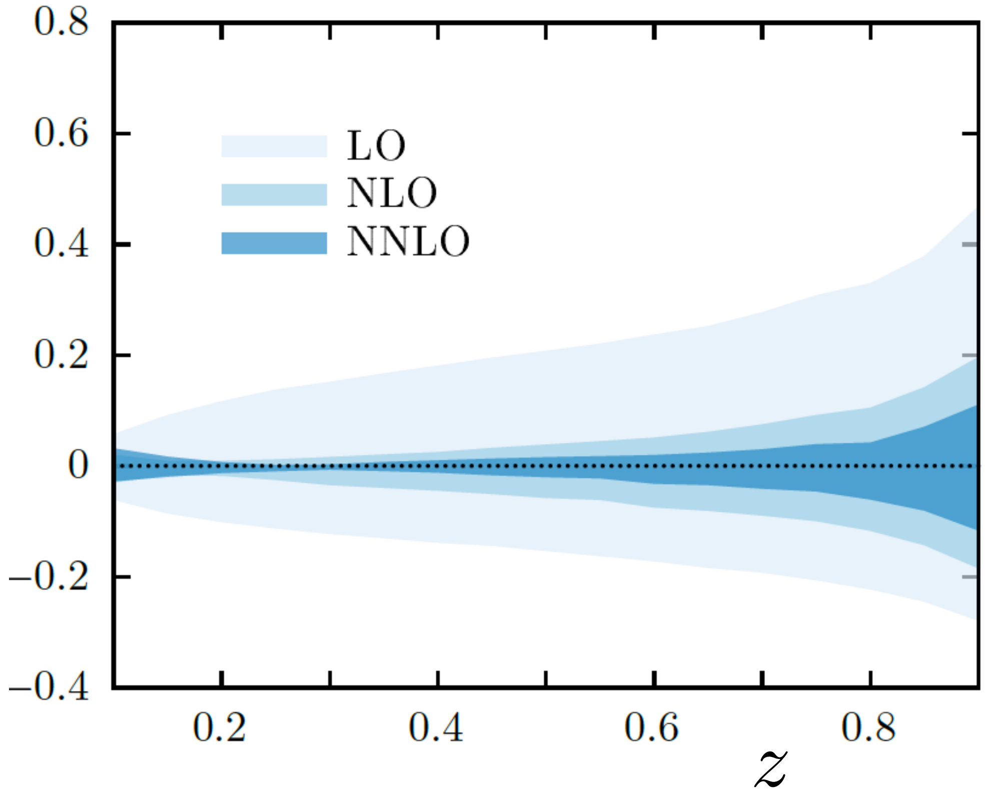

$Q^2 > 5\,\mathrm{GeV}^2$

SIDIS@EIC

Abele, De Florian, WV

- progress in lattice computations

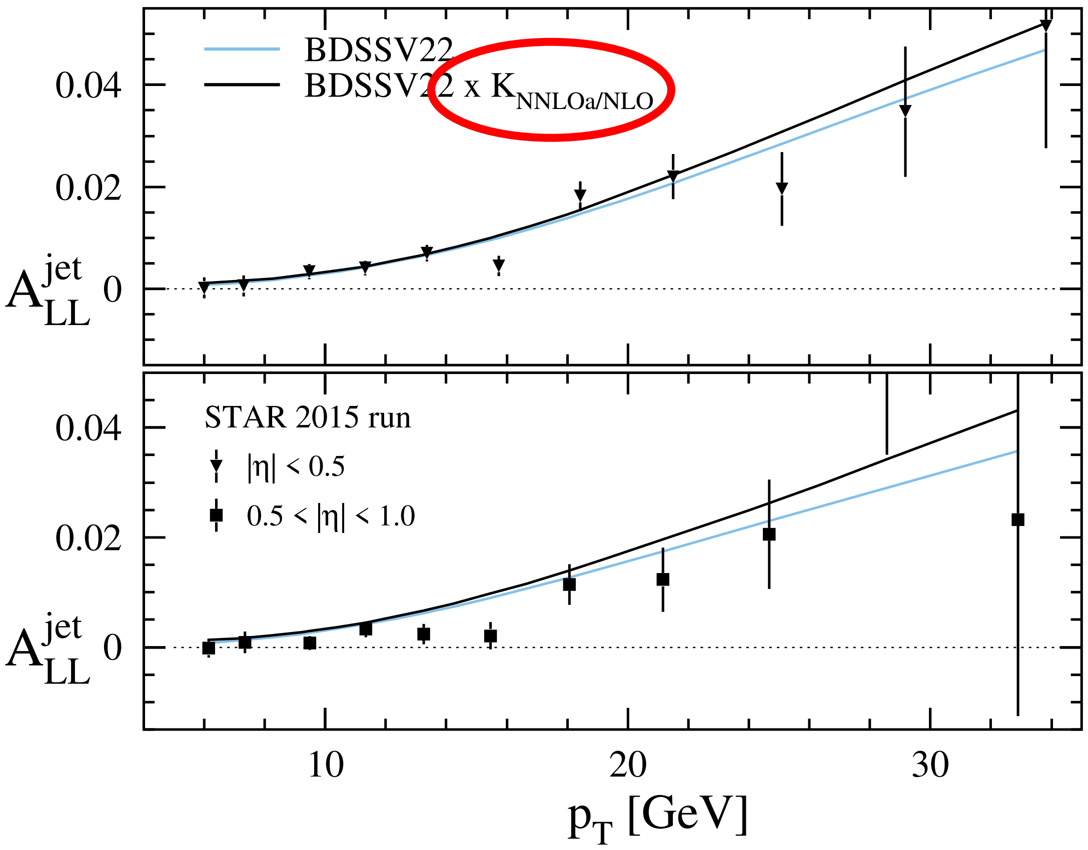

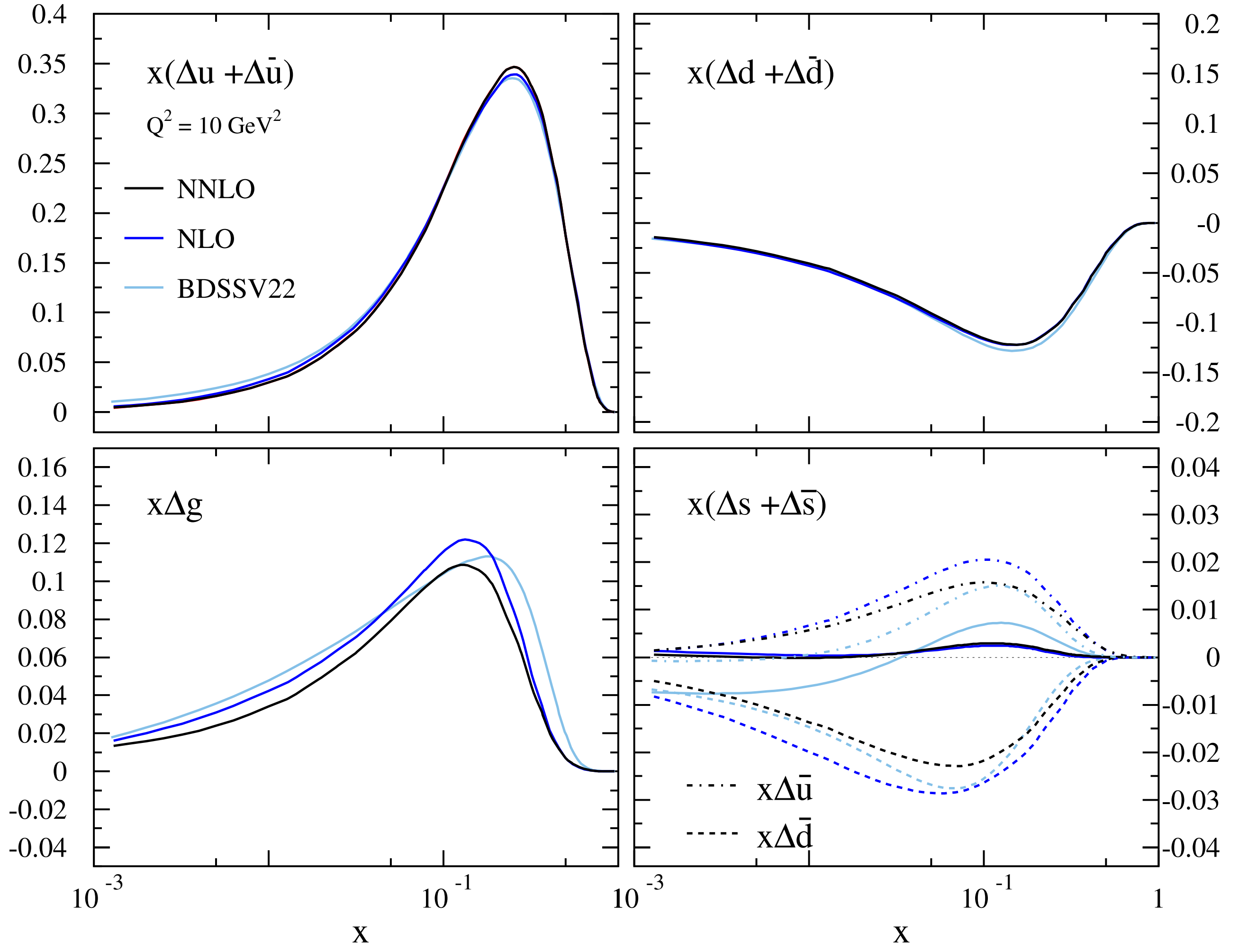

First ever NNLO global analysis of helicty PDFs !

Moos
Schlegel
Gamberg
Zurita
Borsa
Magni
Bertone
Braun
Bhattacharya
Pedron
Tomalak
Hobart

Bacchio
Koutsou
Pefkou
Zhang
Mukherjee
Constantinou
Pittler
Li

Thank you!